HEAT AND MOISTURE TRANSFER IN THE AVIAN RESPIRATORY SYSTEM

Thesis for the Degree of Ph. D.
MICHIGAN STATE UNIVERSITY
WILLIAM EDWARD ROPER
1969

This is to certify that the

thesis entitled

HEAT AND MOISTURE TRANSFER IN THE

AVIAN RESPIRATORY SYSTEM

presented by

William E. Roper

has been accepted towards fulfillment
of the requirements for

Ph D degree in A. E.

Merle L Esmay
Major professor

Date 11/20/69

ABSTRACT

HEAT AND MOISTURE TRANSFER IN THE AVIAN RESPIRATORY SYSTEM

by William E. Roper

Knowledge of the moisture and heat production capabilities of the domestic fowl at various environmental conditions is of primary importance in the design of poultry housing and equipment. Respiratory latent heat production is the major mode of moisture addition to the environment by the bird. However, very little research related to the mechanisms and location of moisture transfer within the bird has been done.

This study was undertaken to gain a better understanding of the heat and moisture transfer in the avian respiratory system. The chicken was choosen as the experimental species because of its commercial value, and the large amount of related information available in the literature.

A simulation model was developed to determine: 1) the portion of the respiratory system where heat and moisture is transfered, and 2) the rate at which this transfer takes place. Two heat and mass balance equations coupled with a respiratory wall temperature equation were used in the model. The model was adapted to thermoneutral conditions.

The results indicate that the majority of the heat and moisture transfer to the respiratory air occurs during inspiration from the respiratory surfaces between the anterior nasal opening and the base of the trachea. The simulation model predicted that air at the base of the trachea was very near lung temperature and saturated. Experimental measurements confirmed the simulation model prediction. Therefore only a small amount of heat and moisture is transfered on the surfaces of the lungs and air sacs under thermoneutral conditions.

The rate of sensible and latent heat production predicted by the simulation model was compared with the heat produced by hens in a specially designed two-compartment respiration calorimeter. The selected hens were adult White Leghorns in active egg production.

Sensible and latent heat production from the head chamber and body chamber of the calorimeter were determined as a function of environmental temperature and humidity. Non-linear least squares analysis was used to develop the regression equations from the calorimeter data. Equations representing heat transfer from a flat plate exposed to laminar air flow was used to estimate convective heat transfer from the comb and wattles. The difference between the heat transferred from the comb and wattle, and the total sensible heat produced in the head chamber was an estimate

of respiratory sensible heat production. The production of sensible and latent heat predicted by the simulation model was within the 95 percent confidence limits of the respiratory sensible and latent heat production values estimated by the non-linear least squares regression equations. These regression equations were developed using the appropriate heat production values from the calorimeter study.

Calorimeter temperatures ranged from 76°F to 96°F. At these temperatures relative humidities of 60%, 70%, and 80% had a very small effect on sensible and latent heat production. The head region of the hen was found to produce approximately 40-46% of the bird's total sensible heat loss at these chamber temperatures. Latent heat transfer from body surfaces other than the head region were negligible.

Approved Merle F Esmay
Major Professor

Approved Carl W Hall
Department Chairman

HEAT AND MOISTURE TRANSFER IN THE AVIAN RESPIRATORY SYSTEM

By

William Edward Roper

A THESIS

Submitted to

Michigan State University

in partial fulfillment of the requirements

for the degree of

DOCTOR OF PHILOSOPHY

Department of Agricultural Engineering

1969

To Kathy

ACKNOWLEDGMENTS

The author wishes to express his appreciation and thanks to Dr. M.L. Esmay, committee chairman, Dr. R.K. Ringer, Dr. J.V. Beck, Dr. D.R. Heldman, the Poultry Science Department, and the Agricultural Engineering Department for their help and support that aided the completion of this study.

TABLE OF CONTENTS

	Page
ACKNOWLEDGMENTS	iii
LIST OF TABLES	vii
LIST OF FIGURES	viii
LIST OF APPENDICES	xi
LIST OF SYMBOLS	xii
Chapter	
1. INTRODUCTION	1
2. LITERATURE REVIEW	4
2.1 General Heat Balance	4
2.1a Metabolism and heat storage	5
2.1b Modes of heat transfer	6
2.2 Heat Production Studies with Avian Species	12
2.2a Total body calorimetry	12
2.2b Respiratory heat loss	17
2.3 Avian Respiratory System	19
2.3a Mechanics of respiration	20
2.3b Air flow in the respiratory system	20
2.4 Respiratory Evaporation	21
3. ANALYTICAL CONSIDERATIONS	27
3.1 Heat Production in the Calorimeter	27
3.2 Estimation of Tidal Volume	32

Chapter Page

3.3 Heat and Moisture Transfer Model of the Respiratory System 33

3.3a Analysis of the transient term. . . 38

3.3b Structure of the respiratory system . 43

4. EXPERIMENTAL PROCEDURE AND EQUIPMENT . . . 46

4.1 Calorimeter Chamber 46

4.1a Temperature measurement 49

4.1b Humidity measurement 52

4.1c Air flow measurement 53

4.1d Experimental procedure 55

4.2 Respiratory Tract Wall Temperature . . . 61

4.3 Trachea Humidity Investigation 63

5. EXPERIMENTAL RESULTS 67

5.1 Heat and Moisture Production; the Calorimeter Studies 67

5.1a Latent heat production 68

5.1b Sensible heat production in the head chamber 71

5.1c Sensible heat production in the body chamber 74

5.1d Total sensible heat production . . 76

5.2 Estimation of Tidal and Minute Volume . . 78

5.3 Wall Temperatures in the Respiratory System 80

5.4 Humidity at the Base of the Trachea . . 83

5.5 Respiratory Simulation Model Results . . 85

5.6 Unequal Duration of Inspiration and Expiration 91

Chapter Page

6. CONCLUSIONS 97

7. RECOMMENDATIONS FOR FUTURE WORK 99

LIST OF REFERENCES 101

APPENDICES 107

LIST OF TABLES

Table		Page
2.1	Forced convection heat transfer equations for average heat transfer coefficients	10
4.1	Thermocouple locations	50
4.2	Temperature and humidity combinations studied in the calorimeter (6 birds were used)	60
5.1	Respiratory tract wall temperatures	82
5.2	Surface temperatures in the head region . . .	83
5.3	Humidity at base of the trachea when subjected to different respiration rates and tidal volumes.	84
A.1	Latent heat production from the head chamber . .	118
A.2	Sensible heat production from the head chamber .	121
A.3	Sensible heat production from the body chamber .	124
A.4	Total sensible heat production from body and head chambers	127
A.5	Sensible heat production from the respiratory system	130

LIST OF FIGURES

Figure		Page
2.1	Metabolism in homeotherms	6
2.2	Total heat produced by caged layer per hour per pound of body weight at different temperatures	14
2.3	Evaporative heat loss of White Leghorn hens in a standing position after eleven weeks of acclimation to a 75°F or a 95°F environment . .	16
4.1	Calorimeter chamber	47
4.2	Inner chamber	47
4.3	Calorimeter recording instruments	47
4.4	Fifty-inch inclined manometer	47
4.5	Air flow through the calorimeter	48
4.6	Chicken position in the calorimeter	58
4.7	Chicken position in the head chamber	58
4.8	Calorimeter training box	58
4.9	Humidity sensor and housing	62
4.10	Trachea humidity test	62
4.11	Respiratory tract temperature test	62
4.12	Schematic diagram of the operation for determination of the humidity at the base of the trachea	64
5.1	Total latent heat production	70
5.2	Total sensible heat production in the head chamber	72

Figure Page

5.3 Respiratory sensible heat production 73

5.4 Sensible heat production in the body chamber 75

5.5 Total sensible heat production 77

5.6 Estimated tidal volume 79

5.7 Estimated minute volume 81

5.8 Temperature of inspired nasal air 87

5.9 Humidity of inspired nasal air 87

5.10 Temperature of inspired nasal to tracheal air 87

5.11 Humidity of inspired nasal to tracheal air . . . 87

5.12 Temperature of inspired tracheal air 88

5.13 Humidity of inspired tracheal air 88

5.14 Temperature of expired tracheal air 88

5.15 Humidity of expired tracheal air 88

5.16 Temperature of expired tracheal to nasal air . . 89

5.17 Humidity of expired tracheal to nasal air . . . 89

5.18 Temperature of expired nasal air 89

5.19 Humidity of expired nasal air 89

5.20 Comparison of respiratory sensible heat production 92

5.21 Comparison of respiratory latent heat production 93

5.22 Respiratory duration cycle of 50% inspiration an 50% expiration 95

5.23 Respiratory duration cycle of 42% inspiration and 58% expiration 95

Figure Page

A.4.1 Individual total latent heat production 113

A.4.2 Individual total sensible heat production in the head chamber 114

A.4.3 Individual respiratory sensible heat production in the head chamber 115

A.4.4 Individual sensible heat production in the body chamber 116

A.4.5 Individual total sensible heat production . . . 117

LIST OF APPENDICES

Appendix		Page
A.1	Derivation of the Energy Balance Equation	107
A.2	Derivation of the Energy Balance Equation with Condensation	109
A.3	Derivation of the Mass Balance Equation	111
A.4	Heat Production Graphs with Individual Bird Regression Lines	113
A.5	Calorimeter Data Tables	118
A.6	Calorimeter Sensible and Latent Heat Production Program	133
A.7	Calorimeter Conduction Heat Transfer Program	140
A.8	Non-Linear Least-Squares Program	142
A.9	Respiration Simulation Model; Air temperature and Humidity as a Function of Location	144
A.10	Respiration Simulation Model; Estimated Heat Production, BTU/hr	153

LIST OF SYMBOLS

ρ_a . . . Density of air, lb/ft^3

V_a . . . Velocity of air, ft/hr

A . . . Cross-sectional area, ft^2

T_a . . . Air temperature, °F

C_a . . . Specific heat of air, BTU/lb °F

dx . . . Increment length, ft

h . . . Convective heat transfer coefficient, BTU/hr ft^2°F

P . . . Perimeter, ft

T_w . . . Wall temperature, °F

t . . . Time, hr

σ . . . Mass transfer coefficient, $lb_{water}/hr\ ft^2 \Delta H$

H_a . . . Specific humidity of air, lb_{water}/lb_{air}

H_w . . . Specific humidity in the boundary layer, lb_{water}/lb_{air}

$\dot{m}$ . . . Air mass flow rate, lb_{air}/hr

Δx . . . Increment length, ft

T_{i+1} . . . Air temperature at outlet of increment i,°F

T_i . . . Air temperature at inlet of increment i,°F

X_{i+1} . . . Distance to outlet of increment i, ft

X_i . . . Distance to inlet of increment i, ft

H' . . . Specific humidity in the boundary layer, lb_{water}/lb_{air}

H_{a_i} . . . Specific air humidity at inlet to increment i, lb_{water}/lb_{air}

$H_{a_{i+1}}$ . . Specific air humidity at outlet from increment i, lb_{water}/lb_{air}

1. INTRODUCTION

Controlled environment housing has become the major type of poultry housing in the last ten to fifteen years. Its major advantage has been the provision of a controlled livestock environment which lends itself to good management practices. Environmental management practices, however, should be linked with a knowledge of which variables to control and in what range to control them in order to produce maximum economic return.

A good deal of work has been done relating environmental temperature to various production variables. Ota and McNally (1961) reported on total body sensible and latent heat production from caged White Leghorn and Rhode Island Red hens in full production. Longhouse (1967), working with Ota, developed regression equations for total body latent, sensible, and total heat production as a function of average live weight for several ambient temperatures.

More recently researchers have attempted to gain a better understanding of physiological behavior of poultry and to relate physiological response to environmental conditions. A close correlation of the hypothalamic temperature and the heart rate with respect to both diurnal

rhythms and rapid changes corresponding to the level of excitement has been found by Scott, Johnson, and Van Tienhoven (1967). Similar work, involving the cat's hypothalamic temperature, has been done in establishing a basis for control theory analogies of the respective thermal regulatory systems (Adams, 1964).

Interest has also expanded into direct calorimeter studies of single birds. W.L. Roller and A.C. Dale (1962) developed regression equations for total body heat production for Leghorn hens as a function of dry-bulb temperature, weight, feed consumption, and dew-point temperature. The equations were based on tests with confined single hens in a thermoelectric, partitioning (convective, radiative, evaporative heat transfer) calorimeter. Other researchers have used the thermoelectric partitioning calorimeter to study the effect of acclimation upon partitioned heat loss for single constrained laying hens (DeShazer, 1968). The turkey has also been studied recently in this type of calorimeter (Malholtra, 1967).

These studies have assumed all moisture loss to be emmitted from the respiratory system. There has been no attempt to separate the respiratory moisture and heat loss from other body surface moisture and heat losses.

This research was undertaken to partition the heat and moisture transfer of the respiratory system from the external body surfaces of adult Leghorn hens in active egg

production as a function of environmental temperature and humidity. A specially designed two-compartment calorimeter was used for separating the amounts of heat and moisture transfer from the head and body sections of the bird.

A simulation model was developed to determine: 1) the portion of the respiratory system where heat and moisture is transfered, and 2) the rate at which this transfer takes place. A breath by breath simulation was used. Theoretical results were compared with laboratory results.

2. LITERATURE REVIEW

2.1 General Heat Balance

Homeothermic animals are capable of maintaining a relatively constant body temperature despite wide changes in ambient conditions. This is accomplished by physiological control of the balance between heat production and heat loss.

Sturkie (1965) expresses this relationship as

$$M \pm S = E \pm R \pm C_1 \pm C_2 \qquad (2.1)$$

where:

M = rate of heat production (metabolism)

S = heat storage within the body

E = rate of evaporation of moisture

R = heat exchange due to radiation

C_1 = rate of heat loss by convection

C_2 = rate of heat loss by conduction

Rearranging equation 2.1 to express the transient condition, Adams (1968) developed the following expression

$$\frac{\partial H}{\partial t} = M \pm S \pm R \pm C_1 \pm C_2 - E \qquad (2.2)$$

where:

$\frac{\partial H}{\partial t}$ = the net heat flux; if $\frac{\partial H}{\partial t}$ is equal to zero, a thermal steady state is achieved.

In some instances a further development of the modes of heat transfer were necessary. Beckett and Vidrine (1969)

considered both free and forced convection heat transfer from swine. Birkebak (1966) divided radiation into solar and infrared components in his development of the heat balance equation. However, equations 2.1 and 2.2 contain the general modes of heat transfer and heat production most authors consider important.

2.1a Metabolism and heat storage

The first research efforts in this area were concerned with the study of metabolic heat production of various animals in resting states. Research then progressed to include the effects of nutritional levels, age, sex, environmental air temperature, seasonal changes, and other parameters.

The various parameters affecting metabolism are given by Brody (1945), Klieber (1961), King and Farner (1961), as well as others. From these works a general scheme of metabolic rates can be discussed. The standard metabolism is found, in most cases, to be independent of environmental air temperatures over a limited range, as shown in Figure 2.1. This region is referred to as the thermoneutral zone and is bracketed between the lower critical temperature, T_{CL}, and the upper critical temperature, T_{CU}. Within this region physiological mechanisms control the various modes of energy exchange and metabolism. When the environmental temperature drops below T_{CL}, the majority of the physiological mechanisms which are used to conserve heat are at their maximum effectiveness and the subsequent added heat

loss must be made up by increasing the metabolic rate. In accordance with the physical laws of heat transfer, the heat loss is proportional to the insulation afforded by the animal's body covering and the temperature difference between the body surface and the environmental temperature.

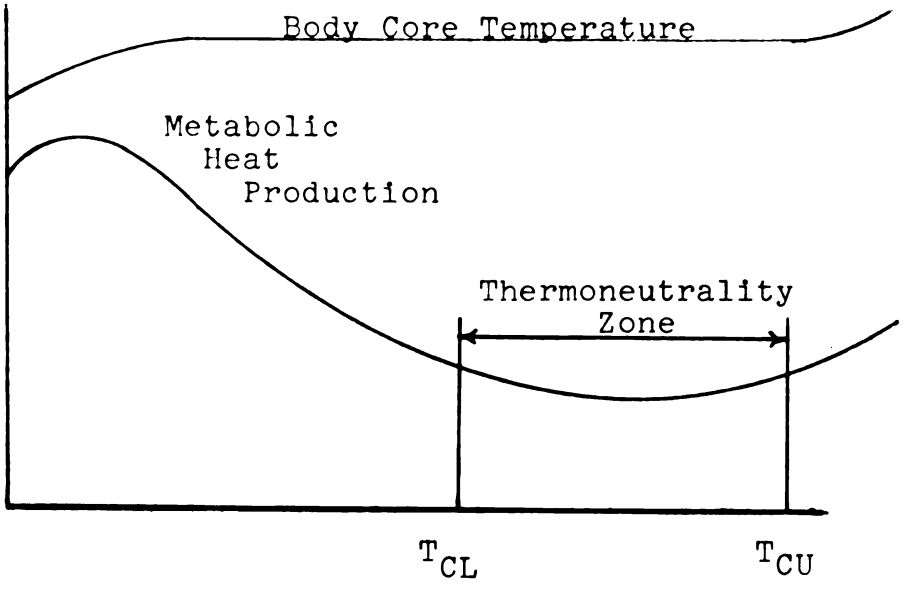

Figure 2.1-- Metabolism in homeotherms

When the environmental temperature rises above the upper critical temperature, T_{CU}, the animal is only able to transfer the excess energy by evaporative cooling. Heat may also be stored, but in doing so, body temperature rises and the metabolic rate increases. This process continues until the upper lethal temperature is reached.

2.1b Modes of heat transfer

Many of the fundamental concepts of heat transfer have been applied to heat exchange studies between animals and

their environment. Particular interest here is with avian species.

Radiation

The rate of radiation heat transfer from a chicken was determined by Clayton and Boyd (1963) as

$$q_r = \frac{A_s \sigma (T_s^4 - T_e^4)}{\frac{1}{E_s} + \frac{A_s}{A_e}\left(\frac{1}{E_e} - 1\right)} \qquad (2.3)$$

where:

q_r = net radiant heat transfer, BTU/hr

σ = Stefan-Boltzmann constant

A_s = area of surface, ft^2

A_e = area of surroundings, ft^2

E_s = effective emissivity of the surface

E_e = effective emissivity of the surroundings

T_s = effective surface temperature of bird surface, °R

T_e = effective surface temperature of surroundings, °R

With the emissivity of chicken feathers and skin being very close to that of a black body (Jordan and Dale, 1961), equation 2.3 reduces to

$$q_r = A_s E_s \sigma (T_s^4 - T_e^4) \qquad (2.4)$$

If the temperature difference between the bird and its environment is small, the radiative heat loss is roughly proportional to the temperature difference (Sturkie, 1965).

Conduction

The fundamental equation for calculating heat transfer by conduction is Fourier's heat conduction equation (Holman, 1963).

$$Q = - KA \frac{\partial T}{\partial x} \tag{2.5}$$

where:

Q = rate of heat flow, BTU/hr

K = thermal conductivity, BTU/ft^{2}hr

A = area perpendicular to the direction of heat flow

$\frac{\partial T}{\partial x}$ = temperature gradient

Because of the low thermal conductivity of air, even of moist air, loss of heat by conduction from the body surface to air is negligible (Sturkie, 1965). There is, however, some heat transfer by conduction from the deep body tissues of a bird to the skin surface. This can be determined by approximating the body form by geometric figures, such as spheres or cylinders, and applying Fourier's equation (Clayton and Boyd, 1963; Birkebak, 1966). Blood flow is another mode of transfering heat to the body surface.

Convection

Heat loss by convection from an animal's skin surface to the surrounding air may be expressed as (Rohsenow and Choi, 1961)

$$Q_c = hA (T_s - T_{air}) \tag{2.6}$$

where:

Q_c = rate of convective heat loss, BTU/hr

h = average heat transfer coefficient, BTU/ft^{2}hr

A = convective surface area, ft^2

T_s = average skin temperature, ^oF

T_{air} = average air temperature, ^oF

There are two fundamental types of convection heat transfer: free convection and forced convection. Free convection occurs where fluid motion is caused by fluid variation due to temperature differences. In this case, the dimensionless heat transfer coefficient is a function of the Grashof and Prandtl numbers.

$$Nu = f(Gr,Pr) \qquad (2.7)$$

The relationship between dimensionless variables for objects of various sizes, forms, and orientations has been determined. The forms or shapes that are of most interest in approximating biological systems are cylindrical surfaces, spherical shapes, and horizontal and vertical flat plates. Simplified equations for calculating the heat transfer coefficient for these shapes at ordinary air temperatures and atmospheric pressures are given by Birkebak (1966).

Heat transfer by convection is increased when fluid motion past the surface is caused by means other than density difference. This is termed forced convection and may be caused by animal movement or by forced movement of air over the animal's surface. In this case, the dimensionless

equation for the average heat transfer coefficient is

$$Nu = f(Re,Pr) \qquad (2.8)$$

Expressing equation 2.8 as a power function, this becomes

$$Nu = C \times Re^n Pr^m$$

The constant C and exponents m and n are contained in Table 2.1 for a variety of shapes and flow conditions as summarized by Birkebak (1966).

Table 2.1 Forced convection heat transfer equations for average heat transfer coefficients

Plane Surface	$Nu = C \times Re^n Pr^m$		
	c	n	m
Laminar range	0.644	.5	.33
Turbulent range	0.037	.8	.33
Cylinder (air flow normal to body)	$Nu = B_1 + B_2 Re^n$		
Re	n	B_1	B_2
0.1 - 1,00	0.52	0.32	0.43
1,000 - 50,000	0.60	0.00	0.24
Spheres	$Nu = 0.37\ Re^{0.6}$		
	for Re = 17 - 70,000		

Evaporation

Birds do not have sweat glands, but are able to lose some heat by vaporization of moisture from their skin (Sturkie, 1965). Most of the evaporative loss, however, occurs from the moist lining membranes of the respiratory tract. It has long been recongnized that respiratory evaporation plays an important part in the heat regulation of birds. When air temperatures reach or exceed body temperature, it is the only avenue of heat dissipation remaining. Evaporative heat loss is dependent upon the difference between aqueous vapor pressure at the evaporating surface and that of the air, as well as upon the rate of air movement over the moist surface. This evaporative heat loss may be represented by an equation suggested by Burton and Edholm (1955).

$$H = V(Q_{sat}T_b Q_a) \times 0.6 \qquad (2.10)$$

where:

H = rate of evaporative heat loss

V = pulmonary ventilation rate

$Q_{sat}T_b$ = quantity of moisture in air saturated at deep body temperature

Q_a = quantity of moisture in ambient air

0.6 = latent heat of vaporization of water, K_{cal}/g

In this equation, as well as others (King and Farner, 1961; Bouchillon, Reece, and Deaton, 1969) used to estimate evaporative heat loss, the exhaled air humidity is assumed to be that of saturated air at deep body or lung temperature.

It seems reasonable that the humidity of exhaled air would be more dependent upon the temperature of the evaporating surfaces (assuming the evaporating surfaces are wetted at all times) throughout the respiratory tract. In this literature survey, however, no studies of air temperature and humidity as a function of location in the respiratory tract were found.

2.2 Heat Production Studies with Avian Species

2.2a Total body calorimetry

Calorimetric methods may be broadly classed as direct calorimetry and indirect calorimetry. Through direct calorimetry sensible and latent heat transferred to the environment is measured directly. Sensible heat can be measured by an increase in the ventilating air temperature (respiration calorimetry) or by a temperature difference in the walls (gradient layer calorimetry) as described by Benzinger (1958). The radiant component of sensible heat may be measured by directional radiometric measurement which is integrated over the subject surface, or by a 4π radiometer measuring the radiation to the calorimeter walls. Latent heat is measured with air-moisture sensing elements or by measurement of the heat of condensing water vapor.

Indirect calormetry, which is based on heat liberation in chemical reactions by concentrations of reactants, requires measurement of oxygen and carbon dioxide

concentrations and often methane or fecal nitrogenous compounds. A method often used with poultry which requires the measurement of oxygen and carbon dioxide was developed by Romijn and Lokhorst (1961). They calculated heat production by the equation

$$T = 3.871\ O_2 + 1.194\ CO_2 \qquad (2.11)$$

where:

T = heat production in Kcal

O_2 = oxygen consumption in liters

CO_2 = carbon dioxide production in liters

The indirect calorimetry method is used for the measurement of heat production in small birds (Dawson and Evans, 1957) and more recently has been used for broiler chicks by Beattie and Freeman (1962)

Indirect calorimetry will not distinguish between the various modes of heat transfer. Thus, only total heat production is determined.

Ota and McNally (1961), in some of the earlier direct respiration calorimeter research, studied total body sensible and latent heat production from caged White Leghorn and Rhode Island Red hens in full production. Some of their results are illustrated in Figure 2.2.

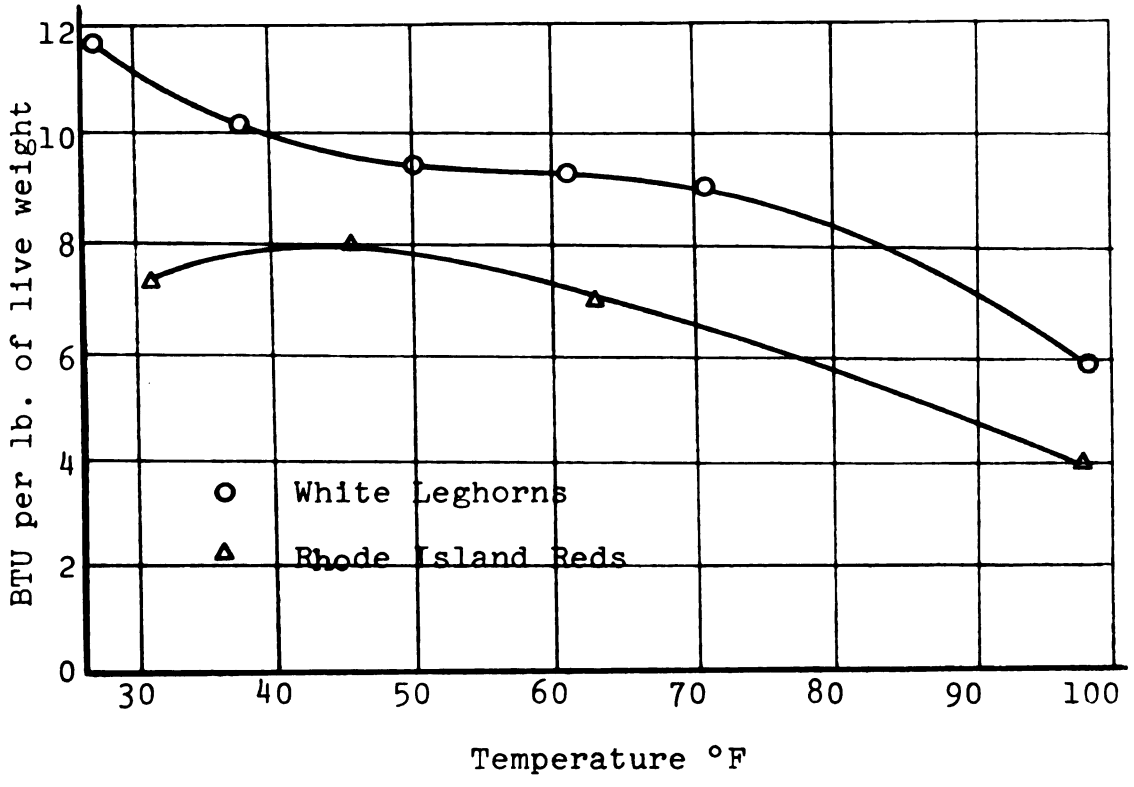

Figure 2.2-- Total heat produced by caged layers per hour per pound of body weight at different temperatures

More recently Longhouse, Ota, Emerson, and Heishman (1967), using a similar calorimeter, developed regression equations for total body latent, sensible, and total heat production of broilers as a function of average live weight for several ambient temperatures. As an example, heat production equations for an ambient temperature of 77° ± 2°F are

$$H_T = 22.68 - 5.24\ x \qquad (2.12)$$

$$H_L = 4.89 - 1.07\ x \qquad (2.13)$$

$$H_S = 17.95 - 4.30\ x \qquad (2.14)$$

where:

H_T = total heat production, BTU/hr/lb live weight

H_L = total latent heat production, BTU/hr/lb live weight

H_S = total sensible heat production, BTU/hr/lb live weight

x = average live weight, lb/bird

Sensible heat loss partitioning from Leghorn layers was further studied by Roller and Dale (1962) in a gradient layer calorimeter constructed at Purdue University. Based upon calorimeter tests of twenty-seven birds (one bird for each test), they developed the following equations by linear multiple regression analysis

$$Y_1 = 19.0-.374X_1+0.0106X_2+3.06X_3+0.298X_4 \quad (2.15)$$

where:

Y_1 = total heat production, BTU/hr

X_1 = dry-bulb temperature, °F

X_2 = bird weight, gms

X_3 = feed consumption, gm/hr

X_4 = dew-point temperature, °F

$$Y_2 = -0.780+.0158X_1+ 0.000117X_2-0.00792X_4 \quad (2.16)$$

$$Y_3 = +1.780-.0158X_1-0.000117X_2+0.00792X_4 \quad (2.17)$$

$$Y_4 = +0.793-.00653X_1-0.0000592X_2+0.00239X_4 \quad (2.18)$$

$$Y_5 = +0.989-.00929X_1-0.0000575X_2+0.00554X_4 \quad (2.19)$$

where:

Y_2 = fraction of Y_1 dissipated as latent heat

Y_3 = fraction of Y_1 dissipated as sensible heat

Y_4 = fraction of Y_1 dissipated as radiant heat

Y_5 = fraction of Y_1 dissipated as convection heat

X's are the same as above

Other researchers using a gradient layer calorimeter at North Carolina State University studied the effect of acclimation upon the partitioning of heat loss by the laying hen (DeShazer, Jordan, and Suggs, 1968). Their results indicate hens lower their evaporative heat loss after eleven weeks of acclimation at 95°F (see Figure 2.3).

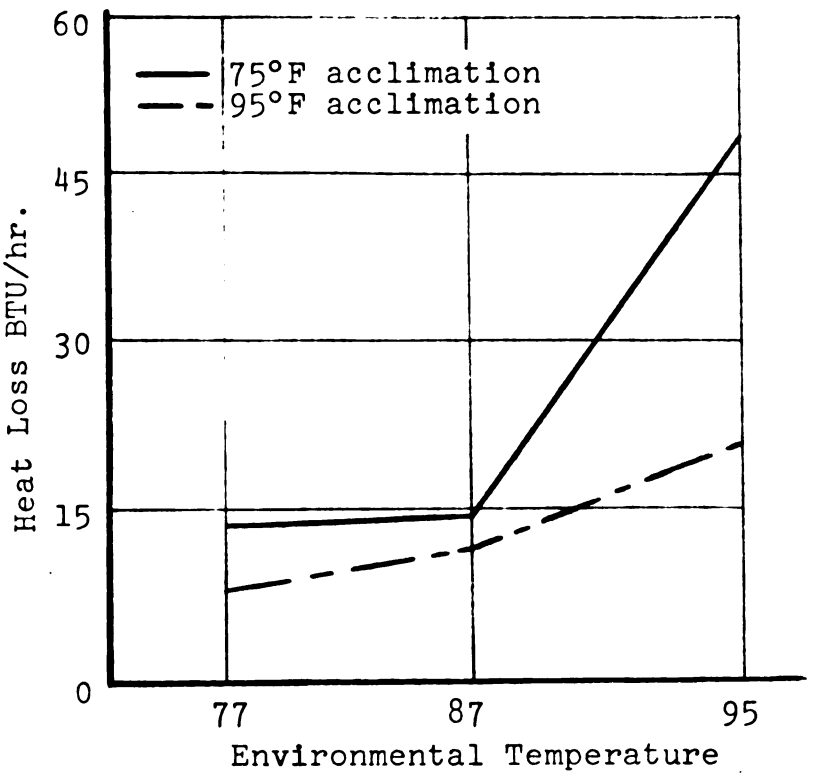

Figure 2.3-- Evaporative heat loss of White Leghorn hens in a standing position after eleven weeks of acclimation to a 75°F or a 95°F environment

Later work by DeShazer, Mather and Jordan (1969), using the same gradient layer calorimeter, showed a standing White Leghorn hen lost heat 40% faster than while sitting. Standing with wings in a 'fully drooped' position caused an increase in convective heat loss of 18%, while radiative heat loss remained fairly constant. Placing the head and neck against the breast caused a 6% decrease in radiative heat loss. However, ruffling the feathers resulted in a small increase in radiative heat loss.

At the University of Missouri, Malhotra (1967), using another gradient layer calorimeter, developed regression equations for the partitioned heat loss from broad breasted Bronze turkeys similar to the equations by Roller and Dale (1962).

However, there has been no attempt to separate respiratory moisture and heat loss from external body moisture and heat loss in calorimetry studies to date. Rather, total body heat and moisture losses have been determined and the total moisture loss is assumed to originate from the respiratory tract. According to Sturkie (1965) and a recent study of insensible heat loss from sheep (Brown and Shanklin, 1969), this may not be a true assumption.

2.2b Respiratory heat loss

The only two-compartment calorimeter study of respiratory moisture (latent heat) loss found in the literature for an avian specie was by Kendeigh (1934). He enclosed the

head of an English sparrow in a ventilated chamber and measured the amount of moisture added to the air at various air temperatures. He was then able to separate the moisture loss from the respiratory tract (and to a small extent from the skin of the head) from that given off from the remainder of the body. The amounts of moisture lost from the head in two-hour periods, at different air temperatures were

Air Temperature (°C)	Weight Loss (g)
0.6	0.154
5.6	0.141
20.0	0.156
27.2	0.181
31.7	0.581
36.1	0.823

Kendeigh, unfortunately, did not publish the evaporative loss from the remaining parts of the body.

Enclosing the head in a ventilated chamber is one method of separating respiratory heat loss, another would be a type of face mask. Though none has been used for the chicken, Tucker (1969) has developed a plastic head mask for gulls and parakeets in his studies of flight metabolism. The mask is held on by a rubber band. Air is allowed to enter between the tabs used to anchor the rubber band. A vacuum pump draws gases from the mask through a small tube while a smaller pump samples the flow continuously for the oxygen and carbon dioxide analyzers. Another type of face mask was developed by Cohn and Shannon (1968) for unanesthetized geese in their study of pulmonary gas exchange. With

a number of adaptive changes a mask system might be used for respiratory heat transfer research with chickens and other fowl.

Respiratory masks have met with varying success in other animal studies. Morrison, Bond, and Heitman (1966), studying lung moisture loss from swine, found their mask caused unnatural breathing. Respiration was lower and per breath volume higher with the mask. Brown and Shanklin (1969), studying the respiratory fraction of total insensible heat loss from shorn and unshorn sheep, reported no adverse effects from the respiration mask that they used.

2.3 Avian Respiratory System

The avian respiratory system is composed of the nasal cavities, pharynx, trachea, syrinx, primary bronchi, lungs, nine air sacs, and a number of pneumatic bones. The lungs, which are small, are attached to the ribs of the thorax. They are flow-through lungs with air passages leading to and from them. The avian lungs are incapable of the elastic recoil characteristics of mammalian lungs (Sturkie, 1965).

Exposed to a thermal neutral environment, a chicken's respiration rate will be about thirty-seven breaths per minute with a tidal volume of 15.4 ml and a minute volume of 554 ml (Weiss, Frankel, and Hollands, 1962).

2.3a Mechanics of respiration

Inspiration in the standing domestic fowl is a passive action with the weight of the viscera moving the sternum and sternal ribs downward and slightly forward. The lungs are thus expanded on inspiration by the pull of the ribs and sternum, while the vertical diameter of the thorax increases greatly and the transverse diameter only slightly (Soum, 1896).

Expiration is the active part of the respiratory cycle in the domestic fowl. The first phase of expiration is due primarily to the elastic recoil of the thoracic cage, aided by the passive tension of the abdominal wall. In the second phase, as confirmed electromyographically, the abdominal muscles, which begin to contract during the first phase, contract actively returning the thorax to its original position (Fedde, Burger, and Kitchell, 1963).

Because of the mechanics of respiration in avian species, Salt and Zeuthen (1960) and King and Payne (1962) emphasize the importance of the upright position of the bird for studying normal respiratory behavior.

2.3b Air flow in the respiratory system

The path air takes after entering the nose or mouth down through the trachea and two primary bronchi in respiration is well understood. However, its path through the lungs and air sacs during inspiration and expiration is open to much conjecture (Salt and Zeuthen, 1960; Vos, 1934;

Hazelhoff, 1951; and Shepard, 1959). There seems to be the most support for Salt and Zeuthen's (1960) theory of reciprocal flow, with the air sacs acting as bellows.

Salt and Zeuthen (1960) speculate that the majority (80%) of the inspired air goes to the abdominal sac and does so via its indirect connections to the primary bronchus. This route offers much less flow resistance than down the smaller primary bronchus. The air sacs are expanded and compressed by the movement of the sternum like bellows and serve to force air in and out through the lung passages. Of the inspired air, 29-48% traverses the parabronchi (gas exchange surfaces) of the lung. During expiration, the direction of flow is reversed with 38-67% of the air from the air sacs traversing the parabronchi. Aerodynamic forces and parabronchial muscle control of the passage diameters are assumed to determine the amount of parabronchial air flow.

2.4 Respiratory Evaporation

In most animals the respiratory surface must be moist for gas exchange to take place. Consequently, water evaporation and related heat loss are going on continuously as a by-product of respiration. In many birds, this process of evaporative loss is controlled, within limits, for the purpose of heat regulation (Salt and Zeuthen, 1960).

As air temperatures increase, the absolute amount of water evaporated per unit time from a bird's respiratory tract increases more or less exponentially (Dawson, 1954). The curve appears to be smooth, but Dawson (1958) showed an abrupt increase in the rate of evaporation at the upper critical temperature in the cardinal. DeShazer, Jordan and Suggs (1968) demonstrated a similar increase in evaporative loss at the onset of panting in the White Leghorn fowl. As air temperatures increase, the relative importance of evaporative heat loss increases. At air temperatures near or above the avian body temperature, evaporation is the only mode of heat loss. Even then it accounts for approximately half the heat produced, so the body temperature rises (King and Farner, 1961). While this rise may be inadvertent, it has the beneficial effect of increasing the rate of heat loss and tends to temporarily restore the heat balance. It also represents heat storage in the body. The water that would be required to dissipate this stored heat through vaporization is a savings to the bird (Hutchinson, 1954).

The rate of respiratory evaporation is influenced by internal and external factors. In addition, there are differences between species. Internally, evaporation varies directly with the volume of air ventilated. When air temperatures rise above the upper limit of the thermoneutral zone in domestic fowl, respiration rate increases and tidal volume decreases slightly. The result is an increase in minute volume. The reduction in tidal volume is thought to

restrict hyperventilation to the surfaces of the respiratory tract, which do not participate in the exchange of blood gases. Thus, it reduces the possibility for the removal of excessive amounts of carbon dioxide from the blood (Sturkie, 1965). At higher air temperatures, heat loss efficiency may be further increased by panting or gular (throat) flutterings. Panting is the more important route in the domestic fowl. Panting rates for White Leghorn hens have been reported as high as 247 breaths per minute at a body temperature of 45.5°C (Lee, Robinson, Yeates, and Scott, 1945).

The importance of the air sacs in evaporative loss within the respiratory system is not well understood. Soum (1896) found fifteen to thirty percent less exhaled water vapor after the air sacs had been destroyed. However, most of this decrease was due to the decreased intake of air (tidal volume) following the operation. After inactivating several of the air sacs of two pigeons and stressing the birds, Victorow (1909) observed an approximately 2°C greater rise in body temperature than the control birds. With the small number of birds, however, these results are not very conclusive. In more recent work by Sturkie (1965) using chickens with destroyed air sacs, there was no change in body temperature that could be attributed to the removed air sacs.

The air sac walls have a small capillary supply, but

are so thin that peritoneal fluid can diffuse through them. The wall consists of a layer of endodermal epithelium, a thin layer of connective tissue, and a layer of serosal epithelium (Biester and Schwarte, 1965). If moisture moves through the air sac wall by diffusion, the humidity of the air in the air sac will be a limiting factor. A determination either theoretically or experimentally, of the humidity in the air sacs was not found in the literature. Under normal breathing, it is usually assumed to be at saturation for deep body temperature.

By comparison, the upper part of the respiratory tract (mainly the nasal passages, mouth, and trachea) has a rich capillary supply and is coated with epithelium cells and mucous secreting goblet glands (Bang and Bang, 1959; and Marshall, 1960). There is an additional moisture supply in the mouth from the tubular salivary glands.

Some work has been reported that develops a theoretical basis for calculations on evaporative cooling in birds. Hutchinson (1955) developed the following equation based on Dalton's Law.

$$E = C\, f(V)\, (ps-pa) \qquad (2.20)$$

where:

E = rate of evaporation

C = constant

f(V) = a function of respiratory ventilation

ps = vapor pressure of saturated air at the temperature of the evaporative surface

pa = vapor pressure of ambient air

Hutchinson, in his experiments, made several assumptions: 1) that in slow breathing the expired air is probably nearly saturated at the temperature of the respiratory passages; 2) that during panting the expired air is probably not saturated; 3) that the rate of evaporation is a function of the ventilation rate; and 4) that the salt content of the fluid covering the respiratory surfaces is so low that its vapor pressure is essentially the same as that of pure water.

He demonstrated that in Brown Leghorn hens, when rectal temperature and respiration rate are constant, the rate of respiratory evaporation is proportional to the vapor pressure gradient between the evaporating surface and the inspired air. He also found a close correlation between rate of evaporation and rectal temperature, and thus estimated that the actual temperature of the evaporating surface in the respiratory system was two to four degrees Fahrenheit lower than rectal temperature.

In a more recent study Bouchillon, Reece, and Deaton (1969) expressed the evaporative water loss from the chicken as

$$\dot{m} = \rho_A V_T N_R (V_2 - V_1) \qquad (2.21)$$

where:

$\dot{m}$ = mass rate of flow of water, lbm/hr

ρ_A = density of air, lbm/ft^3

V_T = tidal volume, ft^3

N_R = respiration rate, cycles/min

V_2 = specific humidity of air at chicken body conditions, lbm/lbm

V_1 = specific humidity of ambient air, lbm/lbm

This equation is based on the assumption of a pseudo-steady state condition where the air entering the lungs is at existing ambient conditions and the air leaving is at chicken body temperature and saturated moisture conditions.

An absence of research related to the location of the heat and moisture transfer in the chicken's respiratory system has been found. There has also been no research attempts (with the chicken) to separate respiratory heat and moisture loss from external body surface heat and moisture loss in direct calorimeter chambers.

3. ANALYTICAL CONSIDERATIONS

3.1 Heat Production in the Calorimeter

Sensible and latent heat production in the calorimeter head chamber and body chamber are based on the following variables

1. the difference between the average inlet and outlet air temperature
2. the difference between the average inlet and outlet humidity
3. the average volume flow rate of air

Heat production was calculated by the following equations

$$QS = (E_2 - E_1) \times 60. \times cfm/V_s \quad (3.1)$$

$$QL = (W_2 - W_1) \times 1040.1 \times 60. \times cfm/V_s \quad (3.2)$$

where:

QS = sensible heat production, BTU/hr

QL = latent heat production, BTU/hr

E_2 = enthalpy at outlet conditions, BTU/lb air

E_1 = enthalpy at inlet conditions, BTU/lb air

W_2 = humidity ratio at outlet conditions, lb H_2O/lb air

W_1 = humidity ratio at inlet conditions, lb H_2O/lb air

cfm = average volume flow rate of air, ft^3/min

V_s = specific volume of air, ft^3/lb

The development of the heat production equations will begin with the two known quantities of dry-bulb temperature and relative humidity. Assuming atmospheric pressure, the saturation pressure at a known dry-bulb temperature is given in the steam tables. Between 70 and 110°F, this relationship can be approximated by the following polynomial

$$P_s = a + bT_d + cT_d^2 + dT_d^3 \qquad (3.3)$$

where:

P_s = saturation pressure at T_d, lb/in^2

T_d = dry-bulb temperature, °F

a = -.430686

b = .209578 x 10^{-1}

c = -.291182 x 10^{-3}

d = .219653 x 10^{-5}

Knowing the relative humidity, vapor pressure may be solved directly by

$$P_v = RH \times P_s \qquad (3.4)$$

where:

P_v = vapor pressure, lb/in^2

RH = relative humidity

P_s = saturation pressure, lb/in^2

The humidity ratio is then determined (Brooker, 1966) by

$$W = \frac{R_a}{R_{wv}} \left[\frac{P_v}{P_{atm} - P_v} \right] \qquad (3.5)$$

where:

W = humidity ratio, lb water/lb air

R_a = gas constant for air, (53.35)

R_{wv} = gas constant for water vapor, (87.78)

P_v = vapor pressure, lb/in^2

P_{atm} = atmospheric pressure, lb/in^2

Enthalpy of the air may then be determined according to Jennings and Lewis (1944, p. 47) as

$$E = C_p \times T_d + W \times (1059.2 + .45 \times T_d) \qquad (3.6)$$

where:

E = enthalpy of air, BTU/lb air

C_p = specific heat of air, BTU/lb °F

T_d = dry-bulb temperature, °F

W = humidity ratio

The solution for latent and sensible heat production is then found by substituting the results of equation 3.6 and 3.5 into equation 3.1 and 3.2. A fortran IV program using this method to calculate latent and sensible heat production from the calorimeter data is shown in Appendix A.6.

The conduction heat transfer through the walls of the head chamber and body chamber is calculated by the following equation (A fortran IV program is at Appendix A.7)

$$Q_{cd} = A_s \times H/DX \times (T_1 - T_2) \qquad (3.7)$$

where:

Q_{cd} = conduction heat transfer, BTU/hr

A_s = surface area of the chamber, in^2

H = thermal conductivity of plexaglass, BTU/hr in °F

DX = thickness of the plexaglass, in

T_1 = inside wall temperature, °F

T_2 = outside wall temperature, °F

The conductive surface areas of the head chamber and body chamber are 20 and 300 square inches, respectively.

Convection heat transfer from the comb and wattle is computed by the following equation

$$Q_{cv} = \bar{h} A (T_w - T_a) \quad (3.8)$$

where:

Q_{cv} = convective heat transfer, BTU/hr

$\bar{h}$ = average heat transfer coefficient, BTU/ft^2°F hr

A = convective surface area of the comb or wattles, ft^2

T_w = average surface temperature of the comb or wattle, °F

T_a = average air temperature in the head chamber, °F

The average heat transfer coefficient ($\bar{h}$) for the comb and wattle is estimated by a flat plate flow analogy. Since the air flow is laminar the estimation equation according to Kreith (1965; p. 296) is

$$\bar{h} = K/B \times 0.664 \, Re^{1/2} \, Pr^{1/3} \quad (3.9)$$

where:

K = air conductivity, BTU/hr ft °F

B = characteristic length in the direction of air flow, ft

Re = Reynolds number

Pr = Prandtl number

The Reynolds number is calculated using measured air velocities in the head chamber about 3/8 inch from the surface of the comb and wattle. The surface dimensions of the comb and wattle are also used in the calculations as

$$Re = VB/\gamma$$

where:

V = average velocity outside the boundary layer, ft/sec

B = characteristic length in the direction of air flow, ft

γ = kinematic viscosity of air, ft^2/sec

Because the other areas in the head and neck region are generally covered with feathers and are well insulated, sensible heat loss is primarily from the comb, wattles, and respiratory tract. There is also a small amount of sensible heat produced from the parts of the face not covered by feathers. The facial heat production, however, was negligable in comparison to that produced by the comb and wattle.

With this understanding, sensible heat loss from the respiratory tract is calculated by adding sensible heat loss from the head chamber (equation 3.1) to the conduction loss through the head chamber walls (equation 3.7) and subtracting the convective heat loss from the comb and wattles (equation 3.8).

The latent heat from the head chamber is assumed to originate entirely from the respiratory tract. Due to the very small amount of moisture transfer from the eye area (the only other important wet surface in the head chamber), this seems to be a reliable assumption.

3.2 Estimation of Tidal Volume

The air expired from the chicken's nose in normal breathing is approximately at 104°F and saturated. Latent heat production in the head chamber is known by earlier calculation and is assumed to be entirely from the respiratory system. If the respiration rate is known, then tidal volume may be estimated by the following equation

$$TV = \frac{Q_L \times V_S}{RR \times 60. \times 1040.1 \times (W_2 - W_1)} \qquad (3.10)$$

where:

TV = tidal volume, ft^3

Q_L = latent heat production, BTU/hr

V_S = specific volume of air, ft^3/lb

RR = respiration rate, breaths/min

W_2 = humidity ratio at exhaled conditions, lb water/lb air

W_1 = humidity ratio at inhaled conditions, lb water/lb air

This is an indirect method for determining tidal volume, but from an instrument and procedure stand-point it was the most direct in this study.

3.3 Heat and Mass Transfer Model of the Respiratory System

The simulation model is composed of three parts: 1) the nasal model, 2) the nasal to tracheal model, and 3) the tracheal model. All three are similar in structure and have the same energy and mass balance equations.

In order to obtain theoretical equations describing respiratory air temperature and humidity as a function of position in the system, heat and moisture balances are written for a small elemental air volume. In writing the equations, the following assumptions are made.

1) Thermal properties of the air are constant within the temperature range studied.
2) Moisture transfer from the wetted surfaces of the respiratory tract occurs at a constant rate.
3) Respiratory wall temperature is a linear function of position.
4) The inlet air temperature and specific humidity are constant.
5) Air velocity may be described as a constant mean air velocity based on cross-sectional area and known tidal volume.
6) The storage of energy and moisture within the air volume with respect to time is negligible.

The results from the simulation model indicate that these are reliable assumptions for the temperature and humidity conditions of this study. Assumptions 5 and 6 are probably the most questionable of the group. For this reason an order of magnitude analysis of the transient term was investigated as shown in section 3.3a. The results indicating that both assumption 5 and 6 are acceptable.

The finite difference equations describing the cooling of the respiratory tract are obtained by writing mass and energy balances on an elemental air volume of length Δx. A set of three equations is the result.

For the energy in the air (see Appendix A.1 for details)

$$\dot{m} C_a \frac{\partial T_a}{\partial \theta} = Ph (T_w - T_a) \qquad (3.11)$$

by separating variables and integrating

$$T_{i+1} = T_w + (T_i - T_w) e^{-\frac{hP\Delta x}{\dot{m}C_a}} \qquad (3.12)$$

where:

$\dot{m}$ = mass flow of air, lb/hr

C_a = specific heat of air, BTU/lb °F

h = convective heat transfer coef., BTU/hr ft^2 °F

P = perimeter, ft

T_i = inlet temperature of elemental volume, °F

T_{i+1} = outlet temperature of elemental volume, °F

T_w = wall temperature, °F

Δx = length of elemental volume, ft

For the mass of the air (see Appendix A.3)

$$\dot{m} \frac{\partial H_a}{\partial x} = P\sigma \, (H^1 - H_a) \tag{3.13}$$

byseparating variables and integrating

$$H_{a_{i+1}} = H^1 + (H_{a_i} - H^1) \, e^{-\frac{\sigma P \Delta x}{\dot{m}}} \tag{3.14}$$

where:

σ = mass transfer coefficient, lb water/hr ft H

H_{a_i} = specific humidity of air at inlet to elemental volume, lb water/lb air

$H_{a_{i+1}}$ = specific humidity of air at outlet from elemental volume, lb water/lb air

In equation 3.14, H^1 and T_w can be obtained from the thermodynamic tables. Between 70 and 110 °F, this relationship can be approximated by the following polynomial

$$H^1 = -4.80741 \times 10^{-3} + 4.21112 \times 10^{-4} \, T_w - 7.42738 \times 10^{-6} \, T_w^2 + 8.01429 \times 10^{-8} \, T_w^3 \tag{3.15}$$

For the wall temperature

Wall temperatures were determined experimentally at four locations in the respiratory tract. These locations are

1) inlet to nose on the beak (T_{c_1})
2) outlet of nasal passage into the mouth (T_{c_2})
3) top of the trachea (T_{c_3})
4) bottom of the trachea (T_{c_4})

Between these points the temperature is assumed to vary linearly with distance. In the nasal passage-ways for example

$$T_w = T_{c_1} + C_1 x \tag{3.16}$$

where:

$$C_1 = \frac{T_{c_1} - T_{c_2}}{L}$$

L = 1 inch for the nose

Similar equations are developed for the wall temperature between the other experimentally measured temperatures.

During expiration equation 3.11 is altered to account for moisture condensation from the expired air to the respiratory tract walls. The derivation of this equation is in Appendix A.2. It is written as

$$\dot{m} C_a \frac{\partial T_a}{\partial x} = Ph (T_w - T_a) - 1060 (H_a - H^1) \tag{3.17}$$

by separating variables and integrating

$$T_{i+1} = T_w + (T_i - T_w) e^{\left(- \frac{Ph\Delta x}{\dot{m}C_a} + \frac{\sigma\rho 1060(H_a - H^1)\Delta x}{\dot{m}C_a (T_w - T_i)} \right)} \tag{3.18}$$

The heat transfer coefficient used in the simulation was based on the equation for the Nusselt number given by Rohsenow and Choi (1961, p. 141)

$$Nu = \frac{hD}{K} \tag{3.19}$$

where:

Nu = Nusselt number

K = thermal conductivity of air, BTU/hr ft °F

D = diameter, ft

Since thermoneutral air flow in the respiratory system is always laminar and the wall temperature is close to uniform, the Nusselt number for tube flow is a constant and equal to 3.66. Knowing the Nusselt number, the heat transfer coefficient can be determined from equation 3.19.

The mass transfer coefficient was determined from the equation for the Sherwood number given by Treybol (1968).

$$Sh = \frac{FD}{CD_{AB}} \tag{3.20}$$

where:

Sh = Sherwood number

F = mass transfer coefficient, lb moles/hr ft^2

D = diameter, ft

C = molar density, lb moles/ft^3

D_{AB} = molecular diffusivity, ft^2/hr

During normal respiration the air flow in the respiratory system is laminar and the Reynolds number is less than 1000. At these air flow conditions the Sherwood number is approximately constant and equal to 3.41. Equation 3.20 may then be solved for the mass transfer coefficient.

Equations 3.11, 3.14, and 3.16 are the working equations for calculating air temperatures and air specific humidities throughout the respiratory model during inspiration.

Equation 3.18 replaces 3.12 for expiration calculations. A fortran IV program using these equations was developed to calculate air temperatures and air specific humidities in the respiratory system during one breathing cycle. It is shown in Appendix A.9. This program has graphical as well as numerical output of air temperature and specific humidity as a function of location.

3.3a Analysis of the transient term

The importance of the transient term was investigated by an order of magnitude analysis. The general energy balance equation from Appendix A.1 is

$$-\frac{\partial}{\partial x}(\rho_a V_a A T_a C_a)dx + h(dxP)(T_w - T_a) = \rho_a C_a (Adx)\frac{\partial Ta}{\partial t} \quad (3.21)$$

where:

ρ_a = density of air, lb/ft^3

V_a = velocity of air, ft/hr

A = cross-sectional area, ft^2

T_a = air temperature, °F

C_a = specific heat of air, $BTU/ft^2hr\ °F$

h = convective heat transfer coef., $BTU/ft^2hr\ °F$

P = perimeter, ft

T_w = wall temperature, °F

x = length, ft

t = time, hr

The following substitutions are made into equation 3.21 to establish dimensionless coefficients.

$$x^+ = \frac{x}{L}$$

$$V^+ = \frac{\rho_a V_{a(max)} A C_a}{hPL}$$

$$t^+ = \frac{t}{t_c}$$

$$T^+ = \frac{\rho_a C_a A}{h P t_c}$$

where:

L = total length of passage, ft

t_c = period of one breath, hr

Substituting these values into equation 3.21

$$(T_w - T_a) - V^+ f(t) \frac{\partial Ta}{\partial x^+} = T^+ \frac{\partial Ta}{\partial t^+} \qquad (3.22)$$

To determine V^+ and T^+ representative values from the nasal model are used since the largest temperature gradients occur in this region of the respiratory tract.

$$V^+ = \frac{.07\ (112)\ (60)\ \left(2\pi \frac{(.2)^2}{4} \frac{1}{144}\right)\ (.24)}{4\ \left(\frac{2 \times 1.75}{12}\right) \frac{1}{12}} = .52$$

$$T^+ = \frac{.07\ (.24)\ \left(2\pi \frac{(.2)^2}{4} \frac{1}{144}\right)}{4\ \left(\frac{2 \times 1.75}{12}\right) \frac{2}{3600}} = .013$$

For the remaining quantities in equation 3.22, the following orders of magnitude could be expected

$T_w - T_a$ . . . . . 3 to 25 °F

$\frac{\partial T_a}{\partial x^+}$ . . . . . 6 to 60 °F

$\frac{\partial T_a}{\partial t^+}$ . . . . . 3 to 25 °F

Since V^+ is approximately fifty times as large as T^+ and the other terms in equation 3.21 are of approximately equal magnitudes, the transient term does not seem important during normal respiration. If respiration rate increased and velocity remained constant, then the transient term would be of greater importance.

A similar analysis can be done with the mass balance equation. From Appendix A.3, the general air mass balance equation is

$$\sigma P (H - H_a) - V_a \rho_a A \frac{\partial H_a}{\partial x} = \rho_a A \frac{\partial H_a}{\partial t} \qquad (3.23)$$

where:

σ = mass transfer coefficient, lb water/hr ft$^2\Delta$H

P = perimeter, ft

H^1 = specific humidity in the boundary layer, lb water/lb air

H_a = specific humidity of the air, lb water/lb air

V_a = velocity of the air, ft/hr

ρ_a = density of the air, lb/ft^3

A = cross-sectional area of passage, ft^2

x = distance, ft

t = time

let:

$$x^+ = \frac{x}{L}$$

$$W^+ = \frac{V_{a(max)}\ \rho_a\ A}{\sigma\ P\ L}$$

$$t^+ = \frac{t}{t_c}$$

$$Z^+ = \frac{\rho_a\ A}{\sigma P\ t_c}$$

where:

L = total length of passage, ft

t_c = period of one breath, hr

Making these substitutions into equation 3.23 to establish dimensionless coefficients

$$(H^1-H_a) - W^+ f(t) \frac{\partial Ha}{\partial x^+} = Z^+ \frac{\partial Ha}{\partial t^+} \qquad (3.24)$$

Again representative values for the nasal passages are used to calculate W^+ and Z^+.

$$W^+ = \frac{.07\ (112)\ (60)\ \left(2\pi\ \frac{(.2)^2}{4}\ \frac{1}{144}\right)}{6\left(\frac{2 \times 1.75}{12}\right)\left(\frac{1}{12}\right)} = 1.445$$

$$Z^+ = \frac{.07\ \left(2\pi\ \frac{(.2)^2}{4}\ \frac{1}{144}\right)}{6\left(\frac{2 \times 1.75}{12}\right)\frac{2}{3600}} = .036$$

For the remaining quantities in equation 3.24, the following orders of magnitude could be expected

$H^1 - H_a$ . . . . . .001 to .03

$\frac{\partial H_a}{\partial x^+}$ . . . . . .001 to .03

$\frac{\partial H_a}{\partial t^+}$ . . . . . .002 to .03

The results show W^+ is approximately fifty times greater than Z^+. Since the other terms in equation 3.24 are of about the same order of magnitude, this would indicate that the transient term in equation 3.24 can be neglected during normal respiration.

In equation 3.22 and 3.24, f(t) represents the sinusoidal function of velocity. It varies between zero and one for either inspiration or expiration. The average velocity is .707 times the maximum velocity. This last time dependent term in the general equation is eliminated by letting the average velocity represent the time dependent velocity function during each phase of the respiration cycle.

This seems like a reliable assumption, since the largest air temperature and humidity variations are between inspiration and this variation was found to be insignificant above. Therefore, the temperature and humidity variations during one half cycle due to velocity changes would tend to be less significant.

The transient effects were further studied by measuring air temperature continuously at two points in the respiratory system with a 40-gauge thermocouple sensor (time constant of 1.14 seconds, with h = 10 BTU/hr ft^2°F). The bird's respiration rate averaged 29 breaths per minute. The maximum recorded change in temperature with time in the anterior nasal passage was 12 °F. In the mouth cavity the maximum temperature change was only 3°F.

This again indicates the anterior portion of the nasal passages experience the greatest temperature variation. The temperature variation with time, however, is much smaller throughout the rest of the respiratory system, as indicated by the maximum temperature change in the mouth.

3.3b Structure of the respiratory system

From the diagrams of a chicken's nasal cavities by Bang and Bang (1959), the cross-sectional area is approximated to be .0314 square inches for each of the two passageways. The perimeter is about 1.75 inches. The effective diameter for calculating the heat transfer coefficient is .1 inch, and the nasal passageways are about one inch long, based on measurements with White Leghorn hens.

With the beak closed, the mouth cavity between the posterior nasal opening and the anterior trachea opening is similar to a slightly flattened cylinder in shape. The average cross-sectional area and perimeter being .0707

square inches and .942 inches. The length of the mouth cavity is also about one inch.

The trachea is essentially a tube approximately six inches long and .15 inches in inside diameter (Bradley and Grahame, 1960). It is circular in cross-section and uniform in diameter. This is primarily due to the many cartilaginous rings which give rigid support to walls of the trachea and prevent collapse. The trachea branches into two mesobronchi just prior to entering the lungs. However, the similation model only includes the trachea.

The sufaces of the nasal passages and trachea are coated with columnar epithelium of the mucoid and ciliated type. The mouth is lined with stratified squamous epithelium and tubular salivary glands (Sturkie, 1965). Because of these structures, the respiratory tract is capable of maintaining a layer of moisture on the wall surfaces, and is the basis for the assumption of a constant rate of moisture transfer in the simulation model.

Rich capillary beds throughout the walls of the respiratory tract act as a heat source as well as a source of nutrients. Homoethermic controls and the heat capacity of the tissue masses near the respiratory tract tend to maintain wall temperatures at a constant level. Areas nearer the mass center of the bird are maintained at a higher temperature. The simulation model uses a linear approximation

of this phenomena, but assumes the temperature at any one point on the respiratory tract wall to be constant.

4. EXPERIMENTAL PROCEDURE AND EQUIPMENT

4.1 Calorimeter Chamber

The calorimeter chamber was constructed with an inner plexaglass chamber (in which the bird was positioned) and an outer insulated box with observation windows. Air, at controlled temperature and humidity conditions, was supplied to the calorimeter by an Aminco-Aire unit. An overall view of the calorimeter and the Aminco-Aire unit is shown in Figure 4.1.

The inner chamber was constructed of 3/16 inch plexaglass with separate areas for the head and body of the chicken. These will be referred to as the head chamber and the body chamber (Figures 4.6 and 4.7). Air flow through the head chamber, body chamber, and air space outside the inner chamber is shown in Figure 4.5. All air flows were controlled with sliding plexglass valves. Their location is shown in Figure 4.5 also.

The outer insulated box was constructed of one-half inch plywood and two-inch Dow Styrofoam (Figure 4.2). All observation windows were double pane 3/16 inch plexaglass. The four-inch diameter flexible tubing and two-inch diameter plexaglass tubing used in connecting the Aminco-Aire unit to

Figure 4.1-- Calorimeter chamber

Figure 4.2-- Inner chamber

Figure 4.3-- Calorimeter recording instruments

Figure 4.4-- Fifty-inch inclined manometer

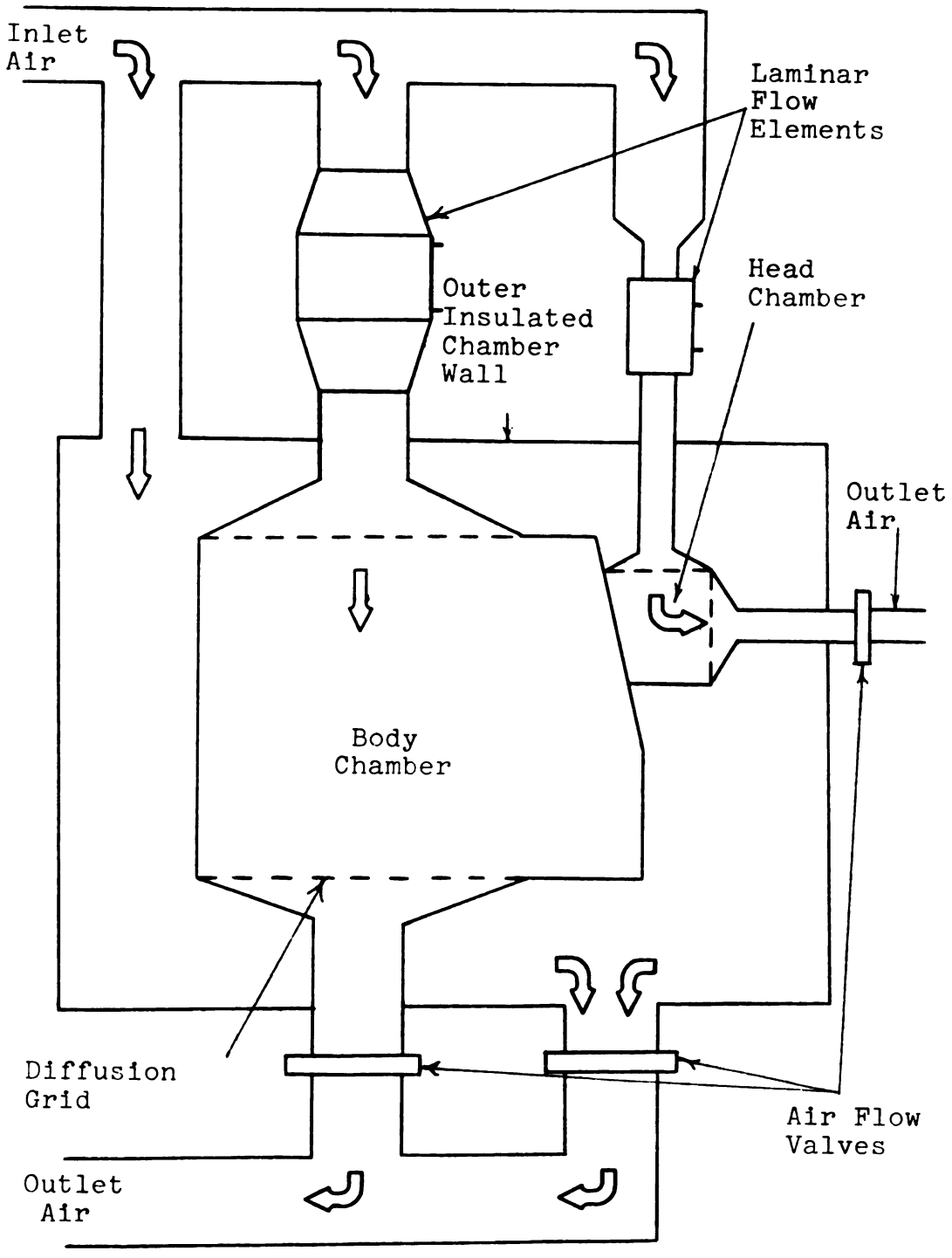

Figure 4.5-- Air Flow Through the Calorimeter

the calorimeter were covered with one-half inch armaflex insulation.

4.1a Temperature measurement

Mean air temperatures and surface temperatures in the calorimeter were measured with fourteen 24-grauge copper-constantan thermocouples. A 24-gauge copper-constantan thermocouple was also used for the silastic coated rectal temperature probe. Thirty-gauge copper-constantan wire was used for the comb and wattle thermocouples. Thermocouple locations are listed in Table 4.1.

Two temperature profiles, perpendicular to the flow of air and perpendicular to each other, were measured at each air inlet and outlet. The inlet profiles were parabolic in form, and the outlet profiles were flat in form. In both cases, the thermocouples were located approximately half-way between the wall and the center line of flow.

Heat conduction through the walls of the inner plexa-glass chamber was determined by four thermocouples which represented the average temperature change through the walls of the chamber. The head chamber and the body chamber were studied separately. Each of the two chambers was divided into sections, and sample temperature changes through the walls were recorded. The heat conduction from all sections were averaged and the section closest to the mean (±.05 BTU/hr) became the thermocouple location. Heat conduction

through the walls of the body chamber were negligible in all sections. The body chamber conduction thermocouples were placed ten inches up and centered on the right wall.

Table 4.1 Thermocouple locations

1.	Outlet air temperature from the head chamber
2.	Outside right wall of the head chamber
3.	Comb
4.	Inlet air temperature to the head chamber
5.	Inside right wall of the head chamber
6.	Inlet air temperature to the head chamber
7.	Inlet air temperature to the body chamber
8.	Inlet air temperature to the body chamber
9.	Inlet air temperature to the body chamber
10.	Wattle
11.	Outlet air temperature from the body chamber
12.	Outlet air temperature from the body chamber
13.	Outside right wall of the body chamber
14.	Inside right wall of the body chamber
15.	Outlet air temperature from the body chamber
16.	Outlet air temperature from the head chamber
17.	Rectal temperature probe

The head chamber conduction thermocouples were centered on the right wall. The average temperature change through the walls of the head chamber was .2°F.

Thermocouples were also used to determine if warm or cold sports were present in the head chamber and the body chamber. This test was done without a bird in the chamber; and the temperature distribution was quite even in both chambers.

Thermocouples were attached to the comb and right wattle after a coating of Dow Corning Medical Adhesive B had been applied to the placement area. Adhesive tape was placed over the thermocouple for additional holding strength. Medical Adhesive B has the advantage of being highly inert, nonirritating, and nonsensitizing to living tissue.

Thermocouples #1-#16 were recorded on a Honeywell Type 153 Electronik sixteen-point recording potentiometer with a print speed of fifteen seconds, a temperature range of -20°F to 120°F, and an accuracy of ±.1% of full scale reading. Rectal temperature (thermocouple #17) was recorded on a Texas Instruments, Incorporated: Multi/riter, Model FMW06B, recording potentiometer with a print speed of five seconds, a temperature range of -10°F to 140°F and an accuracy of ±.25% of full scale reading

All thermocouples were calibrated against a certified mercury in glass thermometer.

4.1b Humidity measurement

Air humidities at the inlet and outlet of the body chamber were measured using two Hygrodynamics, Incorporated, wide-range hygrosensors and Model 15-3001 hygrometer indicators. These instruments have an accuracy of ±3% relative humidity, and a range of 5 to 100% relative humidity. The two hygrometer indicators used with the body chamber humidity sensors are shown in Figure 4.3.

Relative humidity at the outlet of the head chamber was monitored continuously with a Hygrodynamics Incorporated, narrow-range, type H-3, class A hygrosensor and a model 15-3001 hygrometer indicator (Figure 4.1). This instrument has a response time (to 65% of total humidity) of three seconds with an accuracy of ±1.5%, and a sensitivity of .15% relative humidity. The three sensors used had ranges of 51-74%, 68-88%, and 81-99% relative humidity at 80°F. All humidity sensing elements had individual calibration curves determined by the manufacturer.

The output from the hygrometer indicator was continuously recorded on a Esterline Angus E1101E single-point continuous recorder (Figure 4.3) with a range of zero to ten millivolts, a response time of one-half second, and an accuracy of 0.1% of full scale reading. The recorder was calibrated to the hygrometer indicator scale reading. Calibration was checked at the beginning and end of each test run.

A steady-state relative humidity reading from the head chamber outlet was recorded before and after each test run. These recordings were used as a base line for determining the change in relative humidity produced by respiration. The steady-state readings were taken before the chamber was opened to position the chicken for the test run and one-half hour after the chicken had been removed and the chamber closed.

The chickens would occasionally struggle or sleep during the test runs. This activity caused respiration moisture loss to rise or fall respectively, and was noted manually on the recorder output. These periods of struggle and sleep ('abnormal behavior') were not used in determining the average change in relative humidity. Average relative humidity during 'normal behavior' (not struggling or sleeping) in the chamber was determined by a straight line approximation of the mean. A time weighted average of the straight line approximated means was used to calculate the overall mean when 'abnormal behavior' broke up the continuity of the output.

4.1c Air flow measurement

Air flow was measured indirectly as related to pressure drop through laminar flow meters. Air flow into the body chamber was measured with a model 50MC204S Meriam laminar flow meter (200 cfm capacity at four inches of water)

connected to a fifty-five inch Meriam inclined manometer (four inches of water full scale) with an accuracy of ±.002 inches of water. Air flow measurement into the head chamber was measured with a model 50MH10-2 Meriam laminar flow meter (20 cfm capacity at four inches of water) connected to the same monometer (Figure 4.4) through a valving system with an accuracy of ±.002 inches of water. Calibration curves relating pressure drop to air flow in cfm were supplied by the manufacturer (calibration date 2/28/69). The accuracy of air flow measurement through the head and body chamber from the standpoint of cubic feet per minute was ±.01 cfm and ±.10 cfm respectively. Corrections for temperature and air pressure were based on tables provided in the flow meter manuals. Air flow readings were taken every ten minutes during the test runs.

Local air velocities in the head chamber near the comb and wattles were measured with an Alnor thermo-anemometer in order to determine the Reynolds number over these surfaces. The thermo-anemometer, type 8500K, has an air velocity range of 10 to 300 feet/minute with an accuracy of ±3% full scale. With the small fan operating at the top of the head chamber and the Aminco-Aire fan also working, the air velocities measured in the comb and wattle areas were 60 to 65 feet per minute.

4.1d Experimental procedure

Infrared radiant transmission properties through the plexaglass used in the calorimeter were investigated with a Beckman DK-24 ratio photospectrometer. The plexaglass used in the windows and inner chamber was found to transmit radiant energy only in the 340 to 2200 millimicron wavelength range. At all other wavelengths, the plexaglass exhibited zero transmitance behavior. Therefore, all long wave radiation emitted inside the head chamber, for example, would be reflected or absorbed by the plexaglass walls of the head chamber. The majority of the radiant heat production would thus be a portion of the calculated sensible heat.

Equilibrium times for the calorimeter were determined by opening the chamber for fifteen minutes (the time required to position and prepare a bird for a test run), closing the chamber, and determining the time required for the chamber temperature and humidity to reach the equilibrium condition. Humidity in the head chamber was consistently the last variable to reach equilibrium. Equilibrium time tests were done at all temperature and humidity combinations used. The maximum time for all variables to return to equilibrium was thirty minutes.

A twenty-four hour record of ambient temperature and humidity was kept while the calorimeter tests were conducted with a calibrated Bendix Corporation, Model 594 hygrothermograph.

Conduction loss from the feet to the floor of the inner chamber was also studied on several birds. A thermocouple was taped to the bottom of one toe and another to a near-by spot on the floor. The change in temperature was recorded. The heat loss was found to be negligible.

Rectal temperature was used to estimate deep body temperature. The rectal probe used was constructed of 24 gauge copper-constantan thermocouple wire inside Dow Corning Silastic Medical-Grade tubing (ID=.078; OD=.125). The ends were sealed with Silastic 382 Medical-Grade Elastomer. Attempts were made to measure the deep body temperature with a silastic covered 40 gauge copper-constantan thermocouple inserted into the jugular vein near the base of the neck and fed down near the heart. The thermocouple wire exited from the hen's body on her back between the wings. When not recording, the wire was coiled and fastened under a cloth jacket around the hen's mid-section. All four attempts failed because the hens were able to reach the coiled wire and pull at it or catch it on their cage.

Respiration rate was recorded manually with a stop watch every ten minutes. Readings were taken more frequently when respiration rate was not steady. All unusual activity was recorded in the data book. An attempt was made to record respiration rate continuously with a chest operated air bellows, air pressure transducer, amplifier, and recorder system. The chest operated air bellows, however, did not function

properly with the calorimeter holding system used on the bird.

All chickens used is the calorimeter spent a minimum of five hours in the training box (Figure 4.8). This acquainted them with the holding system and the type of confinement they experienced in the chamber. The training box was also used as a proto-type for design dimensions in building the inner plexaglass chamber. The chickens accepted the hammock-type holding system with minimum amount of resistance.

The six chickens used in this research were fifteen-month old White Leghorn hens in active egg production. Except while in the calorimeter, they were housed in the Poultry Science Department cage room. The environmental room has a constant temperature of 78°F with the room lights on from 7:00 a.m. to 11:00 p.m.

Feed (MSU Z-4 Laying Mash) and water were available to the hens at all times in the cage room. While in the calorimeter, they received neither. All six hens used in the tests had been housed in the cage room for at least three months prior to the calorimeter tests and had become accustomed to human handling. The hens were removed from the cage room and weighted just prior to placement in the calorimeter. They were returned to the cage room following each calorimeter test. The first hen tested in the calorimeter chamber each day was taken from the cage room not less than one-half hour after the lights went on in the room. This assured a

Figure 4.6-- Chicken position in the calorimeter

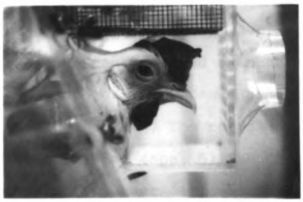

Figure 4.7-- Chicken position in the head chamber

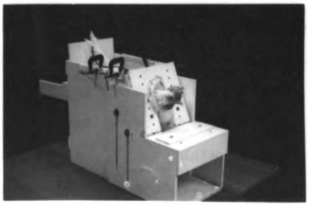

Figure 4.8-- Calorimeter training box

full crop condition in the first hen. The hens were always tested in the same order each day. This minimized diurnal variation between days.

Preparation of the hen for a calorimeter test run included the following: 1) The hen was placed in the holding hammock and secured by tie strings over her back; 2) Two layers of 4 mil surgical rubber about one-half inch apart with holes in the middle were slid over the head and positioned on the neck. The feathers were moved to permit good rubber contack with the skin. Hole size was selected to produce a good air seal at the neck with a minimum amount of pressure. These two separated layers of surgical rubber formed the air seal between the head chamber and the body chamber; 3) The chamber was then opened and the hen was placed in the inner chamber; 4) The rectal probe was inserted and secured with masking tape; 5) The dropping collector was positioned (collected under oil); 6) Comb and wattle thermocouples were secured (as described earlier); and 7) The calorimeter was then closed.

The hens were in the calorimeter one hour and thirty minutes for each test run. Environmental equilibrium was reached during the first thirty minutes. Data values were recorded during the last hour. The only exception to this was at higher temperatures where data values were recorded for only thirty minutes for most of the hens due to the high heat stress. The calorimeter remained closed for

thirty minutes between tests to re-establish equilibrium conditions.

The temperature and humidity conditions used for the test runs are shown in Table 4.2. These conditions are representative of summer environment in commercial laying houses during the day. They also represent upper thermoneutral and lower thermal stress conditions for the chicken.

Table 4.2 Temperature and humidity combinations studied in the calorimeter (6 birds were used)

Number of Tests	Temperature	Relative humidity
6	79.5	59.5
10	79.5	69.7
6	79.5	78.9
6	85.8	59.5
6	85.8	69.7
6	85.8	78.9
6	90.4	59.5
6	90.4	69.7
6	90.4	78.9
6	94.9	59.5
6	94.9	69.7
6	94.9	78.9

4.2 Respiratory Tract Wall Temperature

An investigation of the respiratory wall tissue temperatures at various points in the respiratory system with a 30 gauge copper-constantan thermocouple was done. The thermocouple was held against the tissue for a minimum of thirty seconds at each location. Temperatures were recorded on a Electronik 17 two-pen strip chart recording potentiometer with a temperature range of 0°F to 250°F and an accuracy of ±.25% of full scale reading.

The bird was positioned in a holding rack and tied into the same hammock used in the calorimeter (Figure 4.11) Ten White Leghorn hens of similar age and condition were used. Six of the ten hens had been used in the calorimeter tests. Their weights were recorded just prior to positioning in the holding rack.

The locations of wall tissue temperature measurements were: 1) just inside the nasal opening on the beak, 2) the roof of the mouth where nasal air enters the mouth cavity, 3) at the top of the trachea, and 4) one inch down the trachea. The rectal temperature of each hen was also measured.

Selected surface temperatures were then measured with a Barnes Engineering Company infrared thermometer. This instrument has a range of 10°F to 110°F with an accuracy of ±1.5°F, and a response time of 50 milliseconds. The areas where temperatures were measured included: 1) the eye area, 2) the base of the comb, 3) the left wattle, 4) the right wattle,

Figure 4.9-- Humidity sensor and housing

Figure 4.10-- Trachea humidity test

Figure 4.11-- Respiratory tract temperature test

5) the mouth cavity from between the open beaks, and 6) the nasal opening on the beak. The Model 594 hygro-thermograph was used to record ambient temperature and humidity continuously during the tests.

4.3 Trachea Humidity Investigation

A technique was developed to measure temperature and humidity at the base of the trachea in a living bird under general anesthetic. An air-tight housing (except for the inlet and outlet tube) was developed for the narrow range, type H-3, class A hygroseneor used in the calorimeter head chamber outlet. The inlet tube to the housing was constructed from a 3/16 inch diameter thin wall (.01 inch) rigid plastic tube. This tube was heated and tapered to an outside diameter of .10 inch. A section 1 1/4 inches long was attached to the housing and coated with a thin layer of silastic 382 Elastomer. This tube was placed into the base of the trachea through an incision as shown in Figure 4.9. A 30-gauge copper-constantan thermocouple was also placed inside the housing near the inlet tube to sense air temperature. Air was then moved through the trachea with a Harvard Apparatus Company model 671 small animal respirator pump with a range of 0 to 200 cycles per minute and stroke volume of 20 to 100 cc.

Complete blockage of the trachea in this way would cause death under normal conditions. The chicken's unique air sac

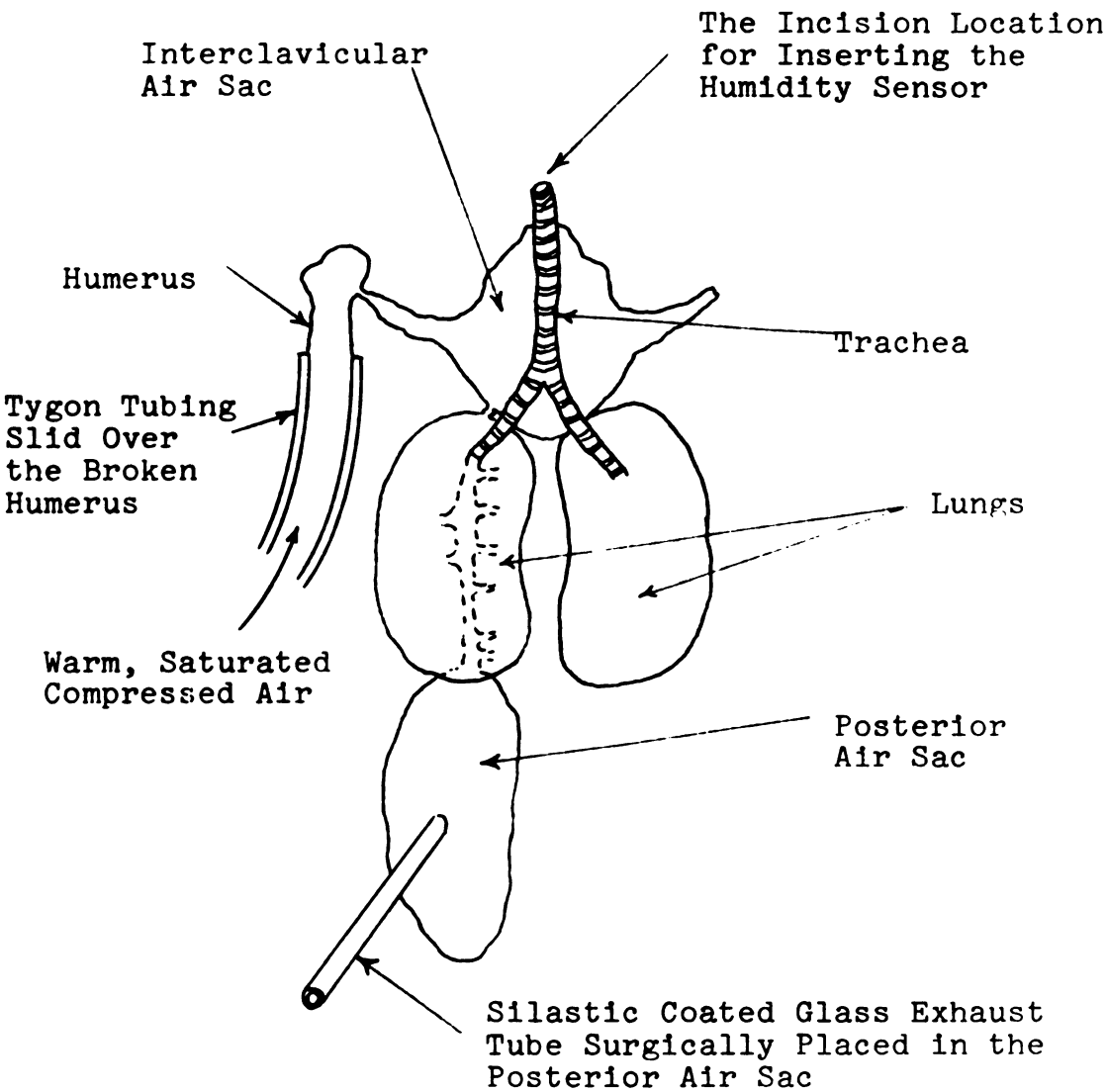

Figure 4.12-- Schematic diagram of the operation for determination of the humidity at the base of the trachea

and pneumatic bone system, however, made it possible to respirate the lungs through surgery.

Nearly saturated air at 107°F was forced at a regulated rate into the broken humerus bone. This pneumatic bone is connected to the interclavicular air sac. The air then travelled through the lungs into the posterior air sac. It was allowed to exit through a surgically placed glass tube coated with silastic 382 Elastomer. A schematic diagram of the operation is shown in Figure 4.12. It took four preliminary operations and many design changes to develop the technique for this operation.

The recording instruments used in this operation have all been described in earlier sections. They include: 1) the hygrosensor and indicator for measuring trachea air relative humidity, 2) the Electronik 17 two-pen recorder for measuring trachea air temperature, and 3) the infrared thermometer for measuring selected surface temperatures. An electric oven was also used to heat the hygrosensor and housing to 107°F before insertion into the trachea. An overall view of the operation and the instruments used is shown in Figure 4.10.

Humidity and temperature tests were conducted for a time span of ten minutes each with a ten minute rest period between tests. The trachea was ventilated at respiration rates of 20, 30, and 40 cycles per minute with tidal volumes of 20 and 25 cc as set on the Harvard respirator. the

position of the respirator tube was also changed from one to two inches down the trachea from the glottis. Comb, wattle, and eye area surface temperatures were also recorded. Ambient temperature and humidity was recorded continuously with the model 594 hygro-thermograph.

5. EXPERIMENTAL RESULTS

5.1 Heat and Moisture Production; the Calorimeter Studies

Sensible and latent heat production from the head chamber and body chamber are presented graphically and discussed in this section. The data are also presented in tabular form in Appendix A.5.

Heat production prediction equations were derived through non-linear least squares analysis of the calorimeter data. The analysis was done on the CDC 3600 with an adapted computer library program (MSU Computer Laboratory No. 000087, GAUSHAUS). The main program and user-supplied subroutine is in Appendix A.8. GAUSHAUS was stored on magnetic tape and called from the main program.

The objective of the regression analysis was to determine the simplest form of regression equation that would adequately represent the data. This was done by comparing the change in the sum of squares after regression as the fitted equation was changed. The residuals were also examined for trends that might indicate improvements in the form of the fitted equation. Finally, the 95% confidence limits for the constant parameters of the fitted equation were examined. If they were not significantly different from zero, that term of the fitted equation was dropped. Therefore,

all the parameters included in the regression equations in this section are significantly different from zero.

Relative humidities relation to heat production for the temperature and humidity conditions of the research was not significant. For this reason there are no humidity terms in the regression equations.

The regression equations are presented in each case with the sum of squares after regression and the variance of residuals. The range of these equations is restricted to 76°F to 96°F dry-bulb temperature.

All the heat production curves are the result of non-linear least squares analysis to fit the given form of the regression equation. There are 76 data points on each graph.

The wide variation in the data from this research is partly due to differences between birds. To illustrate this difference, individual heat production regression curves for each hen were developed and are shown in Appendix A.4. The form of the fitted equation is the same as for the respective pooled heat production data.

5.1a Latent heat production

Latent heat production was found only in the head chamber and this was assumed to be entirely from the respiratory system. These findings support the assumption of Roller and Dale (1962) and DeShazer (1968) that all latent

heat production is from the respiratory system. The diffusion loss of moisture from the skin as discussed by Sturkie (1965) was too small for detection in the body chamber.

Latent heat loss increased with rising temperatures as shown in Figure 5.1. The increase begins between 82°F and 84°F, and continues to increase at a faster rate at the higher temperatures.

The slight decrease in latent heat production between 76°F and 82°F is similar to that found by DeShazer (1968). This drop may be caused by a slight decrease in tidal volume as the bird begins to adjust for thermal stress. The lack of data points in the 76°F to 78°F region of the curves may also have contributed to the increase in that region.

The regression equation for latent heat production is

$$Q_L = 346.45 - 8.62T + .05T^2 \qquad (5.1)$$

sum of squares after regression = 824.6

variance of residuals = 11.3

degrees of freedom = 73

where:

Q_L = latent heat production, BTU/hr

T = temperature, °F

The data subjected to the above regression analysis along with the predicted values and 95% confidence limits for each data value are shown in Table A.1 of Appendix A.5.

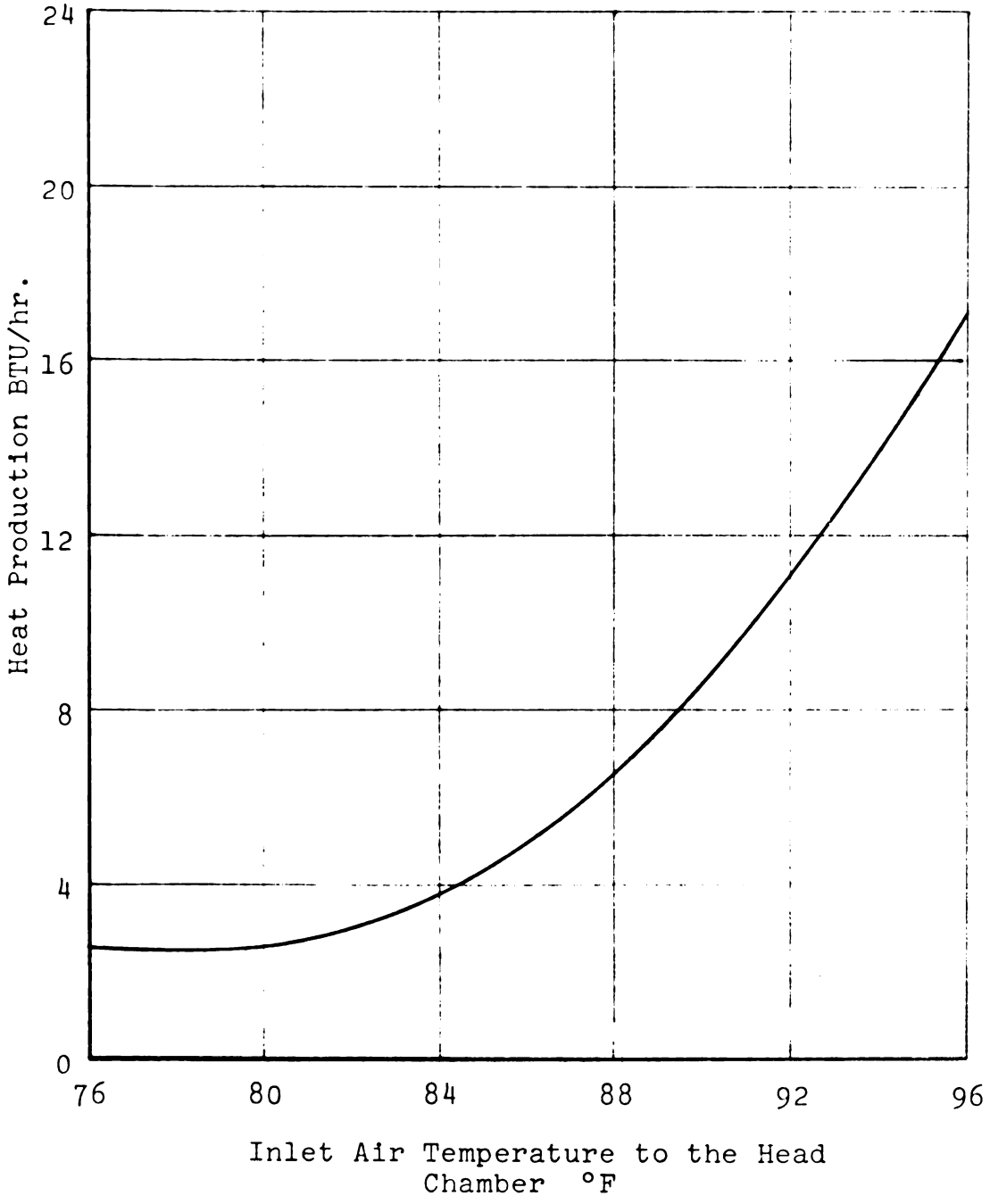

Figure 5.1-- Total latent heat production

The individual bird regression curves are shown in Figure A.4.1 of Appendix A.4.

5.1b Sensible heat production in the head chamber

Total sensible heat production in the head chamber decreases with increasing temperature as shown in Figure 5.2. The respiratory sensible heat production also decreases with increasing air temperature as shown in Figure 5.3. The percentage of total head chamber sensible heat production produced by the respiratory system decreases with increasing temperature. At 76°F, 86°F, and 96°F the percentage of head chamber sensible heat produced from the respiratory system is approximately 67%, 70%, and 80% respectively.

The difference between total sensible heat production in the head chamber and respiratory sensible heat production is an estimate of sensible heat loss from the comb and wattles.

The regression equation for total head chamber sensible heat production is

$$Q_{SH} = 35.88 - .30T \qquad (5.2)$$

sum of squares after regression = 430.7

variance of residuals = 5.8

degrees of freedom = 74

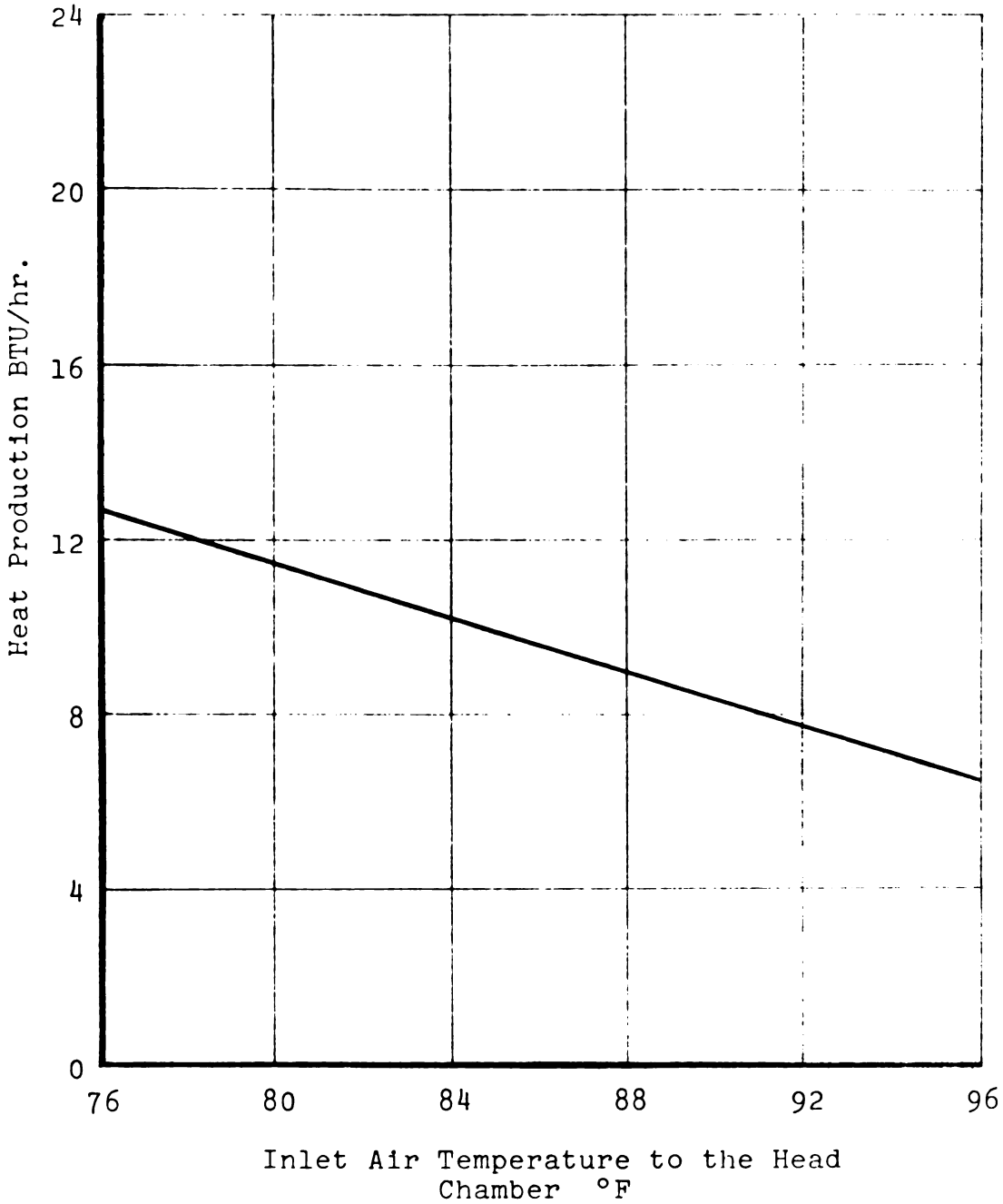

Figure 5.2-- Total sensible heat production in the head chamber

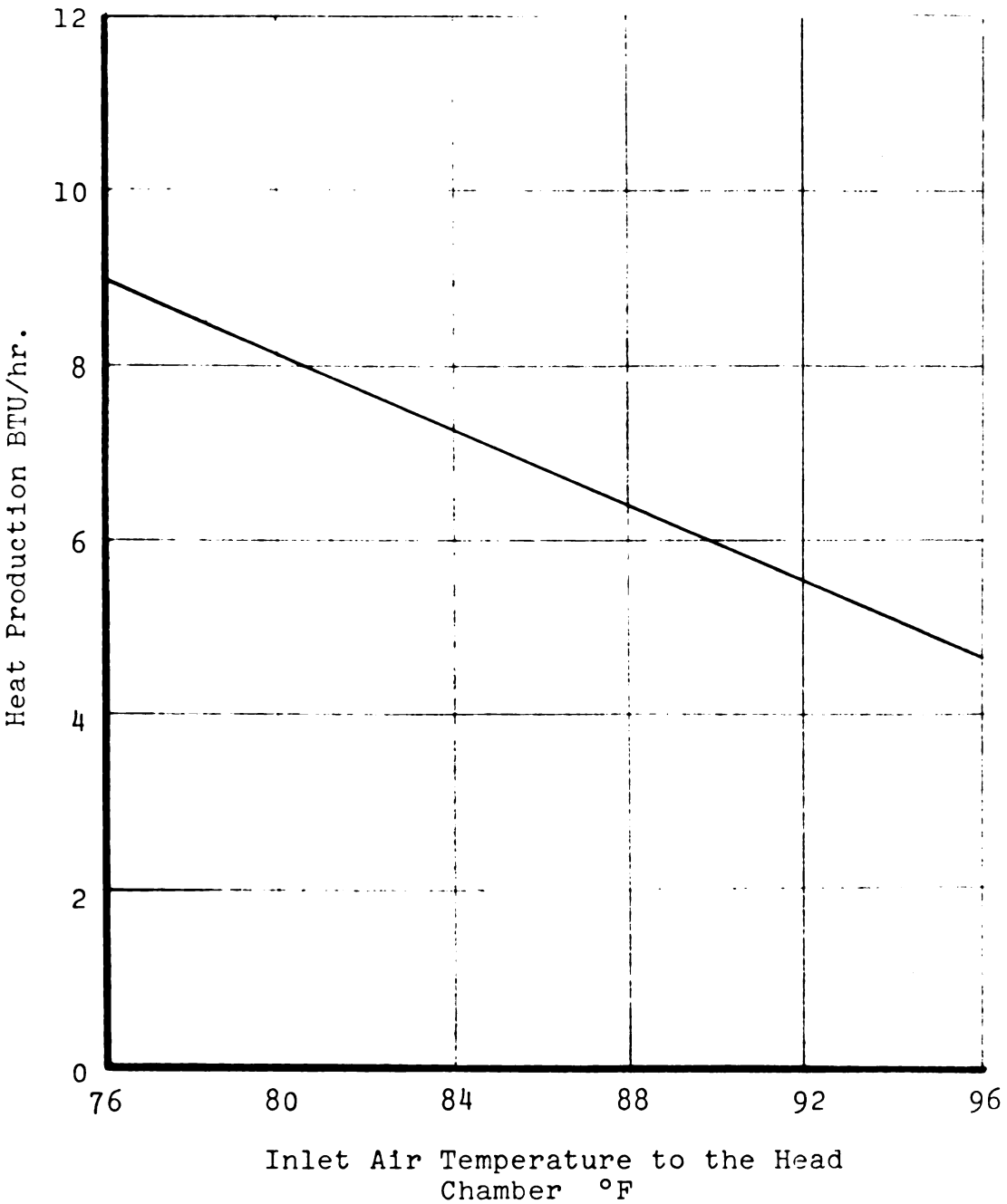

Figure 5.3-- Respiratory sensible heat production

where:

Q_{SH} = sensible heat production in the head chamber, BTU/hr

T = temperature, °F

The regression equation for respiratory sensible heat production is

$$Q_{SR} = 24.52 - .24T \qquad (5.3)$$

sum of squares after regression = 473.9

variance of residuals = 6.4

degrees of freedom = 74

where:

Q_{SR} = respiratory sensible heat production, BTU/hr

T = temperature, °F

The head chamber and respiratory sensible heat production data combined with the predicted values and 95% confidence limits for each data value are shown in Table A.2 and A.3 respectively in Appendix A.5. The individual heat production regression curves are shown in Figures A.4.2 and A.4.3 respectively in Appendix A.4.

5.1c Sensible heat production in the body chamber

Sensible heat production in the body chamber decreases with increasing temperatures as shown in Figure 5.4. The rate of heat production decrease is approximately equal to the rate of total sensible heat loss decrease in the head chamber. The body chamber accounts for 54% to 60% of the

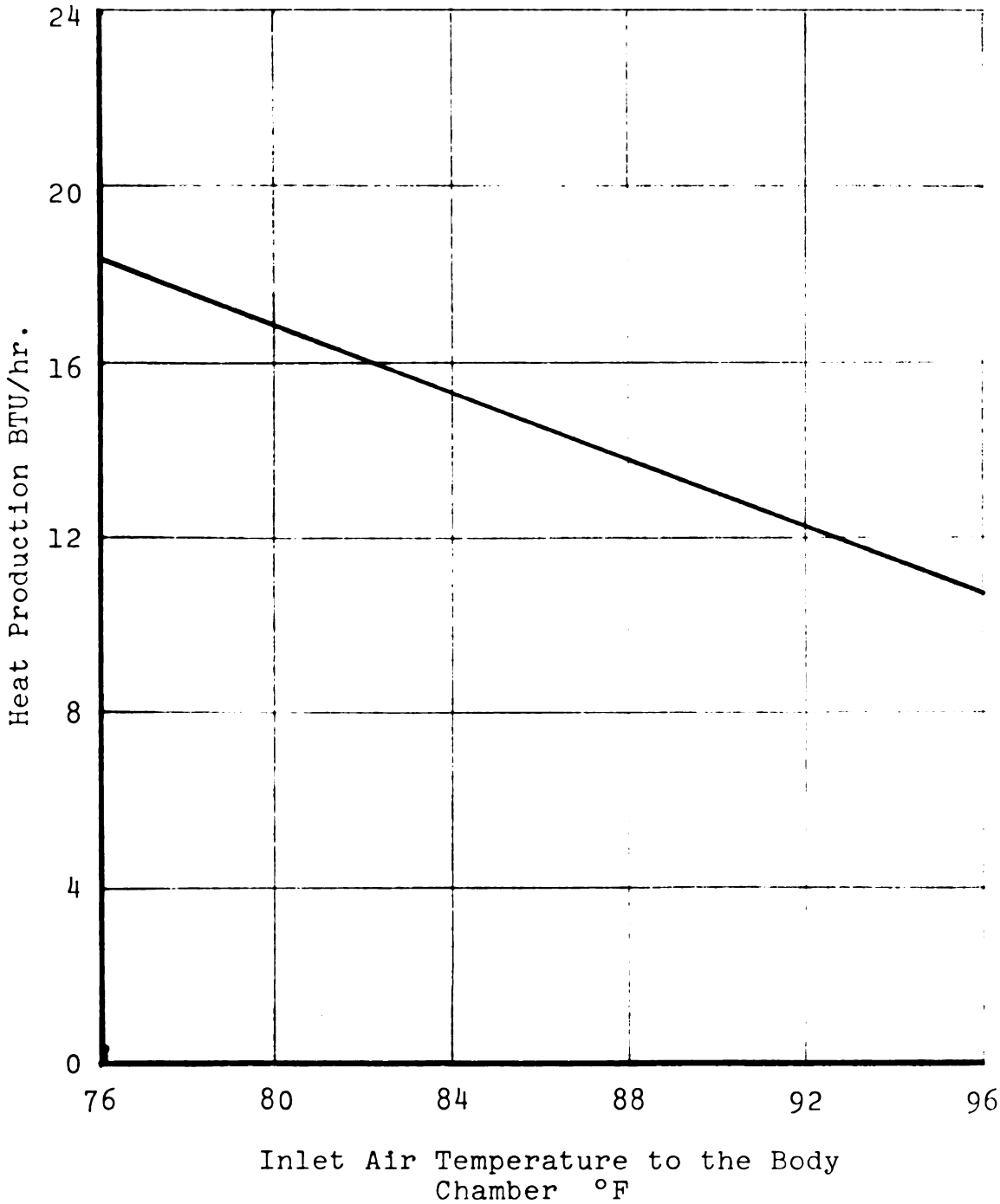

Figure 5.4-- Sensible heat production in the body chamber

total sensible heat produced by the hens in this test. The variation between birds was quite high in sensible heat production in the body chamber as shown in Figure A.4.4. This helps to explain part of the scatter in the pooled data.

The regression equation for sensible heat production in the body chamber is

$$Q_{SB} = 40.16 - .31T \qquad (5.4)$$

sum of squares after regression = 1247.6

variance of residuals = 16.8

degrees of freedom = 74

The body chamber sensible heat production data combined with predicted values and 95% confidence limits for each data value are shown in Table A.3 of Appendix A.5. The individual bird heat production regression curves are shown in Figure A.4.4 of Appendix A.4.

5.1d Total sensible heat production

Total sensible heat production represents the sum of the sensible heat produced in the head chamber and body chamber. It is shown graphically in Figure 5.5. The graph shows, as expected, a decrease in heat production as ambient temperature increases. These results compare very closely with Ota and McNally (1961).

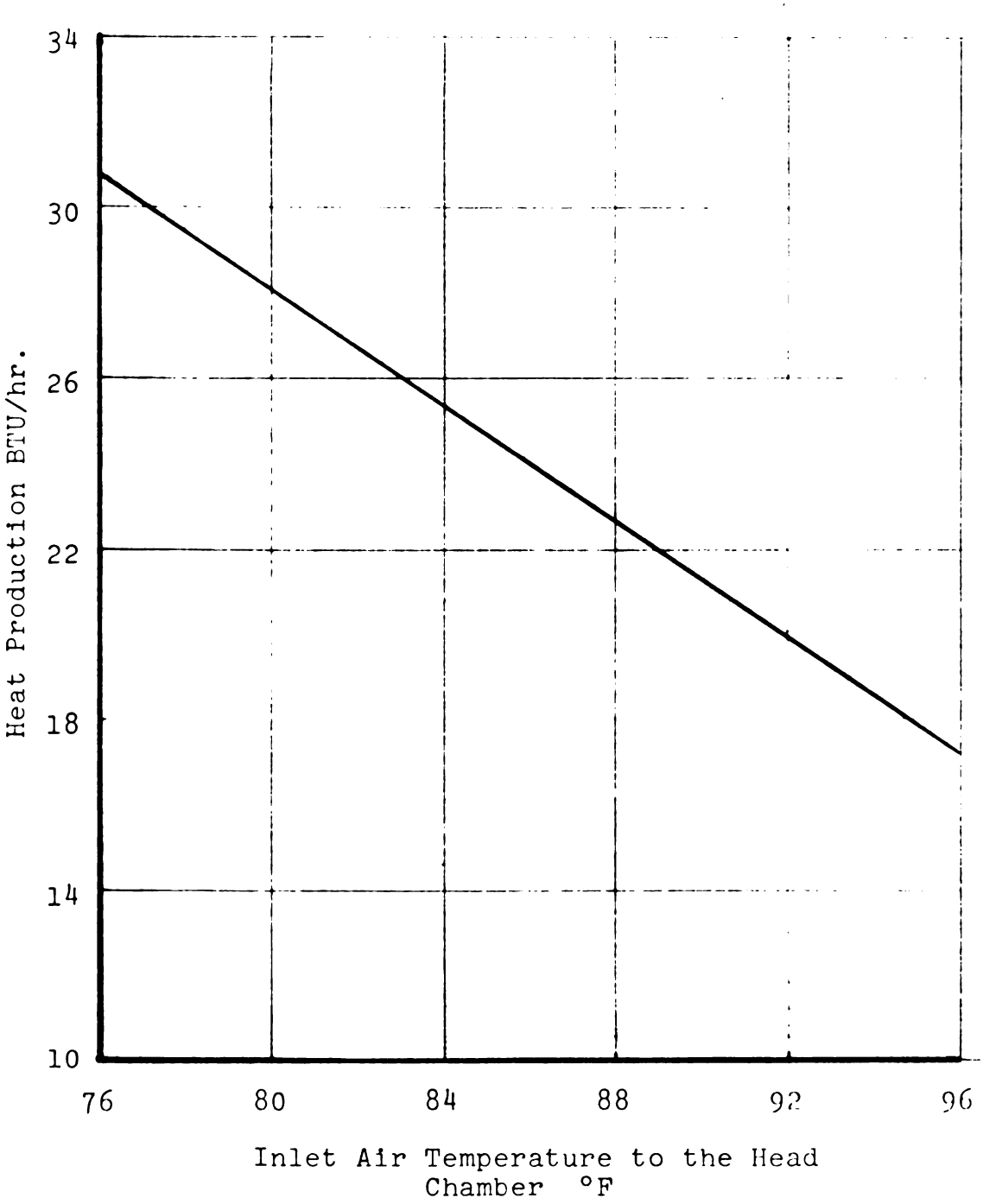

Figure 5.5-- Total sensible heat production

The regression equation for total sensible heat production is

$$Q_S = 76.04 - .61T \qquad (5.5)$$

sum of squares after regression = 1890.2

variance of residuals = 25.5

degrees of freedom = 74

The total sensible heat production data combined with predicted values and 95% confidence limits for each data value are shown in Table A.4 of Appendix A.5. The individual hen heat production regression curves are shown in Figure A.4.5 of Appendix A.4.

5.2 Estimation of Tidal and Minute Volume

Data from the calorimeter experiments were substituted into equation 3.10 in order to estimate tidal volume as a function of temperature. The resulting curve is shown in Figure 5.6. The decrease in tidal volume between 80°F and 86°F agrees with Sturkie's (1965) discussion of tidal volume decrease as a hyperthermic reaction. The estimated tidal volume is somewhat higher, however, than the 6.3×10^{-4} cubic feet determined by Weiss (1962) for normal respiration. Bouchillon, et al. (1969) found tidal volume to be about 8.7×10^{-4} cubic feet for normal respiration. These results would indicate that the hens were breathing a little deeper

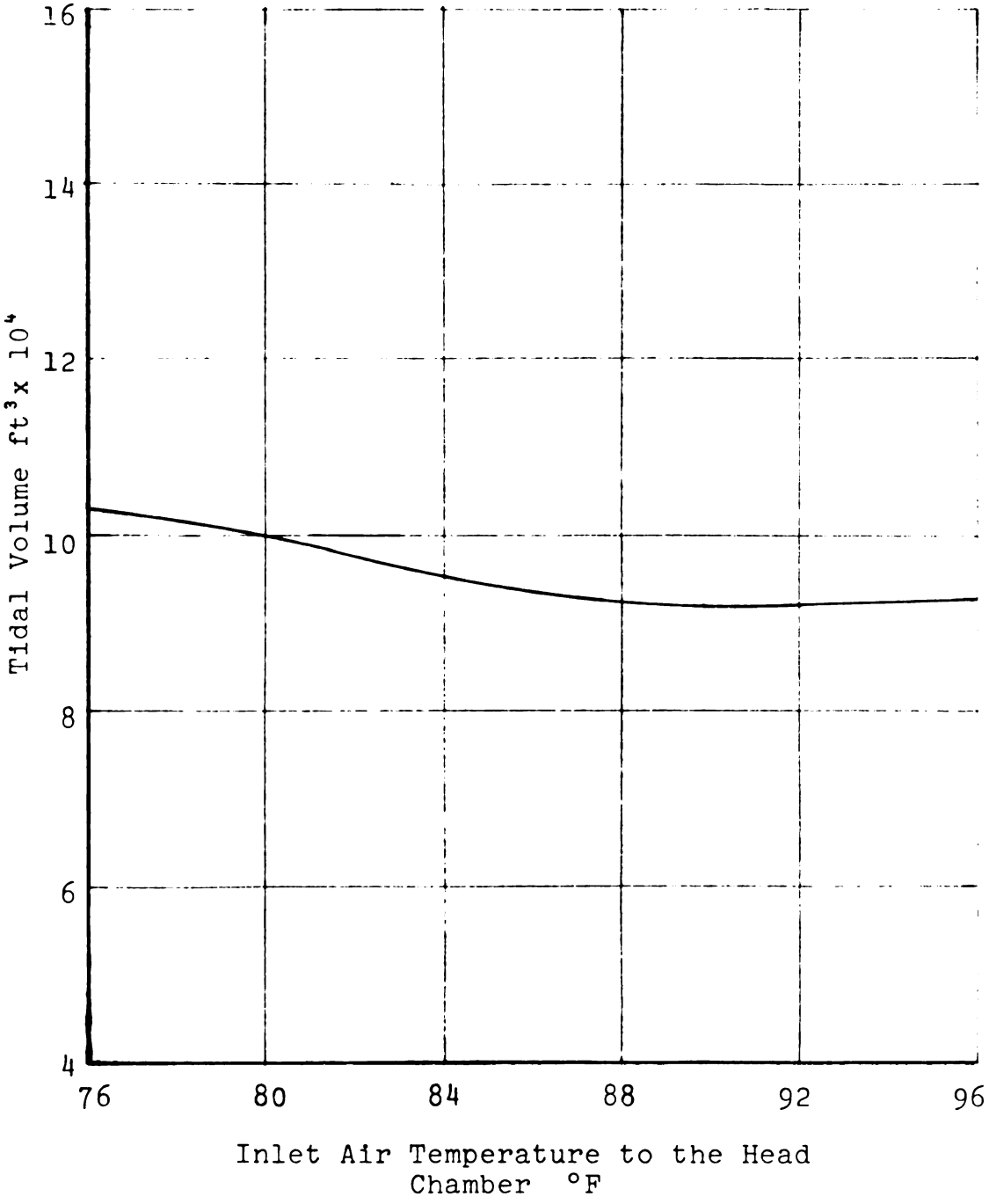

Figure 5.6-- Estimated tidal volume

while in the calorimeter than if they were unconfined under similar environmental conditions.

The minute volume was determined by multiplying tidal volume times respiration rate. Figure 5.7 illustrates the estimated minute volume data from the calorimeter study and the regression line developed from the data. The regression equation is

$$V_M = 12555. - 299.11T + 1.86T^2 \qquad (5.6)$$

sum of squares after regression = 774,152.3

variance of residuals = 10605.0

degrees of freedom = 73

where:

V_M = Minute volume, ml

T = Temperature, °F

In determining the simplest form of the regression equation that would adequately fit the data, relative humidity in the 60% to 80% range was found to have an insignificant effect on minute volume.

Equation 5.6 is in good agreement with the thermoneutral and hyperthemic minute volumes determined by Weiss (1962) for White Leghorn hens.

5.3 Wall Temperatures in the Respiratory System

The surface temperatures at various points in the respiratory system were measured as discussed in section 4.2.

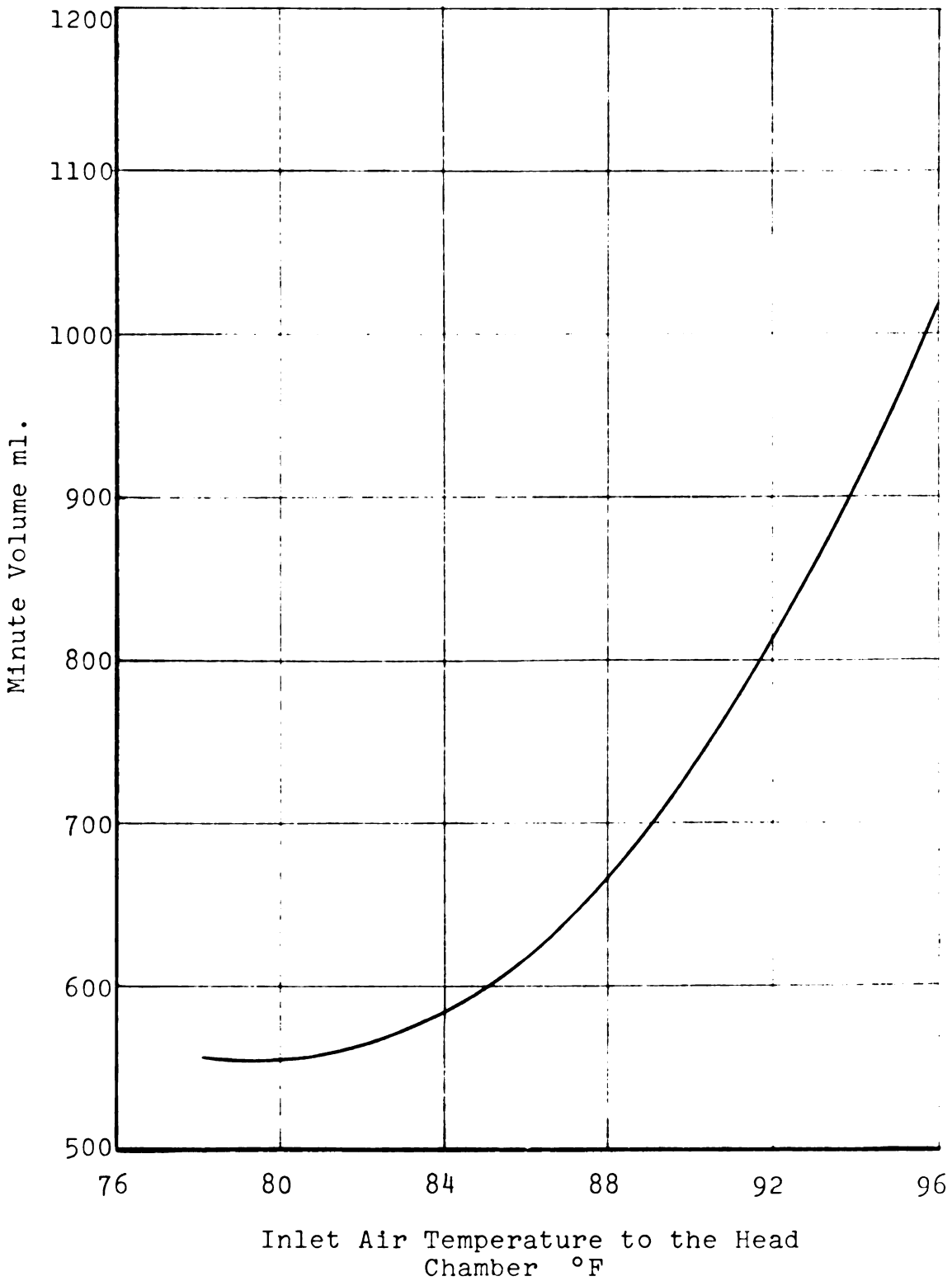

Figure 5.7-- Estimated minute volume

Table 5.1 Respiratory tract wall temperatures

Bird No.	T_{c1}	T_{c2}	T_{c3}	T_{c4}	Wt. (kg)
15	95	103	104	106	2.01
28	95	103	105	106	2.32
35	101	103	104	107	1.97
8	100	103	104	107	2.03
1	98	102	103	107	1.92
2	96	103	105	107	1.75
3	101	103	104	108	1.82
4	99	102	104	107	2.05
5	100	103	103	108	2.12
6	101	103	104	108	2.09
Average	98.6	102.8	104.0	107.1	2.00

where:

T_{c1} = wall temperature at nasal inlet

T_{c2} = wall temperature at nasal outlet to mouth

T_{c3} = wall temperature at the top of the trachea

T_{c4} = wall temperature at the base of the trachea

The results are shown in Table 5.1. The average temperature values at the given locations were used in the simulation model. Rectal temperature was assumed to equal surface temperature at the base of the trachea.

Average surface temperatures were also measured with the infrared thermometer at several locations on the head area. These data are shown in Table 5.2. The absence of insulative feathers in the areas where surface temperatures were measured accounts for the relatively high temperatures. The feathered surfaces in the head region were only 2 to 5°F above the 73°F ambient air temperature.

Table 5.2 Surface temperatures in the head region

Bird No.	Locations eye	comb	l. wattle	r. wattle	mouth
15	96	100	98	98	94
28	99	100	101	101	97
35	97	98	104	100	104
8	97	100	99	100	102
1	99	101	97	98	98
2	99	100	98	99	100
3	98	100	99	100	98
4	97	101	100	99	100
5	99	99	100	98	100
6	98	100	98	99	102
Av.	97.9	99.9	99.4	99.2	99.5

5.4 Humidity at the Base of the Trachea

An experiment was developed to measure air humidity and temperature at the trachea base as described in section 4.3.

The results are shown in Table 5.3. The distance from the humidity sensor to the outlet of the artificial respirator's trachea tube is shown in the first column of Table 5.3.

Table 5.3 Humidity at base of the trachea when subjected to different respiration rates and tidal volumes

D	RR	TV	RH	T
5	20	20	100	103.6
5	30	20	100	101.2
5	40	20	100	100.1
5	20	25	100	102.3
5	30	25	100	100.6
5	40	25	100	99.4

Rectal temperature = 103.2°F

D = distance from sensor, in

RR= respiration rate, cycles/min

TV= tidal volume, cc

RH= relative humidity, percent

T = temperature, °F

The recorded relative humidity remained at 100% for all respiration rates and volume settings used. The air temperature decreased with increasing minute volume, but was lower than expected in all except the first test. This

could have been the result of cooling at the sensor location due to the opened neck and exposed trachea. Careful insulation around the sensor would be an improvement to the experimental procedure. The rectal temperature of this bird was about 3.5°F below average, indicating a cooling trend throughout the body. The anesthesia was probably partly responsible for the decrease in body temperature.

The results of this experiment suggest that the humidity at the base of the trachea is very close to saturation at the respective air temperatures. The air temperature at the base of the trachea in an unanesthetized healthy bird under normal breathing conditions is estimated to be very close to rectal temperature.

5.5 Respiratory Simulation Model Results

The respiratory heat and mass transfer simulation model as discussed in section 3.3 was used to estimate air temperature and humidity as a function of location in the respiratory system. The model is based on thermoneutral conditions with all the inspired and expired air passing through the nasal cavities. The wall temperatures are from the results given in section 5.3. The graphical results of the simulation are shown in Figure 5.8 through 5.19. The solid line represents air temperature or humidity, and the dashed line represents wall temperature or saturated boundary layer humidity.

Temperature and humidity changes occur most rapidly in the nasal passages (Figures 5.8 and 5.9). The transient term in the mass and energy balance equations was studied at nasal conditions because these rapid changes only occur in that region. Air temperature is raised to within 1°F of wall temperature at the posterior end of the nasal passage. Air humidity is within .003 lb water/lb air of the saturated boundary layer humidity. Air temperature and humidity remains slightly less than the respective wall condition in the mouth cavity and trachea during inhalation (Figures 5.10 through 5.13). At the base of the trachea the inspired air is very close to body temperature and saturation.

The air entering the base of the trachea from the lungs and air sacs during expiration is at body temperature and saturated. The temperature and moisture gradients are therefore reversed with respect to the wall conditions during expiration (Figures 5.14 through 5.17). The largest amount of cooling and condensation takes place in the nasal passages with expired air being just a little warmer and more humid than the nasal wall conditions (Figures 5.18 and 5.19).

These results indicate that the majority of heat and moisture transfer to the respiratory air occurs during inspiration from the respiratory tract surfaces between the anterior nasal opening and the base of the trachea during thermoneutral conditions. The heat and moisture transfer

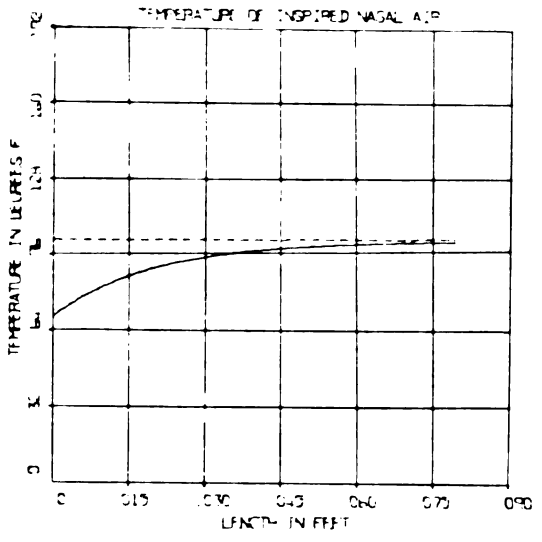

Figure 5.8-- Temperature of inspired nasal air

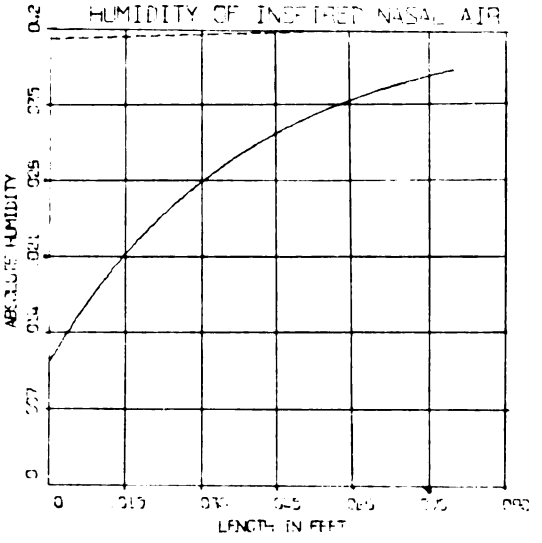

Figure 5.9-- Humidity of inspired nasal air

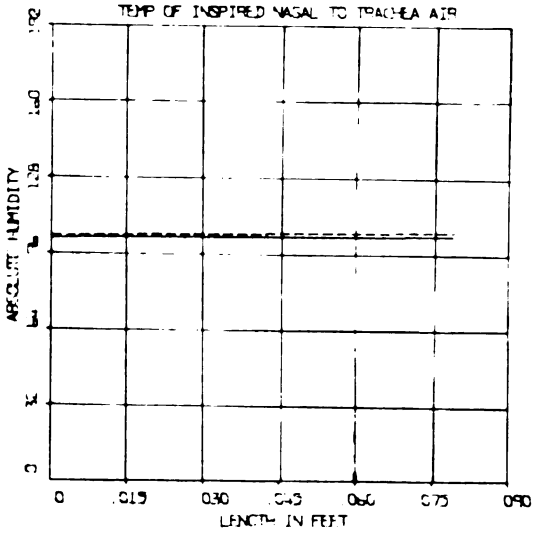

Figure 5.10-- Temperature of inspired nasal to tracheal air

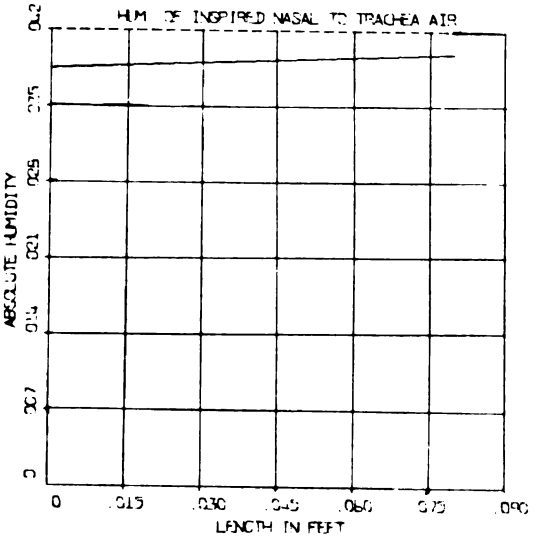

Figure 5.11-- Humidity of inspired nasal to tracheal air

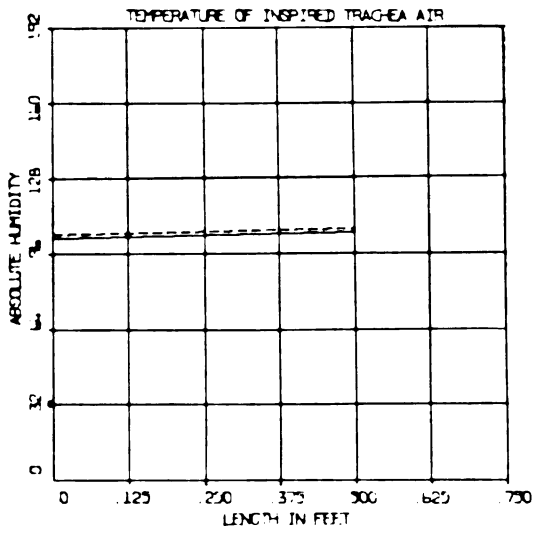

Figure 5.12-- Temperature of inspired tracheal air

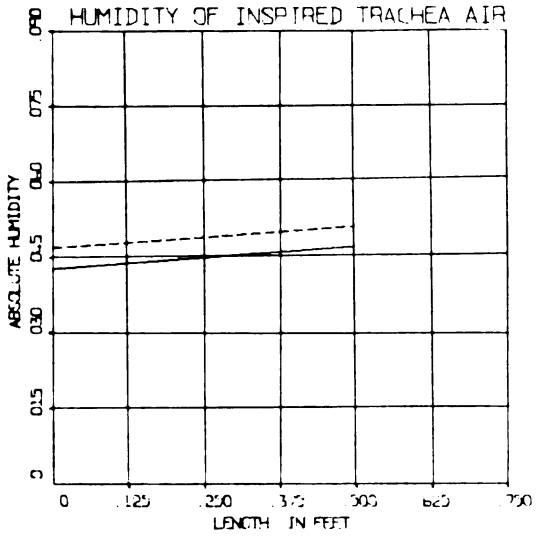

Figure 5.13-- Humidity of inspired tracheal air

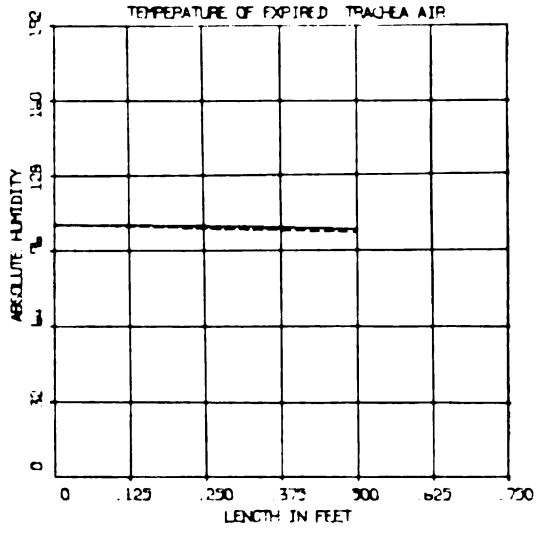

Figure 5.14-- Temperature of expired tracheal air

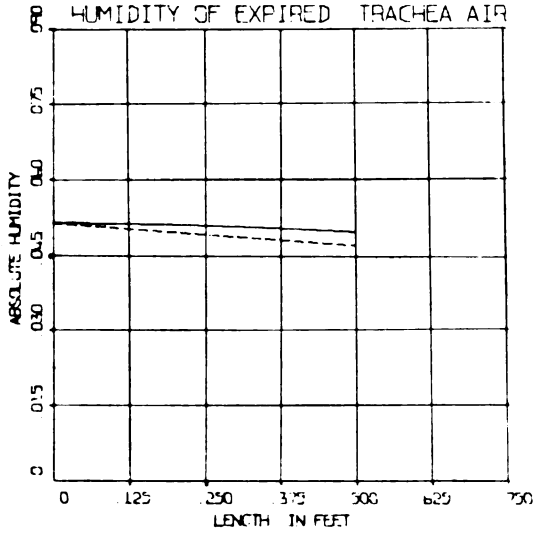

Figure 5.15-- Humidity of expired tracheal air

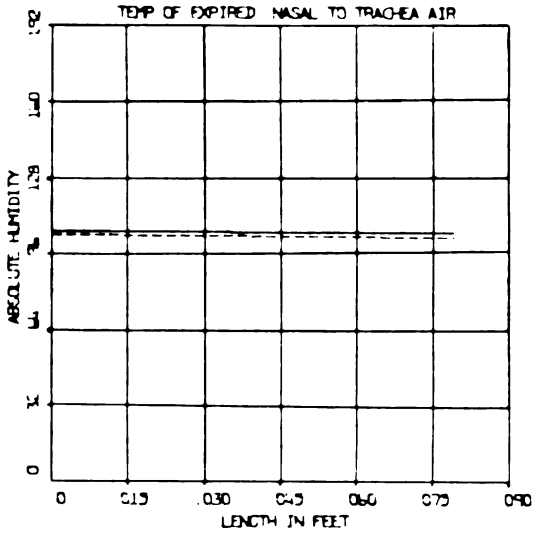

Figure 5.16-- Temperature of expired tracheal to nasal air

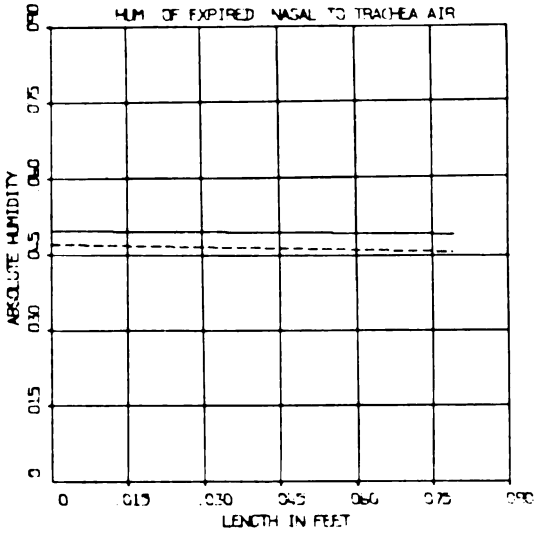

Figure 5.17-- Humidity of expired tracheal to nasal air

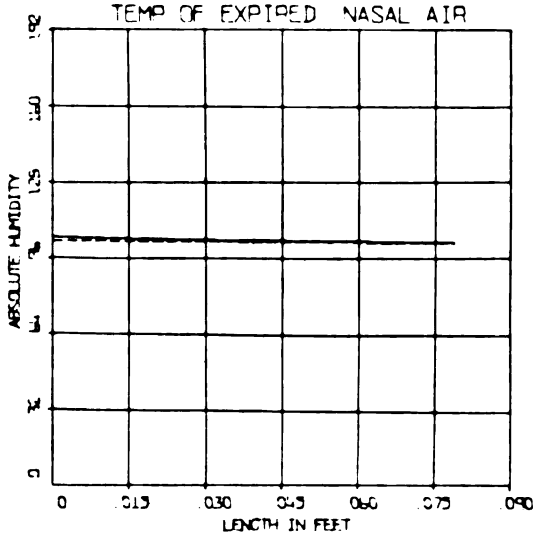

Figure 5.18-- Temperature of expired nasal air

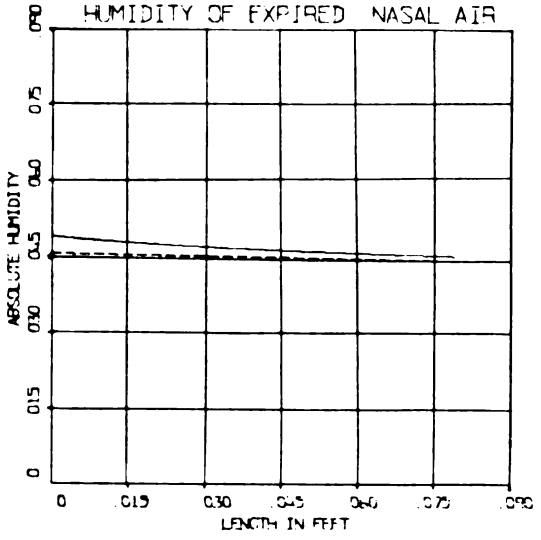

Figure 5.19-- Humidity of expired nasal air

from the surfaces of the lungs and air sacs is small, since the inspired air is very near body temperature and saturated before entering the lungs.

A form of the simulation computer program was developed to estimate sensible and latent respiratory heat production on a BTU/hr basis. Input parameters to this program include the following:

1. bird weight, lb
2. anterior nasal wall temperature, °F
3. posterior nasal wall temperature, °F
4. top of trachea wall temperature, °F
5. base of trachea wall temperature, °F
6. length of nasal passages, ft
7. length of mouth cavity, ft
8. length of trachea, ft
9. average cross-sectional area and perimeter for each structural part of the model, ft^2, ft
10. effective diameter for calculating h for each part of the model, ft
11. mass transfer coefficient for each part of the model, lb water/ft^2hrΔH
12. incremental change in distance between each calculation, ft

With these parameters accessible as input constants, the simulation program may be easily adapted to study the effect of changes in physical structure of the respiratory system and heat or mass transfer characteristics. It might also be adapted to other species of birds, since the

avian respiratory system is very similar in most species. This fortran IV computer program is at Appendix A.10.

The above simulation was used to calculate sensible and latent respiratory heat production under the same conditions the hens were exposed to in the calorimeter experiments. A comparison of the simulation results and the regression equations from the calorimeter data is shown in Figures 5.20 and 5.21. Heat production between 76°F and 86°F was used since the simulation model is designed for thermoneutral conditions.

The simulation results are lower than those of the regression equations, particularly for respiratory sensible heat production. In both cases, however, the simulation results are within the 95% confidence limit of the regression equation. The simulation model is therefore a reasonable approximation of the respiratory sensible and latent heat production recorded in the calorimeter.

5.6 Unequal Duration of Inspiration and Expiration

The discussion and graphs from the respiratory simulation model assume an equal duration of inspiration and expiration. An investigation of this assumption was made to establish: 1) if the White Leghorn hen does have an unequal respiratory cycle, and 2) the magnitude of error that an unequal respiratory cycle would produce in the simulation model.

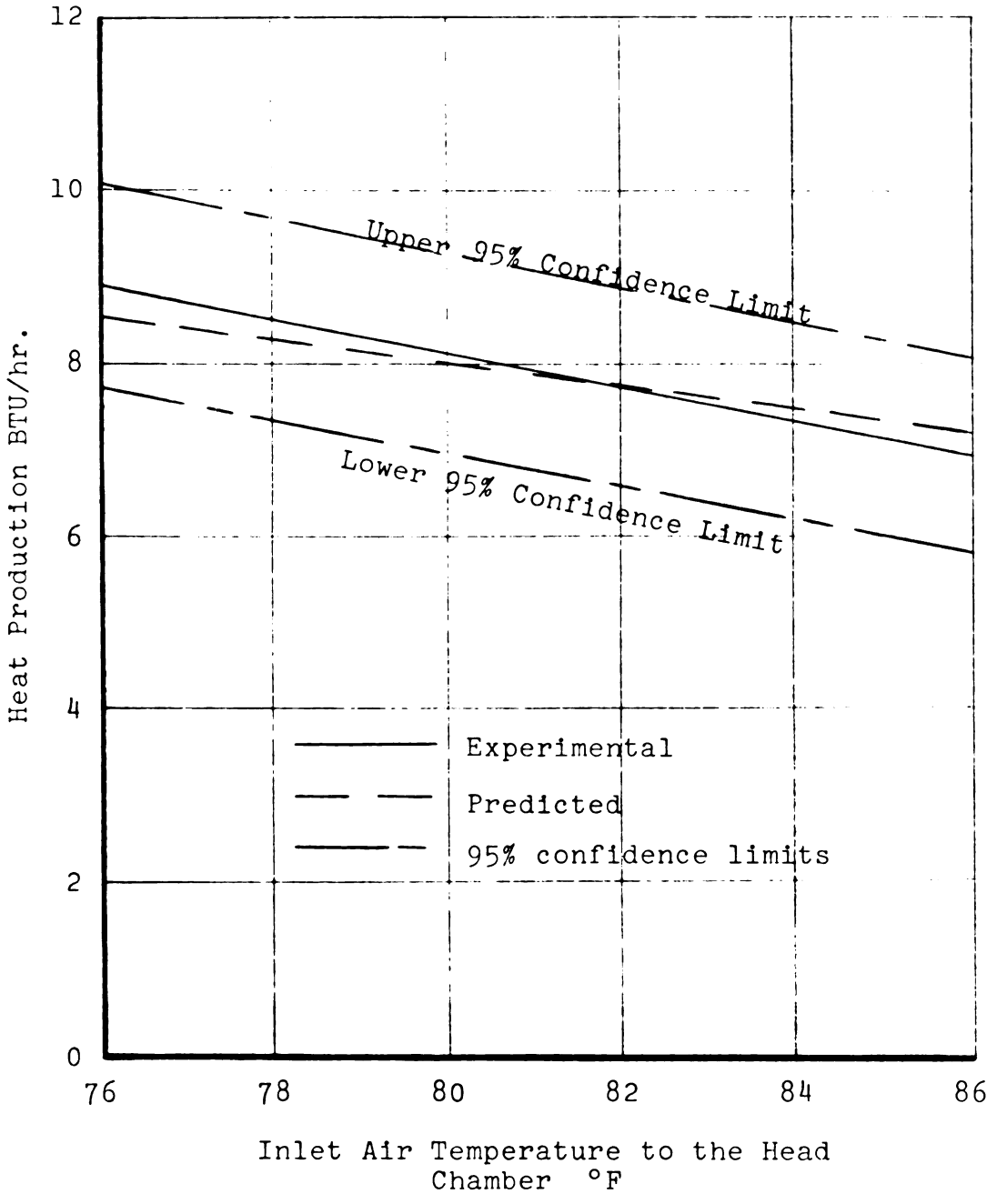

Figure 5.20-- Comparison of respiratory sensible heat production

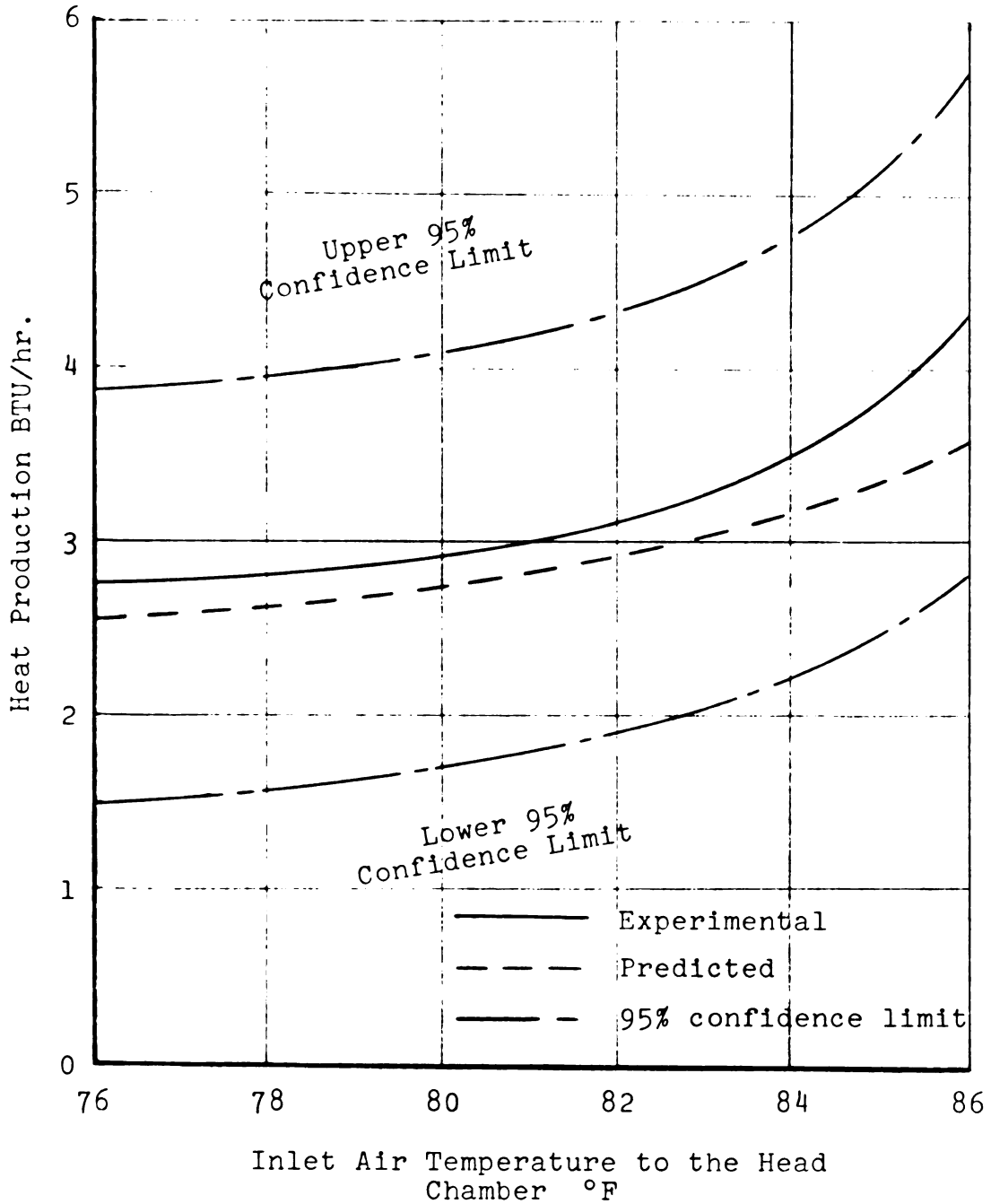

Figure 5.21-- Comparison of respiratory latent heat production

The research on duration of inspiration and expiration for Leghorn hens found in the literature was conflicting. Kaupp (1923) reported inspiration and expiration to be equal, while Graham (1940) found expiration twice as long as inspiration.

Because of these inconclusive results an experiment was developed to measure the respiration cycle durations for the six birds used in the calorimeter chamber tests. An air bellows was secured around the chest of an unanesthetized standing hen. The bellows was then connected to a pressure transducer and the transducer to a Grass model 5 polygraph. With this instrumentation, chest movement as related to respiration phase was recorded as a function of time.

The results indicate that as respiration rate increases inspiration and expiration duration become equal. Even at a respiration rate of 25 breaths per minute, one hen had equal duration times. However, for the other five hens, inspiration was shorter than expiration. The largest duration difference found in all the tests was a 40% inspiration time and a 60% expiration time. Sample polygraph recordings of inspiration and expiration time durations are shown in Figures 5.22 and 5.23. In the figures, the chart speed was 5 mm/sec and the downward deflection represents inspiration.

The simulation model was then changed to represent a 40% inspiration: 60% expiration cycle. Comparing the results

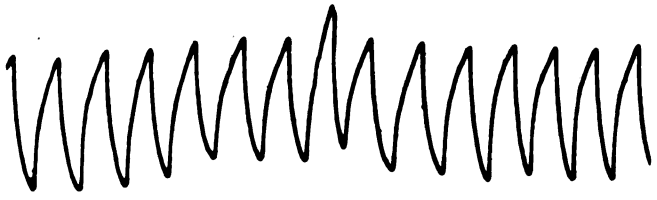

Figure 5.22-- Respiratory duration cycle of 50% inspiration and 50% expiration

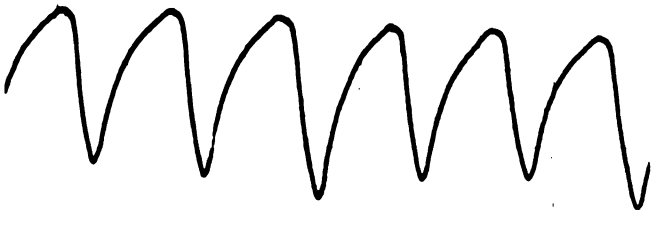

Figure 5.23-- Respiratory duration cycle of 42% inspiration and 58% expiration

with the 50% inspiration: 50% expiration cycle simulation the following differences were found:

1. At the base of the trachea during inspiration the 40%:60% simulation predicted the air temperature change (from ambient conditions) to be .42% smaller and the air specific humidity change to be 1.36% smaller than with the 50%: 50% simulation.

2. At the outlet from the nose during expiration the 40%:60% simulation predicted the air temperature change to be .22% smaller and the air specific humidity change to be .87% smaller than with the 50%:50% simulation.

Thus, even at the extreme 40%:60% case, the predicted temperatures and humidities were not very different from the 50%:50% simulation results.

6. CONCLUSIONS

1. The majority of the heat and moisture transfer during thermoneutrality to the respiratory air occurs during inspiration. The transfer takes place from the respiratory tract surfaces between the anterior nasal opening and the base of the trachea.

2. The heat and moisture transfer from the surfaces of the lungs and air sacs during thermoneutrality is small, since the inspired air is very near lung temperature and saturation as it leaves the trachea.

3. Under thermoneutral conditions the expired respiratory air is four to five degrees cooler than deep body temperature as it leaves the nasal passages.

4. Ambient relative humidities of 60%, 70%, and 80% have a very small effect on sensible and latent heat production at the ambient temperatures and air flows used in this research.

5. The head region of the chicken (including respiratory sensible heat production) accounts for approximately 40% to 60% of the total sensible heat production at the ambient temperatures and air flows used in this study.

6. The head region of the chicken (primarily the respiratory system) accounts for approximately 100% of the total latent heat production. Latent heat production from other body surfaces was negligible.

7. RECOMMENDATIONS FOR FUTURE WORK

The results of this research indicate the need for additional work in the following areas

1. The expansion of the simulation model to include hyperthermic conditions and panting is a logical next step. This would involve simulation of air flow through the lungs and perhaps the air sacs.

2. Solution of the moisture balance and energy balance equations including the transient term and sinusoidal velocity term would improve the simulation model.

3. The development of a face mask and air flow system that facilitates direct measurement of respiratory sensible and latent heat production is needed. This would eliminate the need for estimating sensible heat production from the comb and wattle in order to calculate respiratory sensible heat production.

4. Further investigation is needed in studying the convective and radiate heat transfer capabilities of the comb and wattles at various environmental conditions.

5. Studies with the bird in the chamber for longer periods of time are needed to establish diurnal changes in heat production in the head chamber and the body chamber.

LIST OF REFERENCES

LIST OF REFERENCES

Adams, T.
1964 A method of local heating and cooling of the brain
J. Applied Physiol. 19:338-340

Adams, T.
1968 Temperature Regulation
Exercise Physiology
Academic Press, New York

Bang, B.G., and Bang, F.G.
1959 A comparative study of the vertebrate nasal chamber in relation to upper respiratory infections
Bull. Johns Hopkins Hosp., 104(3):107-149

Beattie, J., and Freeman, B.M.
1962 Gaseous metabolism in the domestic chicken I: oxygen consumption of broiler chickens from hatching to 100 gm. body weight
Brit. Poultry Sci. 3:51

Beckett, F.E., and Vidrene, C.G.
1969 A mathematical model of heat transfer in a pig
ASAE Paper no. 69-437

Benzinger, T.H., Huebscher, R., Minard, D., & Kitzinger, C.
1958 Human calorimetry by means of the gradient principle
J. Applied Physiol. 12(2):547-599

Biester, H.E., and Schwarte, L.H.
1965 Diseases of Poultry, 5th ed.
The Iowa State Univ. Press; Ames, Iowa

Birkebak, R.C.
1966 Heat Transfer in Biological Systems
International Review of General and Experimental Zoology, Vol. II
Academic Press, New York

Bouchillon, C.W, Reece, F.N., & Deaton, J.W.
1969 Mathematical modeling of thermal homeostasis in a chicken
ASAE Paper no. 69-436

Bradley, C.O. and Grahame, T.
1960 The Structure of the Fowl, 4th ed.
Oliver and Boyd, London

Brody, S.
1945 Bioenergetics and Growth
Reinhold, New York

Brooker, D.B.
1966 Mathematical model of the psychrometric chart
ASAE Paper no. 66-815

Brown, W.
1969 Respiratory fraction of total insensible heat loss from shorn and unshorn sheep
ASAE Paper no. 69-458

Burton, A.C. and Edholm, O.G.
1955 Man in a Cold Environment
Edward Arnold (Publishers) Ltd., London

Clayton, J.T. and Boyd, L.L.
1963 Estimating the sensible heat exchange of chickens by simulation
ASAE Paper no. 63-402

Cohn, J.E. and Shannon, R.
1968 Respiration in unanesthetized geese
Resp. Physiol. 5:259-268

Dawson, W.R.
1954 Temperature regulation and water requirements of the brown and Abert towhees, Pipilo fuscus and Pipilo aberti
Univ. Calif. Publ. Zool. 59:81

Dawson, W.R. and Evans, F.C.
1957 Relation of growth and development to temperature regulation in nestling field and chipping sparrows
Physiol. Zool. 30:315

Dawson, W.R.
1958 Relation of oxygen consumption and evaporative water loss to temperature in the cardinal
Physiol. Zool. 31:37

DeShazer, J.A., Jordan, K.A., & Suggs, C.W.
1968 The effect of acclimation upon the partitioning of heat loss by the laying hen
ASAE Paper no. 68-437

DeShazer, J.A., Mather, F.B., & Jordan, K.A.
1969 The dynamic heat loss variations of the laying hen
ASAE Paper no. 69-527

Fedde, M.R., Burger, R.E., & Kitchell, R.
1963 Electronographic study of abdominal muscle movement during respiration
Poultry Sci. 42:1269

Graham, J.D.
1940 Respiratory reflexes in the fowl
J. Physiol. 97:525

Hazelhoff, E.H.
1951 Structure and function of the lung of birds
Poultry Sci. 30:3

Holman, J.P.
1963 Heat Transfer
McGraw-Hill Book Co., Inc.

Hutchinson, J.C.D.
1954 Heat regulation in birds
Progress in the Physiology of Farm Animals, Vol. I; Butterworths Sci. Publ., London

Hutchinson, J.C.D.
1955 Evaporative cooling in fowls
J. Agric. Sci. 45:48'59

Jennings, B.H. and Lewis, S.R.
1944 Air Conditioning and Refrigeration
International Textbook Co., Penn.

Jordan, K.A. and Dale, A.C.
1961 The measurement of heat transmission components of chickens
ASAE Paper no. 61-402

Kaupp, B.F.
1923 The respiration of fowls
Vet. Med. 18:36

Kendeigh, S.C.
1934 The role of environment in the life of birds
Ecol. Monogr. 4:229

King, J.R. and Farner, D.S.
1961 Energy metabolism, thermoregulation and body temperature
Biology and Comparative Physiology of Birds
Vol. II; Academic Press, New York

King, J.R. and Payne, D.C.
1962 The maximum capacities of the lungs and air sacs of Ballus domesticus
J. Anat. 96:495

Klieber, M.
1961 The Fire of Life
Wiley, New York

Kreith, F.
1965 Principles of Heat Transfer, 2nd ed.
International Textbook Co., Penn.

Lee, D.H.K., Robinson, K., Yeates, N. & Scott, M.
1945 Poultry husbandry in hot climates--experimental inquiries
Poultry Sci. 24:195

Longhouse, A.D., Ota, H., Emerson, R., & Heishman, J.
1967 Heat and moisture design data for broiler houses
ASAE Paper no. 67-422

Malhotra, R.K.
1967 Partitional heat losses of mature broad breasted bronze turkeys
Unpublished Ph.D. thesis, Univ. of Missouri

Marshall, A.J. (ed.)
1960 Biology and Comparative Physiology of Birds
Vol. I; Academic Press, New York

Morrison, S.R., Bond, T., & Heitman, H.
1966 Skin and lung moisture loss from swine
ASAE Paper no. 66-441

Ota, H. and McNally, E.H.
1961 Poultry respiration calorimeter studies on laying hens--single comb White Leghorns, Rhode Island Reds, and New Hampshire Cornish Crosses
ARS 42-43, USDA

Rohsenow, W.M. and Choi, H.Y.
1961 Heat, Mass, and Momentum Transfer
Prentice-Hall, Inc., New Jersey

Roller, W.L. and Dale, A.C.
1962 Heat losses from Leghorn Layers at warm temperatures
ASAE Paper no. 62-428

Romijn, C. and Lokhorst, W.
1961 Climate and poultry: heat regulation in the fowl
Tijdschr. Diergeneesk. 86:153

Salt, G.W. and Zeuthen, E.
1960 The respiratory system
Biology and Comparative Physiology of Birds
Vol. I; Academic Press, New York

Scott, N.R., Johnson, A. & Van Tienhoven, A.
1967 Measurement of hypothalamic temperature and heart rate of White Leghorn hens
ASAE Paper no. 67-423

Shephard, R.H., Sladen, B., Peterson, N., & Enns, T.
1959 Path taken by gases through the respiratory system of the chicken
J. Applied Physiol. 14:733

Soum J.M.
1896 Recherches physiologiques sur l'appareil respiratoire des oiseauz
Ann. Univ. Lyon 28:1

Sturkie, P.D.
1965 Avian Physiology, 2nd ed.
Cornell Univ. Press, New York

Threlkeld, J.L.
1962 Thermal Environmental Engineering
Prentice-Hall, Inc., New Jersey

Treybal, R.E.
1968 Mass-Transfer Operations
McGraw-Hill, New York

Tucker, V.A.
1969 The energetics of bird flight
Sci. Amer. 220(5):70

Victorow, C.
1909 Die kuhlende wirkung der luftsacke bei vogeln
Pflugers Arch. 126:300

Vos, H.F.
1934 Uber den web der atemluft in der entenlunge

Weiss, H.S., Frankel, H. and Hollands, K.G.
1962 The effect of extended exposure to a hot environment on the response of the chicken to hyperthermia
Canad. J. Biolchem. Physiol. 41:805

APPENDICES

APPENDIX A.1

APPENDIX

A.1 Derivation of the Energy Balance Equation

The first law of thermodynamics is applied to a representative control volume of air in the respiratory tract during inspiration. The control volume is shown in Figure A.1.1.

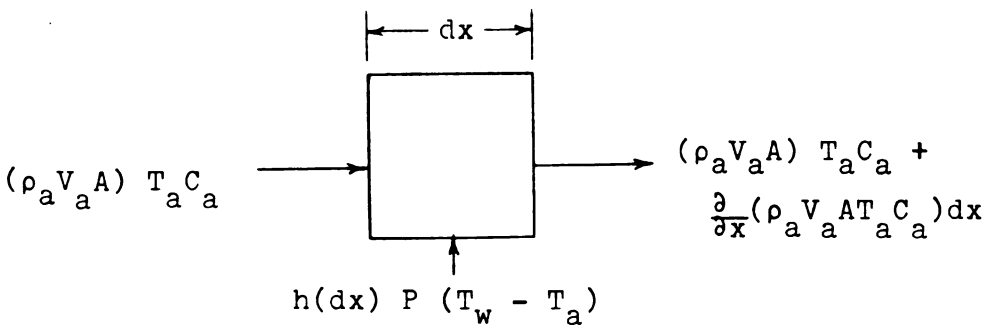

Figure A.1.1-- Energy balance on inspired air

Stating Figure A.1.1 in the form of an energy balance equation

$$(\rho_a V_a A)\ T_a C_a - (\rho_a V_a A T_a C_a + \frac{\partial}{\partial x}(\rho_a V_a A T_a C_a)\ dx)$$

$$+ h(dx)\ P\ (T_w - T_a) = \rho_a C_a (Adx)\ \frac{\partial T_a}{\partial t} \qquad (A.1.1)$$

collecting terms

$$-\frac{\partial}{\partial x}\ (\rho_a V_a A T_a C_a) + h\ P\ (T_w - T_a) = \rho_a C_a A\ \frac{\partial T_a}{\partial t}$$

simplifying

$$h\,P\,(T_w - T_a) - \rho_a V_a A C_a \frac{\partial Ta}{\partial x} = \rho_a C_a A \frac{\partial Ta}{\partial t}$$

Based on the discussion presented in section 3.3a V_a is constant and $\frac{\partial Ta}{\partial t}$ is negligible. The expression then simplifies to

$$h\,P\,(T_w - T_a) = \rho_a V_a A C_a \frac{dTa}{dx} \qquad (A.1.2)$$

separating variables and integrating

$$-\frac{h\,P}{\rho_a V_a A C_a} \int_{x=x_i}^{x=x_{i+1}} dx = \int_{T_i}^{T_{i+1}} \frac{1}{T_a - T_w}\, dT$$

$$\ln \frac{T_{i+1}-T_w}{T_i-T_w} = -\frac{h\,P\,\Delta x}{\rho_a V_a A C_a}$$

let $\dot{m} = \rho_a V_a A$

$$\frac{T_{i+1} - T_w}{T_i - T_w} = e^{\frac{-hP\Delta x}{\dot{m}\,C_a}}$$

$$T_{i+1} = T_w + (T_i - T_w)\, e^{\frac{-hP\Delta x}{\dot{m}C_a}} \qquad (A.1.3)$$

Where $i = 1,2,\cdots,n$ in a finite difference scheme, with $n-1$ being the total number of increments in the given length.

Equation A.1.3 is the finite difference form of the equation used for determining air temperature in the respiratory tract during inspiration.

APPENDIX A.2

APPENDIX

A.2 Derivation of the Energy Balance Equation with Condensation

During expiration condensation on the respiratory tract walls must be considered in determining the air temperature. Applying the first law of thermodynamics to the control volume shown in Figure A.2.1 results in the following

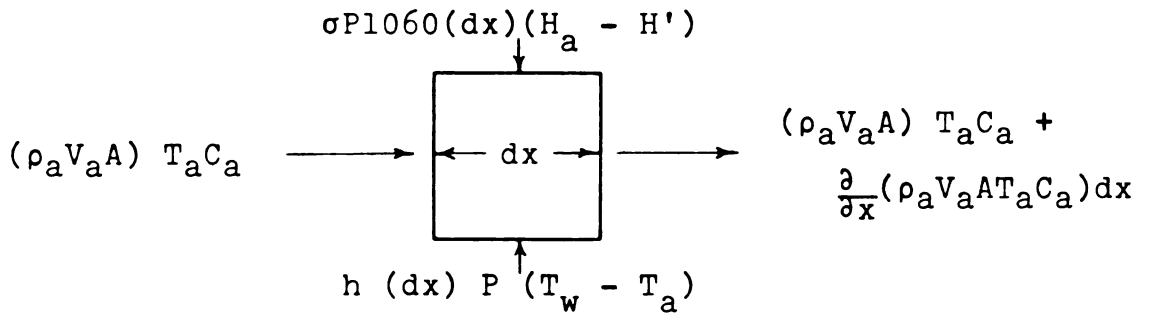

Figure A.2.1-- Energy balance on expired air

$$h\,P\,(T_w - T_a) - \rho_a V_a A C_a \frac{\partial T_a}{\partial x} - \sigma P(1o60)(H_a - H') = \rho_a C_a A \frac{\partial T_a}{\partial t} \qquad (A.2.1)$$

Since V_a constant and $\frac{\partial T_a}{\partial t}$ is negligible as discussed in section 3.3a equation A.2.1 becomes

$$h\,P\,(T_w - T_a) - \sigma P(1o60)(H_a - H') = \rho_a V_a A C_a \frac{dT_a}{dx}$$

let $\dot{m} = \rho_a V_a A$ and simplify

$$\frac{dT_a}{dx} = \frac{hP}{\dot{m}C_a}(T_w - T_a) - \frac{\sigma P(1060)}{\dot{m}C_a}(H_a - H')$$

multiply by $\frac{dx}{dT_a}$ and divide by $(T_w - T_a)$

$$\frac{1}{T_w - T_a} = \frac{a\ h}{\dot{m}\ C_a}\frac{dx}{dT_a} - \frac{\sigma P(1060)(H_a - H')}{\dot{m}\ C_a\ (T_w - T_a)}\frac{dx}{dT_a} \qquad (A.2.2)$$

intergrating

$$\int_{T_i}^{T_{i+1}} \frac{1}{T_w - T_a}\, dT_a = \frac{ah}{\dot{m}C_a} \int_{X_i}^{X_{i+1}} dx - \frac{\sigma P(1060)}{\dot{m}C_a} \int_{X_i}^{X_{i+1}} \frac{(H_a - H')}{T_w - T_a}\, dx$$

$(H_a - H')$ and $(T_w - T_a)$ are functions of x. If the increment change in the x-direction (Δx) is small, they can be assumed constant in that increment and brought outside the integral. Thus, after integration

$$\frac{T_{i+1} - T_w}{T_i - T_w} = e^{-\frac{ah\Delta x}{\dot{m}C_a} + \frac{\sigma P(1060)(H_a - H')\Delta x}{\dot{m}\ C_a\ (T_w - T_i)}}$$

$$T_{i+1} = T_w + (T_i - T_w)\ e^{-\frac{ah\Delta x}{\dot{m}\ C_a} + \frac{\sigma P(1060)(H_a - H')\Delta x}{\dot{m}\ C_a\ (T_w - T_i)}} \qquad (A.2.3)$$

Where $i = 1,2,\cdots,n$ in a finitedifference scheme, with n-1 being the total number of increments in the given length.

Equation A.2.3 is the finitedifference form of the equation used for determining air temperature in the respiratory tract during expiration.

APPENDIX A.3

APPENDIX

A.3 Derivation of the Mass Balance Equation

During both inspiration and expiration there is a transfer of water between the respiratory tract walls and the respiratory air taking place. This moisture transfer is simulated by applying a mass balance on the water transfer terms shown in Figure A.3.1.

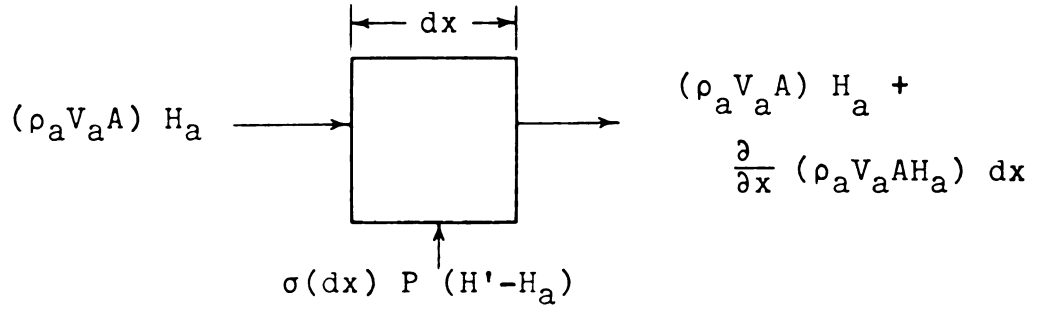

Figure A.3.1-- Mass balance on moisture transfer

The following equation is the result

$$\sigma\ P\ (H' - H_a) - \rho_a V_a A\ \frac{\partial Ha}{\partial x} = \rho_a A\ \frac{\partial Ha}{\partial t} \qquad (A.3.1)$$

Since the time dependent term is negligible as discussed in section 3.3a, equation A.3.1 simplifies to

$$\sigma\ P\ (H' - H_a) = \rho_a V_a A\ \frac{\partial Ha}{\partial x} \qquad (A.3.2)$$

separating variables and integrating

$$-\frac{\sigma P}{\rho_a V_a A}\int_{X_i}^{X_{i+1}} dx = \int_{H_{a_i}}^{H_{a_{i+1}}} \frac{1}{H_a - H'}\, dH$$

let $\dot{m} = \rho_a V_a A$

$$\ln \frac{H_{a_{i+1}} - H'}{H_{a_i} - H'} = -\frac{\sigma P \Delta x}{\dot{m}}$$

$$\frac{H_{a_{i+1}} - H'}{H_{a_i} - H'} = e^{-\frac{\sigma P \Delta x}{\dot{m}}}$$

$$H_{a_{i+1}} = H' + (H_{a_i} - H')\, e^{-\frac{\sigma P \Delta x}{\dot{m}}} \qquad \text{(A.3.3)}$$

Where $i = 1,2,\cdots,n$ in a finite difference scheme with $n - 1$ being the total number of increments in the given length.

Equation A.3.3 is the finite difference from of the equation used for determining the absolute humidity of the respiratory tract air during expiration and inspiration.

APPENDIX A.4

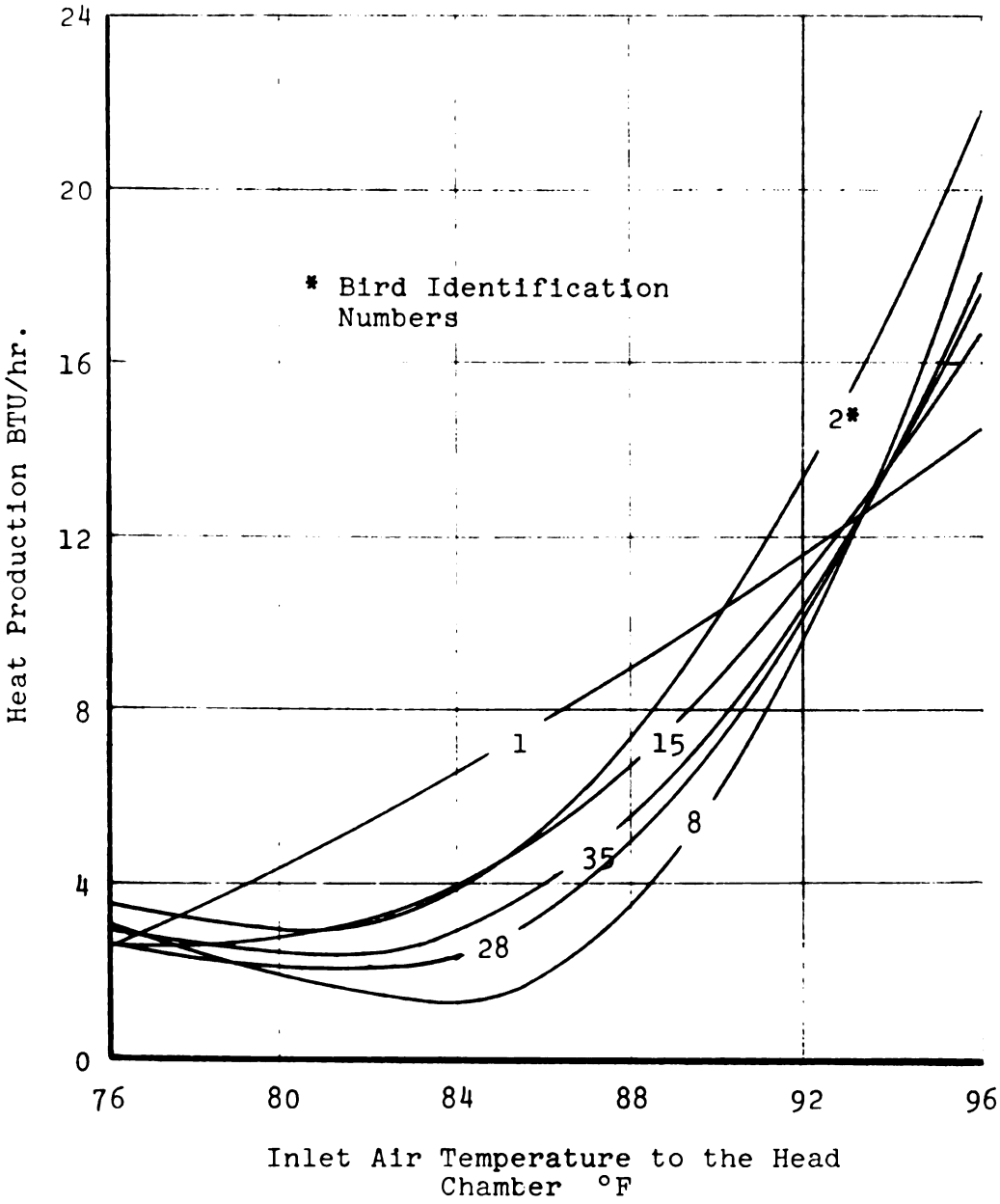

Figure A.4.1-- Individual total latent heat production

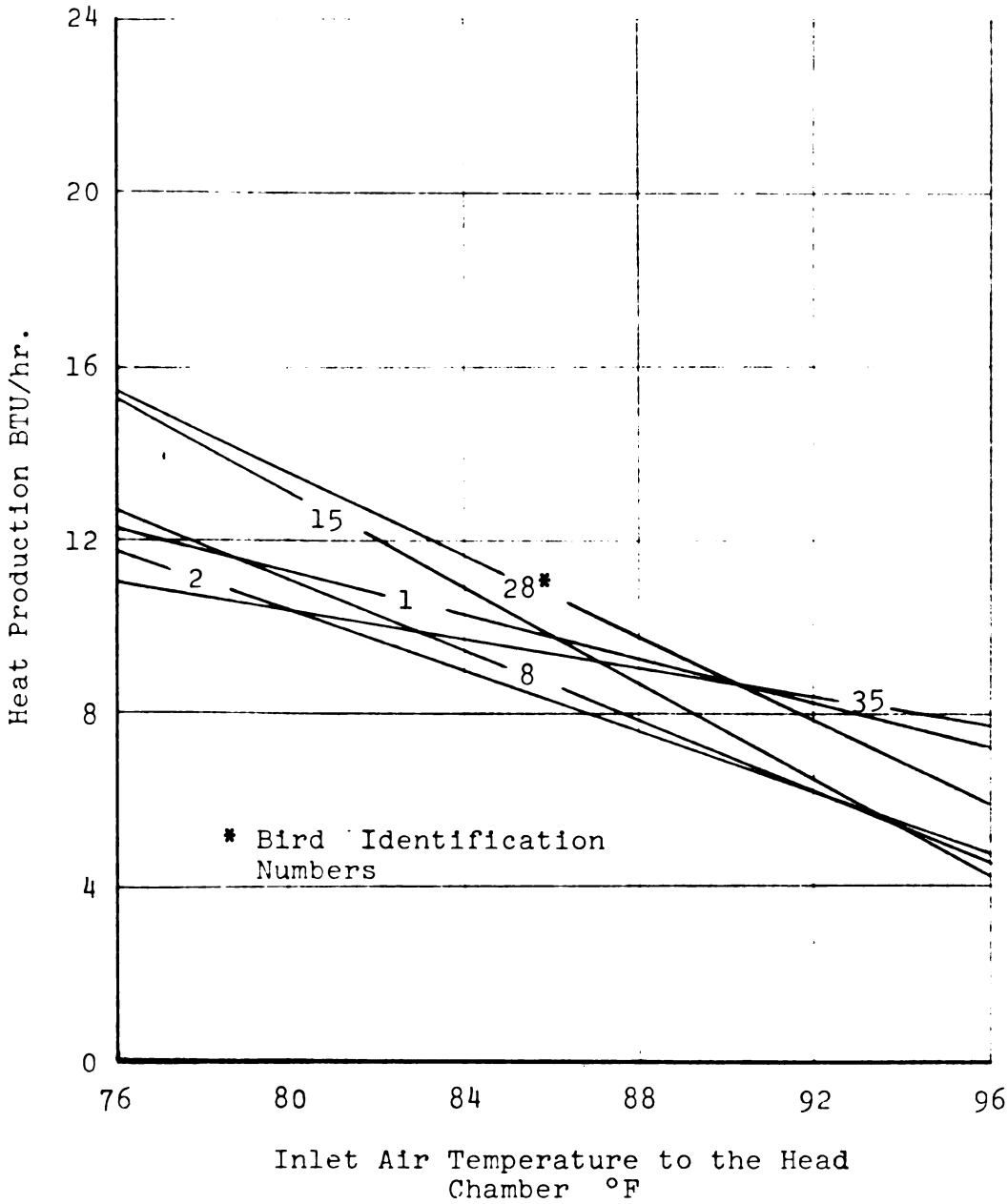

Figure A.4.2-- Individual total sensible heat production in the head chamber

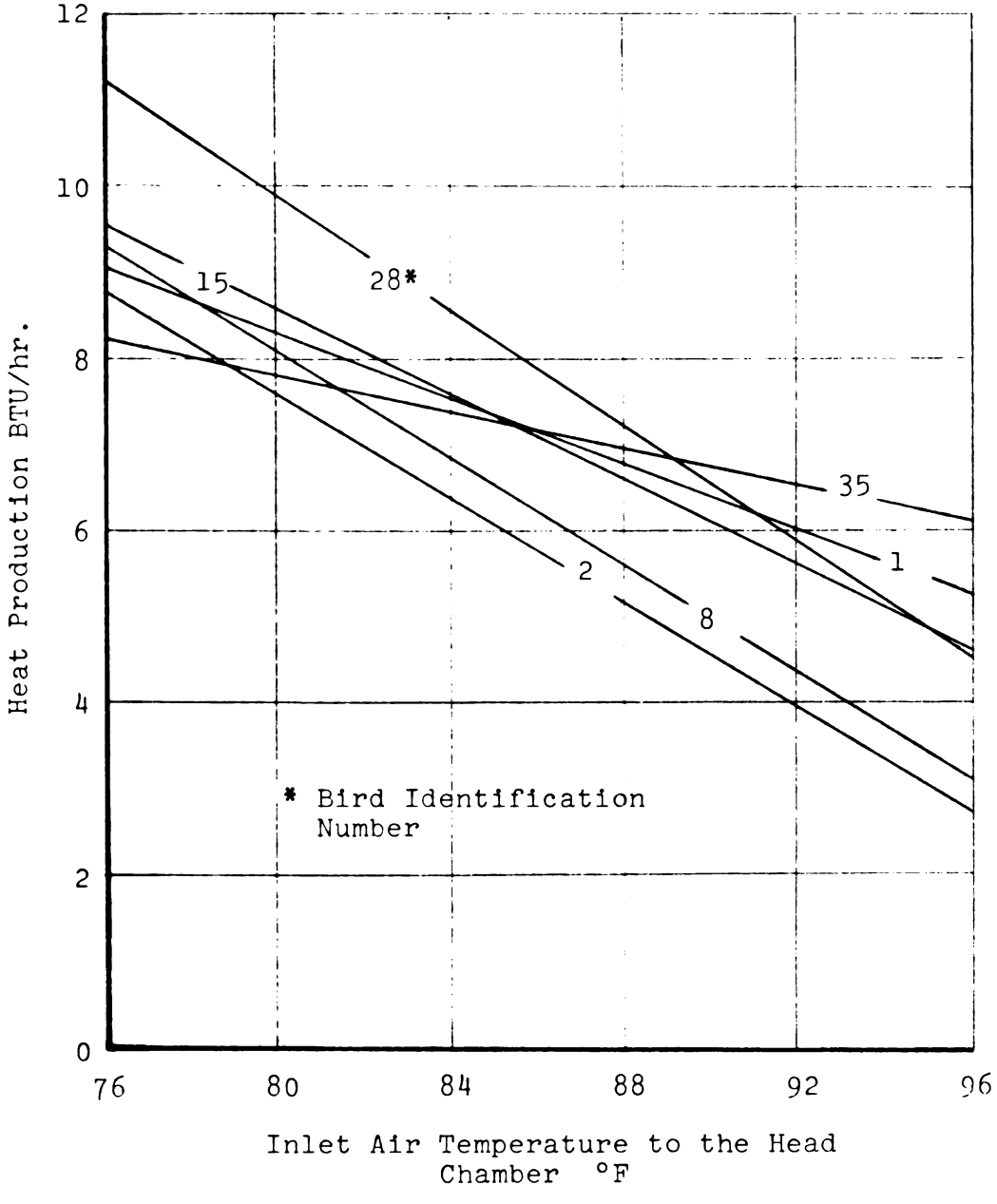

Figure A.4.3-- Individual respiratory sensible heat production

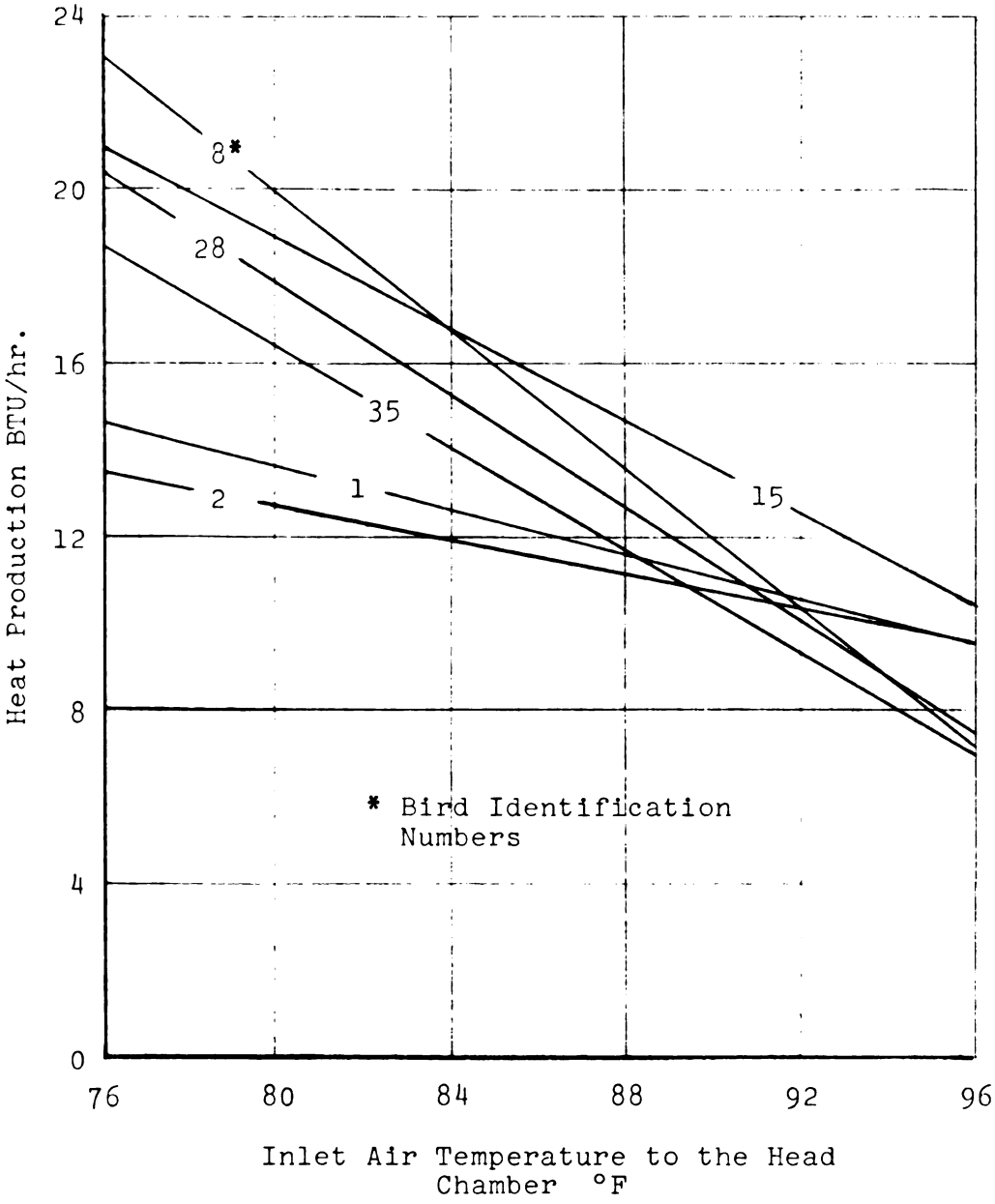

Figure A.4.4-- Individual sensible heat production in the body chamber

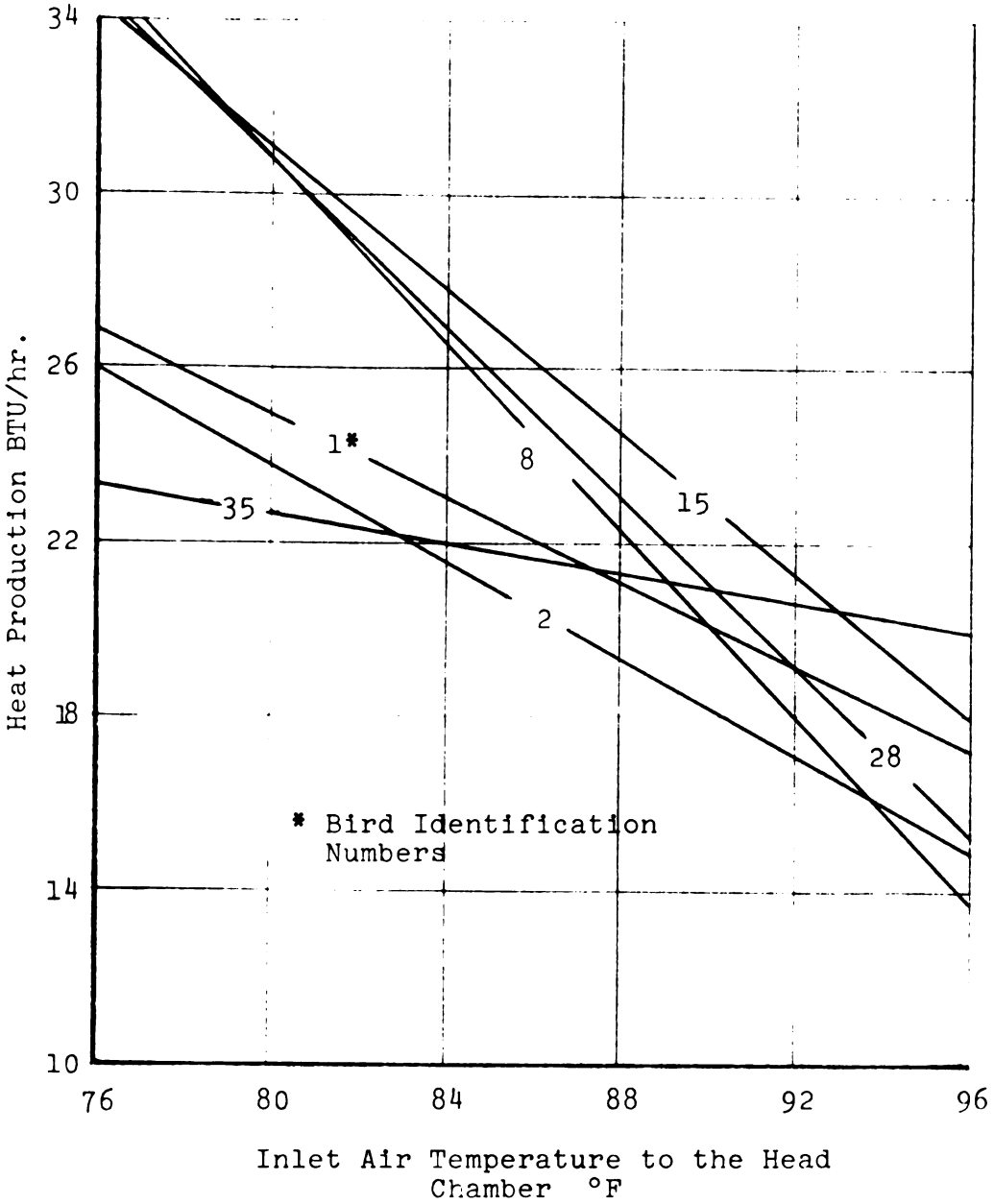

Figure A.4.5-- Individual total sensible heat production

APPENDIX A.5

Table A.1 Latent heat production from the head chamber

Temperature	Humidity	Heat Production	Estimated Heat Production	95% Confidence Limits	
78.99	0.5950	2.04	2.8	4.3	1.3
79.62	0.5950	1.98	2.8	4.1	1.5
79.36	0.5900	1.63	2.8	4.2	1.4
79.22	0.5900	3.12	2.8	4.2	1.4
76.69	0.6050	4.47	3.3	5.6	1.0
78.32	0.6100	2.37	2.9	4.6	1.2
79.48	0.6900	2.41	2.8	4.2	1.4
79.11	0.6800	2.47	2.8	4.3	1.4
79.19	0.6800	3.57	2.8	4.2	1.4
78.53	0.6800	3.00	2.9	4.5	1.3
78.44	0.6990	1.08	2.9	4.5	1.3
77.73	0.6990	3.91	3.0	4.9	1.2
80.00	0.6900	4.56	2.8	4.1	1.6
81.67	0.6800	1.39	3.0	4.1	1.9
80.17	0.6800	2.32	2.8	4.1	1.6
81.44	0.6800	2.13	2.9	4.0	1.9
80.60	0.7900	2.95	2.8	4.0	1.7
81.97	0.7900	2.58	3.1	4.1	2.0
81.79	0.7850	2.69	3.0	4.1	1.9
81.98	0.7850	3.46	3.1	4.1	2.0
77.48	0.7980	4.98	3.1	5.0	1.1
77.96	0.7760	3.64	3.0	4.8	1.2
85.24	0.6000	4.12	4.4	5.5	3.3
85.00	0.5950	5.93	4.3	5.4	3.2
86.64	0.5900	4.85	5.4	6.5	4.2
86.00	0.5900	3.35	4.9	6.0	3.8

Table A.1 (continued)

Temperature	Humidity	Heat Production	Estimated Heat Production	95% Confidence Limits	
85.49	0.6020	8.01	4.6	5.7	3.5
85.52	0.6070	4.61	4.6	5.7	3.5
86.52	0.7020	4.87	5.3	6.4	4.2
85.54	0.7020	3.98	4.6	5.7	3.5
85.51	0.7010	4.20	4.6	5.7	3.5
86.06	0.7020	4.40	4.9	6.1	3.8
84.68	0.7080	6.38	4.1	5.2	3.0
85.70	0.6990	8.75	4.7	5.8	3.6
86.22	0.7850	4.03	5.8	6.9	4.7
86.07	0.7750	4.63	4.9	6.1	3.8
86.90	0.7800	5.01	5.6	6.7	4.4
86.22	0.7750	2.67	5.1	6.2	3.9
84.99	0.7690	8.50	4.3	5.4	3.2
85.75	0.7730	4.45	4.7	5.9	3.6
90.71	0.5970	6.78	9.3	10.3	8.3
91.10	0.5860	5.23	9.8	10.8	8.7
91.50	0.5780	6.61	10.3	11.3	9.2
91.39	0.5870	4.44	10.1	11.1	9.1
88.95	0.5980	5.24	7.4	8.5	6.2
88.92	0.5920	7.82	7.3	8.4	6.2
92.33	0.7000	4.17	11.3	12.4	10.3
92.62	0.7000	8.12	11.7	12.8	10.7
92.75	0.6770	8.55	11.9	12.9	10.9
91.25	0.6960	4.64	9.9	10.9	8.9
88.60	0.7100	4.93	7.0	8.1	5.9
88.65	0.7070	5.34	7.1	8.2	5.9

Table A.1 (continued)

Temperature	Humidity	Heat Production	Estimated Heat Production	95% Confidence Limits	
88.56	0.8000	10.09	7.0	8.1	5.9
91.58	0.7950	5.20	10.4	11.4	9.3
92.03	0.7980	5.36	11.0	12.0	9.9
89.94	0.7960	3.22	8.4	9.4	7.4
87.94	0.7930	7.99	6.4	7.5	5.3
87.87	0.7910	6.68	6.4	7.5	5.2
94.18	0.5950	19.04	14.1	15.3	12.8
93.02	0.5950	16.18	12.3	13.4	11.3
93.06	0.5950	20.07	12.4	13.5	11.3
93.72	0.5950	19.22	13.3	14.5	12.2
99.37	0.5950	12.34	23.6	26.7	20.5
94.63	0.5980	18.05	14.8	16.1	13.5
97.81	0.7000	17.57	20.4	22.8	18.1
96.10	0.7000	16.34	17.2	19.0	15.5
97.38	0.7000	18.83	19.6	21.8	17.4
96.18	0.7000	19.20	17.4	19.1	15.7
94.97	0.7100	20.72	15.3	16.7	13.9
95.36	0.7070	20.42	16.0	17.5	14.5
92.52	0.8000	18.42	11.6	12.7	10.6
94.19	0.8100	15.73	14.1	15.3	12.8
93.96	0.8000	17.24	13.7	14.9	12.5
94.15	0.8050	16.14	14.0	15.2	12.8
94.21	0.8000	19.22	14.1	15.3	12.9
93.40	0.7750	17.71	12.9	13.9	11.8

Table A.2 Sensible heat production from the head chamber

Temperature	Humidity	Heat Production	Estimated Heat Production	95% Confidence Limits	
78.99	0.5950	14.44	11.8	12.7	10.9
79.62	0.5950	13.72	11.6	12.5	10.7
79.36	0.5900	13.49	11.7	12.6	10.7
79.22	0.5900	11.93	11.7	12.6	10.8
76.69	0.6050	9.22	12.5	13.6	11.4
78.32	0.6100	12.68	12.0	13.0	11.0
79.48	0.6900	11.09	11.6	12.5	10.7
79.11	0.6800	12.08	11.8	12.7	10.8
79.19	0.6800	9.05	11.7	12.7	10.8
78.53	0.6800	11.82	11.9	12.9	10.9
78.44	0.6990	17.18	12.0	12.9	11.0
77.73	0.6990	7.05	12.2	13.2	11.1
80.00	0.6900	12.06	11.5	12.3	10.6
81.67	0.6800	9.87	11.0	11.7	10.2
81.44	0.6800	8.08	11.0	11.8	10.3
80.60	0.7900	13.78	11.3	12.1	10.5
81.97	0.7900	14.77	10.9	11.6	10.1
81.79	0.7850	12.86	10.9	11.6	10.1
81.98	0.7850	15.21	10.9	11.6	10.1
77.48	0.7980	8.39	12.3	13.3	11.2
77.96	0.7760	12.93	12.1	13.1	11.1
85.24	0.6000	7.76	9.9	10.5	9.3
85.00	0.5950	8.50	9.9	10.5	9.4
86.64	0.5900	8.68	9.5	10.0	8.9
86.00	0.5900	7.00	9.7	10.2	9.1

Table A.2 (continued)

Temperature	Humidity	Heat Production	Estimated Heat Production	95% Confidence Limits	
85.49	0.6020	10.98	9.7	10.4	9.2
85.52	0.6070	8.27	9.8	10.4	9.2
86.52	0.7020	8.73	9.5	10.0	8.9
85.54	0.7020	10.66	9.8	10.4	9.2
85.51	0.7010	9.99	9.8	10.4	9.2
86.06	0.7020	10.57	9.6	10.2	9.1
84.68	0.7080	11.00	10.1	10.7	9.5
85.70	0.6990	9.28	9.7	10.3	9.2
87.22	0.7850	13.21	9.6	10.2	9.1
86.07	0.7750	11.23	9.7	10.3	9.2
86.90	0.7800	8.62	9.4	9.9	8.8
86.22	0.7750	7.51	9.6	10.1	9.0
84.99	0.7690	11.41	9.9	10.5	9.4
85.75	0.7730	5.25	9.7	10.3	9.2
90.71	0.5970	9.18	8.2	8.9	7.6
91.10	0.5860	8.21	8.1	8.7	7.4
91.50	0.5780	10.73	8.0	8.9	7.3
91.39	0.5870	7.11	8.0	8.7	7.3
88.95	0.5980	8.58	8.8	9.3	8.2
88.92	0.5920	10.73	8.8	9.3	8.2
92.33	0.7000	7.27	7.7	8.4	7.0
92.62	0.7000	13.45	7.6	8.4	6.9
92.75	0.6770	11.45	7.6	8.3	6.8
91.25	0.6960	6.51	8.1	8.7	7.4
88.60	0.7100	8.18	8.9	9.4	8.3
88.65	0.7070	7.72	8.8	9.4	8.3

Table A.2 (continued)

Temperature	Humidity	Heat Production	Estimated Heat Production	95% Confidence Limits	
88.56	0.8000	12.98	8.9	9.4	8.3
91.58	0.7950	9.53	7.9	8.6	7.3
92.03	0.7980	8.94	7.8	8.5	7.1
89.94	0.7960	4.96	8.4	9.1	7.8
87.94	0.7930	13.17	9.1	9.6	8.5
87.87	0.7910	10.40	9.1	9.6	8.5
94.18	0.5950	5.07	7.2	8.0	6.3
93.02	0.5950	6.94	7.5	8.2	6.7
93.06	0.5950	6.92	7.5	8.2	6.7
93.72	0.5950	5.87	7.3	8.1	6.5
99.37	0.5950	8.56	5.6	6.8	4.3
94.63	0.5980	4.01	7.0	7.9	6.1
97.81	0.7000	6.95	6.1	7.2	5.0
96.10	0.7000	6.68	6.6	7.6	5.6
97.38	0.7000	7.47	6.2	7.3	5.1
96.18	0.7000	7.73	6.5	7.5	5.6
94.97	0.7100	5.37	6.9	7.8	6.0
95.36	0.7070	5.95	6.8	7.7	5.9
92.52	0.8000	4.55	7.7	8.4	6.9
94.19	0.8100	3.50	7.2	8.0	6.3
93.96	0.8000	5.88	7.2	8.1	6.4
94.15	0.8050	5.56	7.2	8.0	6.3
94.21	0.8000	5.48	7.1	8.0	6.3
93.40	0.7750	4.96	7.4	8.2	6.6

Table A.3 Sensible heat production from the body chamber

Temperature	Humidity	Heat Production	Estimated Heat Production	95% Confidence Limits	
78.99	0.5950	18.36	17.0	18.6	15.4
79.62	0.5950	15.71	17.0	18.5	15.3
79.36	0.5900	16.63	16.9	18.5	15.4
79.22	0.5900	19.28	17.0	18.6	15.4
76.69	0.6050	15.82	17.5	19.2	15.7
78.32	0.6100	20.89	17.2	18.9	15.6
79.48	0.6900	15.05	17.4	19.1	15.7
79.11	0.6800	17.12	17.4	19.1	15.7
79.19	0.6800	15.78	17.3	19.1	15.7
78.53	0.6800	18.83	17.4	19.1	15.7
78.44	0.6990	16.43	17.6	19.3	15.8
77.73	0.6990	12.38	18.1	20.0	16.2
80.00	0.6900	15.57	17.0	18.6	15.4
81.67	0.6800	16.83	16.9	18.4	15.3
80.17	0.6800	14.98	16.9	18.5	15.3
81.44	0.6800	18.76	16.9	18.4	15.3
80.60	0.7900	20.47	16.7	18.2	15.2
81.97	0.7900	18.39	13.2	14.2	12.3
77.48	0.7980	9.20	16.9	18.5	15.3
81.98	0.7850	21.63	16.4	17.8	14.9
77.96	0.7760	8.45	16.9	18.5	15.3
85.24	0.6000	22.37	14.0	14.9	13.0
85.00	0.5950	15.61	14.0	14.9	13.0
86.64	0.5900	16.74	13.9	14.8	12.9
86.00	0.5900	17.26	14.0	14.9	13.0

Table A.3 (continued)

Temperature	Humidity	Heat Production	Estimated Heat Production	95% Confidence Limits	
85.49	0.6020	16.88	13.6	14.6	12.7
85.52	0.6070	8.79	13.6	14.6	12.7
86.52	0.7020	20.40	13.7	14.6	12.7
85.54	0.7020	14.58	13.8	14.8	12.9
85.51	0.7010	14.56	13.8	14.8	12.8
86.06	0.7020	14.85	13.8	14.8	12.9
84.68	0.7080	8.83	13.4	14.4	12.5
85.70	0.6990	12.29	12.6	13.6	11.6
87.22	0.7850	19.78	13.8	14.7	12.8
86.07	0.7750	16.32	13.7	14.6	12.7
86.90	0.7800	15.67	13.7	14.6	12.7
86.22	0.7750	18.31	13.8	14.8	12.9
84.99	0.7690	14.76	13.3	14.2	12.3
85.75	0.7730	19.48	13.2	14.2	12.3
90.71	0.5970	6.52	11.9	12.9	10.8
91.10	0.5860	9.77	11.7	12.8	10.7
91.50	0.5780	3.05	11.9	13.0	10.9
91.39	0.5870	7.56	12.0	13.0	10.9
88.95	0.5980	3.82	12.6	13.6	11.6
88.92	0.5920	5.97	12.5	13.5	11.6
92.33	0.7000	13.74	11.2	12.4	10.0
92.62	0.7000	18.48	11.0	12.2	9.7
92.75	0.6770	12.62	10.9	12.2	9.7
91.25	0.6960	15.76	11.6	12.8	10.5
88.60	0.7100	16.84	12.4	13.5	11.5
88.65	0.7070	4.45	12.5	13.5	11.5

Table A.3 (continued)

Temperature	Humidity	Heat Production	Estimated Heat Production	95% Confidence Limits	
88.56	0.8000	14.76	12.0	13.0	10.9
91.58	0.7950	12.84	11.9	12.7	10.5
92.03	0.7980	15.80	11.6	12.7	10.5
89.94	0.7960	5.83	12.0	13.1	11.1
87.94	0.7930	12.79	12.6	13.5	11.6
87.87	0.7910	13.83	12.5	13.5	11.5
94.18	0.5950	13.04	10.9	12.2	9.6
93.02	0.5950	5.78	10.8	12.1	9.5
93.06	0.5950	7.11	10.8	12.1	9.6
93.72	0.5950	11.23	10.8	12.1	9.5
99.37	0.5950	10.60	9.5	11.1	7.8
94.63	0.5980	15.39	9.5	11.1	7.8
97.81	0.7000	10.67	10.2	11.6	8.7
96.10	0.7000	3.35	10.1	11.5	8.5
97.38	0.7000	8.74	10.0	11.5	8.5
96.18	0.7000	9.54	10.0	11.5	8.5
94.97	0.7100	9.84	9.3	11.0	7.6
95.36	0.7070	8.64	9.2	10.9	7.4
92.52	0.8000	13.61	10.4	11.8	9.1
94.19	0.8100	10.16	10.3	11.7	8.8
93.96	0.8000	4.61	10.3	11.7	8.8
94.15	0.8050	9.56	10.3	11.7	8.9
94.21	0.8000	6.33	9.2	10.9	7.5
93.40	0.7750	8.94	9.5	11.1	7.8

Table A.4 Total sensible heat production from body and head chambers

Temperature	Humidity	Heat Production	Estimated Heat Production	95% Confidence Limits	
78.99	0.5950	32.80	28.8	30.7	26.8
79.62	0.5950	29.43	28.7	30.7	26.8
79.36	0.5900	30.12	28.7	30.7	26.7
79.22	0.5900	31.21	28.8	30.7	26.8
76.69	0.6050	25.04	30.0	31.7	27.4
78.32	0.6100	33.57	29.2	31.2	27.1
79.48	0.6900	26.14	29.4	31.6	27.3
79.11	0.6800	29.20	29.4	31.6	27.3
79.19	0.6800	24.83	29.3	31.4	27.2
78.53	0.6800	30.65	29.4	31.5	27.3
78.44	0.6990	33.61	29.7	31.9	27.5
77.73	0.6990	19.43	30.6	33.0	28.2
80.00	0.6900	27.64	28.7	30.7	26.7
81.67	0.6800	26.70	28.5	30.5	26.6
80.17	0.6800	22.13	28.6	30.5	26.6
81.44	0.6800	26.84	28.5	30.5	26.6
80.60	0.7900	34.21	28.2	30.0	26.3
81.97	0.7900	33.16	22.5	23.6	21.3
81.79	0.7850	30.24	27.5	29.2	25.8
81.98	0.7850	36.84	27.7	29.5	25.9
77.48	0.7980	17.59	28.7	30.6	26.7
77.96	0.7760	21.38	28.6	30.5	26.6
85.24	0.6000	30.13	23.7	24.9	22.5
85.00	0.5950	24.11	23.7	24.9	22.5
86.64	0.5900	25.42	23.5	27.7	22.3
86.00	0.5900	24.26	23.7	24.9	22.5

Table A.4 (continued)

Temperature	Humidity	Heat Production	Estimated Heat Production	95% Confidence Limits	
85.49	0.6020	27.86	23.1	24.3	22.0
85.52	0.6070	17.06	23.1	24.3	22.0
86.52	0.7020	29.13	23.2	24.3	22.0
85.54	0.7020	25.24	23.4	24.6	22.3
85.51	0.7010	24.55	23.5	24.6	22.3
86.06	0.7020	25.42	23.5	24.6	22.3
84.86	0.7080	19.82	22.8	24.0	21.6
85.70	0.6990	23.52	21.3	22.6	20.1
87.22	0.7850	29.06	23.4	24.5	22.2
86.07	0.7750	29.53	23.2	24.3	22.0
86.90	0.7800	24.29	23.2	24.3	22.0
86.22	0.7750	25.82	23.5	24.7	22.3
84.99	0.7690	26.17	22.5	23.6	21.3
85.75	0.7730	24.73	22.4	23.6	21.3
90.71	0.6970	15.69	20.2	21.5	18.9
91.10	0.5860	17.98	19.9	21.3	18.6
91.50	0.5780	14.81	20.4	21.6	19.1
91.39	0.5870	14.67	20.3	21.6	19.0
88.95	0.5980	12.39	21.4	22.6	20.2
88.92	0.5920	16.69	21.3	22.5	20.1
92.33	0.7000	21.02	19.0	20.5	17.5
92.62	0.7000	31.93	18.7	20.2	17.1
92.75	0.6770	24.07	18.6	20.1	17.0
91.25	0.6960	22.27	19.8	21.2	18.4
88.60	0.7100	25.02	21.2	22.4	20.0
88.65	0.7070	12.17	21.2	22.4	20.0

Table A.4 (Continued)

Temperature	Humidity	Heat Production	Estimated Heat Production	95% Confidence Limits	
88.56	0.8000	27.74	20.3	21.6	19.0
91.58	0.7950	22.38	19.7	21.1	18.3
92.03	0.7980	24.74	19.8	21.1	18.3
89.94	0.7960	10.79	20.4	21.7	19.1
87.94	0.7930	25.96	21.3	22.5	20.1
87.87	0.7910	24.23	21.1	22.4	20.0
94.18	0.5950	18.11	18.5	20.1	16.9
93.02	0.5950	12.72	18.4	20.0	16.8
93.06	0.5950	14.03	18.5	20.1	16.9
93.72	0.5950	17.09	18.4	20.0	16.8
99.37	0.5950	19.16	16.2	18.2	14.1
94.63	0.5980	19.40	16.1	18.2	14.1
97.81	0.7000	17.61	17.3	19.1	15.5
96.10	0.7000	10.03	17.1	18.9	15.2
97.38	0.7000	16.21	17.0	18.8	15.1
96.18	0.7000	17.26	17.0	18.9	15.2
94.97	0.7100	15.19	15.8	17.9	13.7
95.36	0.7070	14.59	15.7	17.8	13.5
92.52	0.8000	18.15	17.8	19.5	16.1
94.19	0.8100	13.66	17.5	19.3	15.7
93.96	0.8000	10.49	17.5	19.3	15.7
94.15	0.8050	15.12	17.5	19.3	15.7
94.21	0.8000	11.81	15.7	17.8	13.6
93.40	0.7750	13.90	16.1	18.2	14.1

Table A.5 Sensible heat loss from the respiratory system

Temperature	Humidity	Heat Production	Estimated Heat Production	95% Confidence Limits	
78.99	0.5950	4.82	8.6	9.6	7.6
79.63	0.5950	10.76	8.5	9.6	7.6
79.36	0.5900	9.10	8.5	9.5	7.6
79.22	0.5900	8.76	8.6	9.5	7.6
76.69	0.6050	9.12	9.2	10.3	8.0
78.32	0.6100	8.99	8.8	9.8	7.7
79.48	0.6900	8.66	8.5	9.4	7.5
79.11	0.6800	9.46	8.6	9.6	7.6
79.19	0.6800	5.29	8.6	9.5	7.6
78.53	0.6800	9.77	8.7	9.7	7.7
78.44	0.6990	8.13	8.7	9.8	7.8
77.73	0.6990	10.78	8.9	10.0	7.8
80.00	0.6900	5.64	8.4	9.3	7.5
81.67	0.6800	7.66	8.0	8.8	7.2
80.17	0.6800	11.82	8.3	9.2	7.4
81.44	0.6800	6.44	8.0	8.8	7.2
80.60	0.7900	11.40	8.2	9.1	7.4
81.97	0.7900	12.10	7.9	8.7	7.1
81.79	0.7850	11.04	7.9	8.7	7.2
81.98	0.7850	13.10	7.9	8.7	7.2
77.48	0.7980	5.00	8.9	10.1	7.9
85.24	0.6000	6.06	7.1	7.7	6.5
85.00	0.5950	5.18	7.2	7.8	6.6
86.64	0.5900	6.11	6.8	7.4	6.2
86.00	0.5900	4.07	6.9	7.5	6.3

Table A.5 (continued)

Temperature	Humidity	Heat Production	Estimated Heat Production	95% Confidence Limits	
85.49	0.6020	7.30	7.1	7.7	6.4
85.52	0.6070	4.81	7.0	7.7	6.4
86.52	0.7020	6.55	6.8	7.4	6.2
85.54	0.7020	8.23	7.0	7.6	6.4
85.51	0.7010	7.20	7.0	7.7	6.4
86.06	0.7020	7.81	6.9	7.5	6.3
84.68	0.7080	7.42	7.2	7.9	6.6
85.70	0.6990	8.01	7.0	7.6	6.4
87.22	0.7850	7.11	6.6	7.2	6.1
86.07	0.7750	10.18	6.9	7.5	6.3
86.90	0.7800	6.06	6.7	7.3	6.1
86.22	0.7750	4.39	6.9	7.5	6.3
84.99	0.7690	8.14	7.2	7.8	6.6
85.75	0.7730	2.22	7.0	7.6	6.4
90.71	0.5970	7.72	5.8	6.5	5.1
91.10	0.5860	5.33	5.7	6.4	5.0
91.50	0.5780	9.53	5.6	6.3	4.9
91.39	0.5870	4.33	5.6	6.3	4.9
88.95	0.5980	5.94	6.2	6.8	5.6
88.92	0.5920	7.89	6.2	6.8	5.6
92.33	0.7000	5.06	5.4	6.2	4.7
92.62	0.7000	10.77	5.3	6.1	4.6
92.75	0.6770	9.90	5.3	6.1	4.5
91.25	0.6960	3.97	5.7	6.4	5.0
88.60	0.7100	5.27	6.3	6.9	5.7
88.65	0.7070	4.84	6.3	6.9	5.7

Table A.5 (continued)

Temperature	Humidity	Heat Production	Estimated Heat Production	95% Confidence Limits	
88.56	0.8000	10.57	6.3	6.9	5.7
91.58	0.7950	6.43	5.6	6.3	4.9
92.03	0.7980	6.61	5.5	6.2	4.6
89.94	0.7960	2.85	6.0	6.6	5.4
87.94	0.7930	10.48	6.5	7.1	5.9
87.87	0.7910	7.56	6.5	7.1	5.9
94.18	0.5950	3.09	5.0	5.9	4.1
93.02	0.5950	4.56	5.2	6.1	4.4
93.06	0.5950	4.67	5.2	6.0	4.4
93.72	0.5950	3.88	5.1	5.9	4.2
99.37	0.5950	6.92	3.7	5.0	2.4
94.63	0.5980	1.55	4.9	5.8	3.9
97.81	0.7000	5.43	4.1	5.3	2.9
96.10	0.7000	4.87	4.5	5.5	3.6
97.38	0.7000	5.28	4.2	5.3	3.1
96.18	0.7000	5.61	4.5	5.5	3.5
94.97	0.7100	3.69	4.8	5.7	3.8
95.36	0.7070	3.61	4.7	5.7	3.7
92.52	0.8000	2.51	5.4	6.1	4.6
94.19	0.8100	1.49	5.0	5.9	4.1
93.96	0.8000	3.99	5.0	5.9	4.2
94.15	0.8050	3.75	5.0	5.9	4.1
94.21	0.8000	3.04	5.0	5.9	4.1
93.40	0.7750	2.36	5.2	6.0	4.3

APPENDIX A.6

```
      PROGRAM TEST
      COMMON X1,X2,VSA,CFM
      DIMENSION D(100),B(100)
      CFM=.420
      RH1=61.0
      RH2=.615
      PRINT 50
50    FORMAT(1H1,15X,*HC  INLET  OUTLET  TEMP(4,6 AND 1,16)*////)
      PRINT 21
      N=1
32    READ(60,20) D(N)
      IF(9999.-D(N))2,2,1
 1    N=N+1
      NN=N-1
      GO TO 32
 2    WRITE(61,20)(D(J),J=1,NN)
      PRINT22
      M=1
33    READ(60,20)B(M)
      IF(9999.-B(M))4,4,3
 3    M=M+1
      MM=M-1
      GO TO 33
 4    WRITE(61,20) (B(J),J=1,MM)
      SUM1=0.
      AUM1=0.
      SUM2=0.
      AUM2=0.
      DO 5 J=1,NN
 5    SUM1=D(J)+SUM1
      E=NN
      X1=SUM1/E
      DO 6 J=1,NN
```

```
6     AUM1=(B(J)-X1)**2+AUM1
            V1=AUM1/(E-1.)
      S1=SQRT(V1)
      PRINT 7
      WRITE(61,8) X1,S1,V1
 7    FORMAT(1H0,10X,*MEAN*,10X,*STANDARD DEVIATION *,10X,*VARIANCE*//)
 8    FORMAT(F16.4,F23.4,F23.4////)
      DO 9 J=1,MM
 9    SUM2=B(J)+SUM2
      F=MM
      X2=SUM2/F
      DO 10 J=1,MM
10    AUM2=(B(J)-X2)**2+AUM2
      V2=AUM2/(F-1.)
      S2=SQRT(V2)
      PRINT 7
      WRITE(61,8)X2,S2,V2
      A=X1-X2
      BB=(E*V1+F*V2)/(E+F-2.)
      A1=N-1
      A2=M-1
      CC=(1./A1+1./A2)
      T=A/(SQRT(BB)*SQRT(CC))
      PRINT 23
      WRITE(61,20) T
20    FORMAT(F30.6)
21    FORMAT(1H0,20X,*X INPUTS*////)
22    FORMAT(1H0,20X,*Y INPUTS*////)
23    FORMAT(1H0,20X,*T TEST RESULTS*//)
      PS1=-.430686+.020957**X1-.000291183*X1**2+.000002196S3*X1**3
      PV1=PH1*PS1
      PS2=-.430686+.020957**X2-.000291183*X2**2+.000002196S3*X2**3
      PV2=PH2*PS2
```

```
      VSA=1.*53.35*(X1+460.69)/(144.*(14.696-PV1))
      W1=53.35/97.79*(PV1/(14.696-PV1))
      W2=53.35/97.79*(PV2/(14.696-PV2))
      EH1=.24*X1+W1*(1061.2+.45*X1)
      EH2=.24*X2+W2*(1061.2+.45*X2)
      PRINT 27
   27 FORMAT(1H0,10X,*VAPOR PRESS IN*,10X,*S VAPOR PRESS IN*,10X,
     1*VAPOR PRESS OUT*,10X,*S VAPOR PRESS OUT*//)
      WRITE(61,28)PV1,PS1,PV2,PS2
   28 FORMAT(1H ,10X,F10.4,14X,F12.4,10X,F10.4,14X,F12.4////)
      PRINT 29
   29 FORMAT(1H0,10X,*ABS. HUMIDITY IN*,10X,*ABS. HUMIDITY OUT*,10X,
     1*ENTHALPY IN*,10X,*ENTHALPY OUT*//)
      WRITE(61,30)W1,W2,EH1,EH2
   30 FORMAT(1H ,10X,F12.4,14X,F13.4,14X,F14.4,12X,F10.4////)
      QS=(EH2-EH1)*CFM/VSA*60.
      QL=(W2-W1)*1040.1* CFM/VSA*60.
      WRITE(61,24)QS
   24 FORMAT(1H0,10X,*SENSIPLE HEAT TRANSFER IN HC = *,F6.3,* BTU/HR*
     1//)
      WRITE(61,25)QL
   25 FORMAT(1H0,10X,* LATENT HEAT TRANSFER IN HC   = *,F6.3,* BTU/HR*
     1////)
      CALL COMB
      CALL WADDLE
      CONTINUE
      END
```

```
      SUBROUTINE PADDLE
      COMMON X1,X2,VSA,CFM
      DIMENSION D(100)
      PRINT 50
   50 FORMAT(1H1,15X,*PADDLE TEMPERATURE (10)*////)
      PRINT 23
      N=1
   22 READ(60,20)D(N)
      IF(2220.-D(N))2,2,1
    1 N=N+1
      NN=N-1
      GO TO 22
    2 WRITE(61,20)(D(J),J=1,NN)
      SUM=0.
      AUM=0.
      DO 3 J=1,NN
    3 SUM=D(J)+SUM
      R=NN
      X=SUM/R
      DO 4 J=1,NN
    4 AUM=(D(J)-X)**2+AUM
      V=AUM/(R-1.)
      S=SQRT(V)
      PRINT 5
      WRITE(61,6)X,S,V
    5 FORMAT(1H0,10X,*MEAN*,10X,*STANDARD DEVIATION *,10X,*VARIANCE*//)
    6 FORMAT(F16.4,F23.4,F23.4)
   20 FORMAT(F30.6)
   23 FORMAT(1H0,20X,*INPUT VALUES*//)
      DL=2.
      DX=1.
      RU=5.
```

```
      ADD=DX**2+DY**2+DZ**2
      DT=1.0/SQRT(X-X3)
      WRITE(6,30)DT
   30 FORMAT(1H0,10X,*HEAT LOSS FROM THE PANELS = *,F6.3,*  BTU/HR*///)
      RETURN
      END
```

```
      SUBROUTINE COMB
      COMMON X1,X2,VSA,CEN
      DIMENSION D(100)
      PRINT 50
   50 FORMAT(1H1,15X,*COMB TEMPERATURE (3)*////)
      PRINT 23
      N=1
   22 READ(60,20)D(N)
      IF(2000.-D(N))2,2,1
    1 N=N+1
      NN=N-1
      GO TO 22
    2 WRITE(61,20)(D(J),J=1,NN)
      SUM=0.
      AUM=0.
      DO 3 J=1,NN
    3 SUM=D(J)+SUM
      B=NN
      X=SUM/B
      DO 4 J=1,NN
    4 AUM=(D(J)-X)**2+AUM
      V=AUM/(B-1.)
      S=SQRT(V)
      PRINT 5
      WRITE(61,6)X,S,V
    5 FORMAT(1H0,10X,*MEAN*,10X,*STANDARD DEVIATION *,10X,*VARIANCE*//)
    6 FORMAT(F16.4,F23.4,F23.4)
   20 FORMAT(F30.6)
   23 FORMAT(1H0 20X,*INPUT VALUES*//)
      DL=4.2
      DX=2.4
      BH=5.
      AR=DX*DL+1.5/144.
```

```
      X3=(X1+X2)/2.
      QT=PH*AP*(X-X3)
      WRITE(61,30)QT
30    FORMAT(1H0,10X,*HEAT LOSS FROM THE COND    =*,F6.3,*  BTU/HR*////)
        RETURN
      END
```

APPENDIX A.7

```
      PROGRAM TEST
      DIMENSION D(100),B(100)
      PRINT 50
50    FORMAT(1H1,15X,*HC INSIDE AND OUTSIDE TEMP (K,2)*////)
      PRINT 21
      N=1
33    READ(60,20) D(N)
      IF(9999.-D(N))2,2,1
 1    N=N+1
      NN=N-1
      GO TO 33
 2    WRITE(61,20)(D(J),J=1,NN)
      PRINT22
      M=1
33    READ(60,20)B(M)
      IF(9999.-B(M))4,4,3
 3    M=M+1
      MM=M-1
      GO TO 33
 4    WRITE(61,20) (B(J),J=1,MM)
      SUM1=0.
      AUM1=0.
      SUM2=0.
      AUM2=0.
      DO 5 J=1,NN
 5    SUM1=D(J)+SUM1
      E=NN
      X1=SUM1/E
      DO 6 J=1,NN
6     AUM1=(D(J)-X1)**2+AUM1
          V1=AUM1/(E-1.)
      S1=SQRT(V1)
      PRINT 7
```

```
      WRITE(61,8) X1,S1,V1
    7 FORMAT(1H0,10X,*MEAN*,10X,*STANDARD DEVIATION *,10X,*VARIANCE *//)
    8 FORMAT(F16.4,F23.4,F23.4////)
      DO 9 J=1,MM
    9 SUM2=B(J)+SUM2
      F=MM
      X2=SUM2/F
      DO 10 J=1,MM
   10 AUM2=(B(J)-X2)**2+AUM2
      V2=AUM2/(F-1.)
      S2=SQRT(V2)
      PRINT 7
      WRITE(61,8)X2,S2,V2
      A=X1-X2
      BB=(F*V1+F*V2)/(F+F-2.)
      A1=N-1
      A2=M-1
      CC=(1./A1+1./A2)
      T=A/(SQRT(BB)*SQRT(CC))
      PRINT 23
      WRITE(61,20) T
   20 FORMAT(F30.6)
   21 FORMAT(1H0 20X,*X INPUTS*////)
   22 FORMAT(1H0,20X,*Y INPUTS*////)
   23 FORMAT(1H0,20X,*T TEST RESULTS*//)
      Q=20.*.2002/(.1875*12.)*(X1 -X2)
      WRITE(61,24)Q
   24 FORMAT(1H0,10X,*HEAT LOSS BY CONDUCTION THROUGH HC=*,F6.3,*BTU/HR*
     1////)
      END
```

APPENDIX A.8

```
      PROGRAM ANAL
      DIMENSION T(100),E(100),PH(100),R(80,76),W(100),S(100)
      DIMENSION D(100)
      DIMENSION TH(10),SIGNS(6),DIFF(6)
      COMMON T,PH
      EXTERNAL MODEL
      NOR=76
    1 FORMAT(11E7.0)
   16 FORMAT(7E7.0)
   19 FORMAT(11E10.4)
   20 FORMAT(7E10.4)
      WRITE(61,3)
      DO 14 I=1,76
      READ(60,1)(D(J),J=1,33)
      WRITE(61,19)(D(J),J=1,33)
      READ(60,16)(D(J),J=34,40)
      WRITE(61,20)(D(J),J=34,40)
      DO 21 J=1,40
   21 R(I,J)=D(J)
   14 CONTINUE
      WRITE(61,3)
    3 FORMAT(1H1)
      PRINT 23
   23 FORMAT(1H ,*TEMPERATURE*,5X,*HUMIDITY*,5X,*HEAT PRODUCTION*)
      DO 4 I=1,NOR
      R(I,14)=R(I,14)+R(I,34)-R(I,19)-R(I,21)
      R(I,27)=R(I,27)+R(I,40)
      S(I)=R(I,14)+R(I,27)
      W(I)=R(I,15)+R(I,28)
      E(I)=R(I,27)
      T(I)=R(I,22)
      PH(I)=R(I,7)
      WRITE(61,22)T(I),PH(I),E(I)
```

```
22   FORMAT(3X,F6.2,8X,F6.4,8X,F8.2)
 4   CONTINUE
     TH(1)=1.
     TH(2)=1.
     DO 11 I=1,2
     SIGNS(I)=0.
11   DIFF(I)=.01
     EPS1=1.0E-5
     EPS2=1.0E-5
     CALL GAUSHAUS(1,MODEL,NOB,F,2,TH,DIFF,SIGNS,EPS1,EPS2,10,.01,10.)
     END
     SUBROUTINE MODEL(NPROB,TH,F,NOB,NP)
     DIMENSION TH(1),F(1),T(100),RH(100)
     COMMON T,RH
      DO 8 J=1,NOB
7    F(J)=TH(1)+TH(2)*T(J)
 8   CONTINUE
     RETURN
     END
```

APPENDIX A.9

```
      PROGRAM NOSE
      DIMENSION T(700),P(700),S(700),V(700),W(700)
20    FORMAT(1H1,3E30.4)
21    FORMAT(1H0,I10,7E16.4)
22    FORMAT(1H0,4E30.4)
      AP=1.75/12.
      DX=.01/12.
      AL=1./12.
      AR=.0760
      AD=.2/12.
      AV=67.5*60./(2.*3.1415*(AD*12.)**2/4.*12.)
      AH=4.*.015/(.1/12.)
      AA=3.1415*AD**2/4.
      AB=16.
      AC=.24
      AM=AV*AP*3.141592*AD**2/4.
      SUM=0.
      Z1=.000000801429
      Z2=-.00000742738
      Z3=.0004211112
      Z4=-.00480741
      N=1
      AU=.0125
      AT=70.
      TW=102.
      UP1=.0706
      Y1=AT
      Y2=AU
      WRITE(61,20)AT,TW,AU
      S(N)=TW
 1    TW=102.+12.*SUM
      T2=TW+(AT-TW)*EXP(-AH*AP*DX/(AM*AC))
      BP=Z1*TW**3+Z2*TW**2+Z3*TW+Z4
```

```
      B2=BP+(AU-BP)*EXP(-AR*AP*DX/AM)
      WRITE(61,21)N,TW,T2,BP,B2,AT, AU,SUM
      T(N)=SUM
      R(N)=AT
      V(N)=AU
      W(N)=BP
      AT=T2
      AU=B2
      N=N+1
      SUM=DX+SUM
      S(N)=TW
      IF(AL-SUM)2,1,1
    2 CONTINUE
      CALL PLOT(0.0,0.0,0.0,100.,100.)
      CALL PLOT(0.0,-30.,2)
      CALL PLOT(0.0,5.,2)
      CALL PLOT(0.0,0.0,0)
      CALL GRAPH1(T,R,100,5H06X06,4HAUTO,36H TEMPERATURE OF INSPIRED NAS
     1AL AIR...17H LENGTH IN FEET...27H TEMPERATURE IN DEGREES F..)
      CALL GRAPH1(T,S,100,7HOVERLAY,4HSAME)
      CALL PLOT(0.0,0.0,0.0,100.,100.)
      CALL PLOT(23.,0.0,3)
      CALL PLOT(0.0,0.0,0)
      CALL GRAPH1(T,V,100,5H06X06,4HAUTO,34H  HUMIDITY OF INSPIRED NASAL
     1 AIR...17H LENGTH IN FEET...20H ABSOLUTE HUMIDITY..)
      CALL GRAPH1(T,W,100,7HOVERLAY,4HSAME)
      AP=3.141592*.3/12.
      DX=.01/12.
      AL=1./12.
      AR=.0760
      AD=.3/12.
      AH=4.*.015/AD
      AV=67.5*60./(    3.1415*(AD*12.)**2/4.*12.)
```

```
      AA=3.141593*AD**2/4.
      AP=10.
      AC=.24
      AM=AV*A2*3.141593*AD**2/4.
      SUM=0.
      Z1=.000000903429
      Z2=-.000007427?8
      Z3=.000421112
      Z4=-.00489?41
      N=1
      UP1=.0706
      WRITE(61,20)AT,TW,AU
      S(N)=TW
3     TW=103.+12.*SUM
      T2=TW+(AT-TW)*EXP(-AH*AP*DX/(AM*AC))
      BP=Z1*TW**3+Z2*TW**2+Z3*TW+Z4
      B2=BP+(AU-BP)*EXP(-AP*AP*DX/AM)
      WRITE(61,21)N,TW,T2,BP,B2,AT, AU,SUM
      W(N)=BP
      V(N)=AU
      R(N)=AT
      T(N)=SUM
      AT=T2
      AU=B2
      N=N+1
      SUM=DX+SUM
      S(N)=TW
      IF(AL-SUM)4,3,3
4     CONTINUE
      CALL PLOT(0.0,0.0,0,0,100.,100.)
       CALL PLOT(23.,0.0,3)
      CALL PLOT(0.0,0.0,0)
      CALL GRAPH1(T,R,100,5H06X06,4HAUTO,40H TEMP OF INSPIRED NASAL TO T
```

```
     1RACHEA AIR...17H LENGTH IN FEET...20H ABSOLUTE HUMIDITY..)
      CALL GRAPH1(T,S,100.,7HOVERLAY,4HSAME)
      CALL PLOT(0.0,0.0,0.0,100.,100.)
       CALL PLOT(23.,0.0,3)
      CALL PLOT(0.0,0.0,0)
      CALL GRAPH1(T,V,100,5H06X06,4HAUTO,40H HUM. OF INSPIRED NASAL TO T
     1RACHEA AIR...17H LENGTH IN FEET...20H ABSOLUTE HUMIDITY..)
      CALL GRAPH1(T,W,100,7HOVERLAY,4HSAME)
      AP=3.141593*.15/12.
      AL=6./12.
      AD=.15/12.
      AV=67.5*60./(    3.1415*(AD*12.)**2/4.*12.)
      AH=4.*.015/AD
      AM=AV*AP*3.141593*AD**2/4.
      SUM=0.
      Z1=.000000801429
      Z2=-.00000742738
      Z3=.000421112
      Z4=-.00480741
      N=1
      UP1=.0706
      WRITE(61,20)AT,TW,AU
      S(N)=TW
    5 TW=104.+6.*SUM
      T2=TW+(AT-TW)*EXP(-AH*AP*DX/(AM*AC))
      BP=Z1*TW**3+Z2*TW**2+Z3*TW+Z4
      B2=BP+(AU-BP)*EXP(-AB*AP*DX/AM)
      WRITE(61,21)N,TW,T2,BP,B2,AT, AU,SUM
      W(N)=BP
      V(N)=AU
      R(N)=AT
      T(N)=SUM
      AT=T2
```

```
      AU=B2
      N=N+1
      SUM=DX+SUM
      S(N)=TW
      IF(AL-SUM)6,5,5
    6 CONTINUE
      CALL PLOT(0.0,0.0,0,100.,100.)
       CALL PLOT(23.,0.0,3)
      CALL PLOT(0.0,0.0,0)
      CALL GRAPH1(T,R,600,5H06X06,4HAUTO,38H TEMPERATURE OF INSPIRED TRA
     1CHEA AIR...17H LENGTH IN FEET...20H ABSOLUTE HUMIDITY..)
      CALL GRAPH1(T,S,600,7HOVERLAY,4HSAME)
      CALL PLOT(0.0,0.0,0.0,100.,100.)
       CALL PLOT(23.,0.0,3)
      CALL PLOT(0.0,0.0,0)
      CALL GRAPH1(T,V,600,5H06X06,4HAUTO,35H HUMIDITY OF INSPIRED TRACHE
     1A AIR...17HLENGTH  IN FEET...20H ABSOLUTE HUMIDITY..)
      CALL GRAPH1(T,W,600,7HOVERLAY,4HSAME)
      SUM=0.
      N=1
      AU=BP
      AT=TW
      WRITE(61,20)AT,TW,AU
      S(N)=TW
    7 TW=107.-6.*SUM
      BP=Z1*TW**3+Z2*TW**2+Z3*TW+Z4
      B2=BP+(AU-BP)*EXP(-AB*AP*DX/AM)
      T2=TW+(AT-TW)*EXP(-AH*AP*DX/(AM*AC)+(1060*DX*(B2-AU))/(AM*AC*
     1(TW-AT)))
      WRITE(61,21)N,TW,T2,BP,B2,AT, AU,SUM
      W(N)=BP
      V(N)=AU
      R(N)=AT
```

```
      T(N)=SUM
      AT=T2
      AU=B2
      N=N+1
      SUM=DX+SUM
      S(N)=TW
      IF(AL-SUM)8,7,7
    8 CONTINUE
      CALL PLOT(0.0,0.0,0.0,100.,100.)
       CALL PLOT(23.,0.0,3)
      CALL PLOT(0.0,0.0,0)
      CALL GRAPH1(T,R,600,5H06X06,4HAUTO,38H TEMPERATURE OF EXPIRED  TRA
     1CHEA AIR...17H LENGTH IN FEET...20H ABSOLUTE HUMIDITY..)
      CALL GRAPH1(T,S,600,7HOVERLAY,4HSAME)
      CALL PLOT(0.0,0.0,0.0,100.,100.)
       CALL PLOT(23.,0.0,3)
      CALL PLOT(0.0,0.0,0)
      CALL GRAPH1(T,V,600,5H06X06,4HAUTO,35H HUMIDITY OF EXPIRED  TRACHE
     1A AIR...17HLENGTH  IN FEET...20H ABSOLUTE HUMIDITY..)
      CALL GRAPH1(T,W,600,7HOVERLAY,4HSAME)
      AL=1./12.
      AD=.3/12.
      AH=4.*.015/AD
      AV=67.5*60./(    3.1415*(AD*12.)**2/4.*12.)
      AM=AV*AR*3.141592*AD**2/4.
      SUM=0.
      N=1
      WRITE(61,20)AT,TW,AU
      S(N)=TW
    9 TW=104.-12.*SUM
      BP=Z1*TW**3+Z2*TW**2+Z3*TW+Z4
      B2=BP+(AU-BP)*EXP(-AB*AP*DX/AM)
      T2=TW+(AT-TW)*EXP(-AH*AP*DX/(AM*AC)+(1060*DX*(B2-AU))/(AM*AC*
```

```
     1(TW-AT)))
      WRITE(61,21)N,TW,T2,BP,B2,AT, AU,SUM
      W(N)=BP
      V(N)=AU
      R(N)=AT
      T(N)=SUM
      AT=T2
      AU=B2
      N=N+1
      SUM=DX+SUM
      S(N)=TW
      IF(AL-SUM)10,9,9
10    CONTINUE
      CALL PLOT(0.0,0.0,0.0,100.,100.)
       CALL PLOT(23.,0.0,3)
      CALL PLOT(0.0,0.0,0)
      CALL GRAPH1(T,R,100,5H06X06,4HAUTO,40H TEMP OF EXPIRED  NASAL TO T
     1RACHEA AIR...17H LENGTH IN FEET...20H ABSOLUTE HUMIDITY..)
      CALL GRAPH1(T,S,100,7HOVERLAY,4HSAME)
      CALL PLOT(0.0,0.0,0.0,100.,100.)
       CALL PLOT(23.,0.0,3)
      CALL PLOT(0.0,0.0,0)
      CALL GRAPH1(T,V,100,5H06X06,4HAUTO,40H HUM. OF EXPIRED  NASAL TO T
     1RACHEA AIR...17H LENGTH IN FEET...20H ABSOLUTE HUMIDITY..)
      CALL GRAPH1(T,W,100,7HOVERLAY,4HSAME)
      AP=1.75/12.
      DX=.01/12.
      AL=1./12.
      AR=.0760
      AD=.2/12.
      AH=4.*.015/(.1/12.)
      AA=3.1415*AD**2/4.
      AV=67.5*60./(2.*3.1415*(AD*12.)**2/4.*12.)
```

```
      AM=AV*AP*3.141592*AD**2/4.
      AB=16.
      AC=.24
      AM=AV*AP*3.141592*AD**2/4.
      SUM=0.
      N=1
      WRITE(61,20)AT,TW,AU
      S(N)=TW
   11 TW=103.-12.*SUM
      BP=Z1*TW**3+Z2*TW**2+Z3*TW+Z4
      B2=BP+(AU-BP)*EXP(-AB*AP*DX/AM)
      T2=TW+(AT-TW)*EXP(-AH*AP*DX/(AM*AC)+(1060*DX*(B2-AU))/(AM*AC*
     1(TW-AT)))
      WRITE(61,21)N,TW,T2,BP,B2,AT, AU,SUM
      W(N)=BP
      V(N)=AU
      R(N)=AT
      T(N)=SUM
      AT=T2
      AU=B2
      N=N+1
      SUM=DX+SUM
      S(N)=TW
      IF(AL-SUM)12,11,11
   12 CONTINUE
      CALL PLOT(0.0,0.0,0.0,100.,100.)
       CALL PLOT(23.,0.0,3)
      CALL PLOT(0.0,0.0,0)
      CALL GRAPH1(T,R,100,5H06X06,4HAUTO,29H TEMP OF EXPIRED  NASAL AIR,
     1,17H LENGTH IN FEET,,20H ABSOLUTE HUMIDITY,,)
      CALL GRAPH1(T,S,100,7HOVERLAY,4HSAME)
      CALL PLOT(0.0,0.0,0.0,100.,100.)
       CALL PLOT(23.,0.0,3)
```

```
      CALL PLOT(0.0,0.0,0)
      CALL GRAPH1(T,V,100,5H06X06,4HACTO,35H HUMIDITY OF EXPIRED NASAL
     1AIR...17H LENGTH IN FEET...20H ABSOLUTE HUMIDITY..)
      CALL GRAPH1(T,V,100,7HOVERLAY,4HSAME)
      AM=AM*6.
      V1=AT
      V2=AU
      DELT=V1-Y1
      DELH=V2-Y2
      Y3=DELH*AM
      Y4=DELH*1060.*AM
      Y5=DELT*.24*AM
      WRITE(61,13)DELT,DELH,Y3,Y4,Y5
13    FORMAT(1H0,5F20.6)
      END
```

APPENDIX A.10

```
      PROGRAM MAIN
      DIMENSION T(500),RH(500),Q(500),RL(500),RR(500)
      COMMON TW1,TW2,TW3,TW4,AL1,AL2,AL3,AD1,AD2,AD3,     DX,AH,AB,KK
    1 FORMAT(1H1)
    2 FORMAT(6X,8F15.2)
    3 FORMAT(7F10.0)
    4 FORMAT(7F10.0)
      READ(60,16)KK
   16 FORMAT(I10)
   17 FORMAT(F10.2)
      READ(60,3)TW1,TW2,TW3,TW4,AL1,AL2,AL3
      READ(60,4)AD1,AD2,AD3,TV,DX,AH,AB
      PRINT 5
    5 FORMAT(1H0,5X,*NASAL TEMP*,5X,*MOUTH TEMP*,5X,*TOP TRACHEA TEMP*,
     15X,*BOTTOM TRACHEA TEMP*,5X,*NOSE LENGTH*,5X,*MOUTH LENGTH*//)
      WRITE(61,6) TW1,TW2,TW3,TW4,AL1,AL2
    6 FORMAT(8X,F6.2,9X,F6.2,11X,F6.2,10X,F6.2,12X,F6.4,10X,F6.4////)
      PRINT 7
    7 FORMAT(1H0,5X,*NASAL PASSAGE DIA*,5X,*MOUTH DIA*,5X,*TRACHEA DIA*,
     15X,*TIDAL VOLUME*,5X,*TRACHEA LENGTH*,5X,*LENGTH X*//)
      WRITE(61,8) AD1,AD2,AD3,TV,AL3,DX
    8 FORMAT(1H ,11X,F6.4,10X,F6.4,10X,F6.4,12X,F6.4,13X,F6.4,8X,F6.4///
     11/)
      READ(60,17)W
      ZZ=0.
      N=0
      K=0
      DO 40 J=1,2
      T(K)=70.
      RH(J)=.025+ZZ
      ZZ=ZZ+.001
      Z=0.
      DO 14 I=1,KK
```

```
      T(I)=T(I-1)+Z
      T(1)=70.
      RH(I)=RH(J)
      TW1=(T(I)-T(I-1))/3.+TW1
      TW2=(T(I)-T(I-1))/8.+TW2
      TW3=(T(I)-T(I-1))/10.+TW3
      TW4=(T(I)-T(I-1))/20.+TW4
      Z=Z+20.
      CALL MODEL (T,RH,QS,QL,RR,DELT,DELH,TV,I,J)
      WRITE(61,2)T(I),RH(I),QS(I),QL(I),RR(I),DELT,DELH,TV
14    CONTINUE
      WRITE(61,1)
      IF(N-1)37,38,38
37    CALL PLOT(0.0,0.0,0.0,100.,100.)
      CALL PLOT(0.0,-30.,2)
      CALL PLOT(0.0,0.0,0.0)
      CALL GRAPH1(T ,QL,KK,5H08X06,4HAUTO,27H   LATENT HEAT PRODUCTION,,
     1,  19H TEMPERATURE      ,,,25H HEAT PRODUCTION BTU/HR,,)
      GO TO 39
38    CALL GRAPH1(T,QL,25,7HOVERLAY,4HSAME)
39    N=N+1
40    CONTINUE
      END
```

```
      SUBROUTINE RATE(T,RH,TV,I,RP)
      DIMENSION T(5  ),RH(5  ),TV(  ,  ),AL(  ,  ),RP(  ,  )
      COMMON TA1,TA2,TA3,TA4,AL1,AL2,AL3,AD1,AD2,AD3,      ,      ,
   20 FORMAT(1H1,5E13.4)
   21 FORMAT(1H0,I10,7E16.4)
   22 FORMAT(1H0,4E31.4)
   13 FORMAT(1H0,5E20.6)
   15 FORMAT(2F40.3)
      CALL RATE(T,RH,TV,I,  ,RP)
      AP=1.75/12.
      AL=AL1/12.
      AD=AD1/12.
      AR=.0760
      AA=3.1415*AD**2/4.
      AC=.24
      AH=4.*.015/(.1/12.)
      AV=RP(I)*TV*5./(2.*3.141592*AD1**2/4.)
      AM=AV*AP*3.141592*AD**2/4.
      SUM=0.
      Z1=.000000801429
      Z2=-.000000742738
      Z3=.000421112
      Z4=-.00480741
      N=1
      AU=RH(I)
      AT=T(I)
      TW=TW1
      UP1=.0706
      Y1=AT
      Y2=AU
    1 TW=TW1+(TW2-TW1)/AL*SUM
      T2=TW+(AT-TW)*EXP(-AH*AP*DX/(AP*AC))
      BP=Z1*TW**3+Z2*TW**2+Z3*TW+Z4
```

```
      B2=BP+(AU-BP)*EXP(-AB*AP*DX/AM)
      WRITE(61,15)TW,T2
      AT=T2
      AU=B2
      N=N+1
      SUM=DX+SUM
      IF(AL-SUM)2,1,1
    2 CONTINUE
      AP=3.141592*AD2/12.
      AL=AL2/12.
      AD=AD2/12.
      AA=3.1415*AD**2/4.
      AH=4.*.015/AD
      AV=RR(I)*TV*5./(    3.141592*AD1**2/4.)
      AM=AV*AP*3.141592*AD**2/4.
      SUM=0.
      N=1
    3 TW=TW2+(TW3-TW2)/AL*SUM
      T2=TW+(AT-TW)*EXP(-AH*AP*DX/(AM*AC))
      BP=Z1*TW**3+Z2*TW**2+Z3*TW+Z4
      B2=BP+(AU-BP)*EXP(-AB*AP*DX/AM)
      WRITE(61,15)TW,T2
      AT=T2
      AU=B2
      N=N+1
      SUM=DX+SUM
      IF(AL-SUM)4,3,3
    4 CONTINUE
      AP=3.141592*AD3/12.
      AL=AL3/12.
      AD=AD3/12.
      AH=4.*.015/AD
      AV=RR(I)*TV*5./(    3.141592*AD1**2/4.)
```

```
      AM=AV*AP*3.141592*AD**2/4.
      SUM=0.
      N=1
5     TW=TW3+(TW4-TW3)/AL*SUM
      T2=TW+(AT-TW)*EXP(-AH*AP*DX/(AM*AC))
      BP=Z1*TW**3+Z2*TW**2+Z3*TW+Z4
      B2=BP+(AU-BP)*EXP(-AB*AP*DX/AM)
      WRITE(61,15)TW,T2
      AT=T2
      AU=B2
      N=N+1
      SUM=DX+SUM
      IF(AL-SUM)6,5,5
6     CONTINUE
      SUM=0.
      N=1
7     TW=TW4-(TW4-TW3)/AL*SUM
      BP=Z1*TW**3+Z2*TW**2+Z3*TW+Z4
      B2=BP+(AU-BP)*EXP(-AB*AP*DX/AM)
      T2=TW+(AT-TW)*EXP(-AH*AP*DX/(AM*AC)+(1060*DX*(B2-AU))/(AM*AC*
     1(TW-AT)))
      WRITE(61,15)TW,T2
      AT=T2
      AU=B2
      N=N+1
      SUM=DX+SUM
      IF(AL-SUM)8,7,7
8     CONTINUE
      AL=AL2/12.
      AD=AD2/12.
      AP=3.141592*AD2/12.
      AH=4.*.015/AD
      AV=RR(I)*TV*5./(    3.141592*AD1**2/4.)
```

```
      AM=AV*AR*3.1415*2*AD**2/4.
      SUM=0.
      N=1
    9 TW=TW3-(TW3-TW2)/AL*SUM
      BP=Z1*TW**3+Z2*TW**2+Z3*TW+Z4
      B2=BP+(AU-BP)*EXP(-AB*AP*DX/AM)
      T2=TW+(AT-TW)*EXP(-AH*AP*DX/(AM*AC)+(1060*DX*(B2-AU))/(AM*AC*
     1(TW-AT)))
      WRITE(61,15)TW,T2
      AT=T2
      AU=B2
      N=N+1
      SUM=DX+SUM
      IF(AL-SUM)10,9,9
   10 CONTINUE
      AP=1.75/12.
      AL=AL1/12.
      AD=AD1/12.
      AA=3.1415*AD**2/4.
      AH=4.*.015/(.1/12.)
      AV=RP(I)*TV*5./(2.*3.141592*AD1**2/4.)
      AM=AV*AP*3.141592*AD**2/4.
      SUM=0.
      N=1
   11 TW=TW2-(TW2-TW1)/AL*SUM
      BP=Z1*TW**3+Z2*TW**2+Z3*TW+Z4
      B2=BP+(AU-BP)*EXP(-AB*AP*DX/AM)
      T2=TW+(AT-TW)*EXP(-AH*AP*DX/(AM*AC)+(1060*DX*(B2-AU))/(AM*AC*
     1(TW-AT)))
      WRITE(61,15)TW,T2
      AT=T2
      AU=B2
      N=N+1
```

```
      SUM=DX+SUM
      IF(AL-SUM)12,11,11
12    CONTINUE
      V1=AT
      V1=103.
      V2=AU
      DELT=V1-Y1
      DELH=V2-Y2
      Y3=DELH*AM
      Y4=DELH*1060.*AM
      Y5=DELT*.24*AM
      VOL=PR(I)*TV
      WRITE(61,21)N,TM,T2,BP,B2,AT,AU,SUM
      WRITE(61,13)DELT,DELH,Y3,Y4,Y5
      X1=Y1
      X2=V1
      RH1=Y2
      RH2=V2
      PS1=-.430686+.0209578*X1-.00029118?*X1**2+.00000219653*X1**3
      PV1=RH1*PS1
      PS2=-.430686+.0209578*X2-.00029118?*X2**2+.00000219653*X2**3
      PV2=RH2*PS2
      VSA=1.*53.35*(X1+459.69)/(144.*(14.696-PV1))
      W1=PV1/(14.696-PV1)
      W2=PV2/(14.696-PV2)
      EH1=.24*X1+W1*(1059.2+.45*X1)
      EH2=.24*X2+W2*(1059.2+.45*X2)
      QL(I)=VOL*.076/(144.*12.)*DELH*60.*1060.
      QS(I)=VOL*.076/(144.*12.)*(EH2-EH1)*60.
      RETURN
      END
```

```
      SUBROUTINE RATE (T,RH,RR,TV,I,W)
      DIMENSION T(500),RH(500),RR(500)
      RR(I)=105.-22.7*W
      TV=(2.  +81.7*W)*(3.53*.0001)
      RETURN
      END
```